risks

Quantitative Risk Assessment in Life, Health and Pension Insurance

Edited by
Anna Rita Bacinello

Printed Edition of the Special Issue Published in *Risks*

www.mdpi.com/journal/risks

MDPI

Quantitative Risk Assessment in Life, Health and Pension Insurance

Quantitative Risk Assessment in Life, Health and Pension Insurance

Editor

Anna Rita Bacinello

MDPI • Basel • Beijing • Wuhan • Barcelona • Belgrade • Manchester • Tokyo • Cluj • Tianjin

Editor
Anna Rita Bacinello
University of Trieste
Italy

Editorial Office
MDPI
St. Alban-Anlage 66
4052 Basel, Switzerland

This is a reprint of articles from the Special Issue published online in the open access journal *Risks* (ISSN 2227-9091) (available at: https://www.mdpi.com/journal/risks/special_issues/Quantitative_Risk_Assessment).

For citation purposes, cite each article independently as indicated on the article page online and as indicated below:

LastName, A.A.; LastName, B.B.; LastName, C.C. Article Title. *Journal Name* **Year**, *Volume Number*, Page Range.

ISBN 978-3-0365-3827-3 (Hbk)
ISBN 978-3-0365-3828-0 (PDF)

Contents

About the Editor

Anna Rita Bacinello is a Full Professor of Mathematical Methods for Economics and Actuarial and Financial Sciences at the Department of Economics, Business, Mathematics and Statistics "Bruno de Finetti" of the University of Trieste, Italy. She currently teaches financial mathematics, mathematical finance, and financial risk management. Her main fields of research are finance and insurance, with particular focus on the valuation of life insurance contracts with minimum guarantees and other embedded options.

risks

MDPI

Editorial

Special Issue "Quantitative Risk Assessment in Life, Health and Pension Insurance"

Anna Rita Bacinello

Department of Economics, Business, Mathematics and Statistics "Bruno de Finetti", University of Trieste, 34100 Trieste, Italy; bacinel@units.it

The high volatility in financial markets, together with the ultra-low interest rates environment and the increased expectation of life, constitute serious threats for providers of long-term investment guarantees and lifelong benefits. Even if the COVID-19 pandemic is currently causing a mortality shock, its influence on future mortality is not clear, and one possible scenario could be a further increase in the life expectancy of survivors. The risk involved by all these "exogenous" factors is amplified by the uncertainty characterizing the individual behavior when taking decisions concerning, e.g., surrender, partial withdrawals, annuitization. The study of suitable solutions allowing to build resilience against these risks is a real challenge.

This Special Issue contributes to this challenge, and collects five high-quality research papers analyzing theoretical or practical aspects related to the following topics:

(i) Design of new pension insurance products and risk-management of loan insurance (Olivieri 2021; Planchet et al. 2022);
(ii) Assessing capital requirements for demographic risk in a life insurance portfolio—stochastic models and numerical techniques (Clemente et al. 2021; Costabile and Viviano 2021);
(iii) Analysis and risk-management of the long-term impact of COVID-19 on the life insurance business (Carannante et al. 2022).

In detail, the paper by (Clemente et al. 2021) focuses on the evaluation of capital requirements for both mortality and longevity risk. To this end, a stochastic model for traditional life insurance contracts is proposed and framed within the Solvency II Directive. In this context, the authors extend the classical methodologies developed in a local accounting framework, and prove that that the valuation of demographic profit can be significantly affected by the financial conditions in the market, so that the financial component cannot be completely separated from a purely demographic one. The paper ends with the presentation of a case study of a portfolio of life insurance contracts, which testifies the effectiveness of the model in highlighting the main drivers of capital requirement evaluation.

The paper by Costabile and Viviano (2021) addresses the problem of approximating the future value distribution of a large and heterogeneous life insurance portfolio by proposing two regression-based methodologies: the former is an extension of the well-known least squares Monte Carlo approach; the latter is grounded on the class of generalized beta distribution of the second kind. Extensive numerical experiments are conducted in order to assess the performance of the proposed methods, both in terms of accuracy and efficiency. To this end, a solid benchmark based on nested simulations is considered. The obtained results show that both methods represent valid alternatives to the benchmark in terms of accuracy, but strongly outperform it in terms of computational time. These conclusions are particularly relevant for insurance companies, helping them to reduce the computational effort needed to evaluate solvency capital requirements.

The paper by Olivieri (2021) introduces some elements of flexibility in the traditional annuity design that can better meet the preferences of annuitants, hence fighting their

Citation: Bacinello, Anna Rita. 2022. Special Issue "Quantitative Risk Assessment in Life, Health and Pension Insurance". *Risks* 10: 72. https://doi.org/10.3390/risks10040072

Received: 22 March 2022
Accepted: 24 March 2022
Published: 28 March 2022

Publisher's Note: MDPI stays neutral with regard to jurisdictional claims in published maps and institutional affiliations.

lack of attractiveness observed in many markets. In more detail, on one hand, the new design allows the benefit amount to fluctuate according to a given mortality/longevity experience, and on the other, provides a pricing structure alternative to classical upfront loading. This structure is based on periodical fees applied to the policy account, as usually occurs in the case of variable annuities. The fees can be assessed in order to incorporate an allowance for both the expected profit and the risk retained by the insurer. This product can be particularly appealing for individuals that need a longevity protection different from that supplied by traditional annuities: even if they are exposed to the risk of future benefit reductions as a consequence of higher longevity, this risk can be compensated by a lower premium loading.

The paper by Carannante et al. (2022) investigates the long-term effects of COVID-19 on life insurance profitability, and proposes a proactive mortality risk management based on dynamic premium adjustments which allows to prevent these effects and to increase the resilience of the business. In particular, the authors explore how the COVID-19 pandemic mortality shock has affected the profitability of annuity providers, and conclude that, unlike what might be expected, the involved mortality acceleration does not increase the profitability if their portfolios are well diversified in terms of age of the annuitants. Then, the longevity improvements continue to represent the main issue for these providers and lead them to frequently adjust their mortality assumptions, particularly if their portfolio is composed by contracts held by relatively young people.

The paper by Planchet et al. (2022) starts from the observation that many loans are currently rejected due to the presence of a pathology in the applicant, and analyzes how improvements in the knowledge of health and pooling risks, based on open data and risk pooling scenarios, can broaden access to loan insurance. In particular, the authors show how to use open data to estimate loan insurance premiums for a variety of diseases, and prove that through these data, the descriptions of the risks of mortality and disability for serious pathologies can be significantly refined. Then, a more accurate assessment of these risks enables enlargement of the insurance portfolios and to keep premiums at reasonable levels.

All the papers appearing in this Special Issue underwent a refereeing process subject to the usual high standards of *Risks*. I would like to thank all the authors for their excellent contributions and all the referees for their thorough and timely reviews. I would also like to extend my heartfelt thanks to the MDPI Editorial Team, especially to Mr. Ivan Wang.

Funding: This research received no external funding.

Conflicts of Interest: The author declares no conflict of interest.

References

Carannante, Maria, Valeria D'Amato, Paola Fersini, Salvatore Forte, and Giuseppe Melisi. 2022. Disruption of Life Insurance Profitability in the Aftermath of the COVID-19 Pandemic. *Risks* 10: 40. [CrossRef]

Clemente, Gian Paolo, Francesco Della Corte, and Nino Savelli. 2021. A Bridge between Local GAAP and Solvency II Frameworks to Quantify Capital Requirement for Demographic Risk. *Risks* 9: 175. [CrossRef]

Costabile, Massimo, and Fabio Viviano. 2021. Modeling the Future Value Distribution of a Life Insurance Portfolio. *Risks* 9: 177. [CrossRef]

Olivieri, Annamaria. 2021. Designing Annuities with Flexibility Opportunities in an Uncertain Mortality Scenario. *Risks* 9: 189. [CrossRef]

Planchet, Frédéric, Édouard Debonneuil, and Marie Péju. 2022. Proposal to Extend Access to Loans for Serious Illnesses Using Open Data. *Risks* 10: 51. [CrossRef]

risks

MDPI

Article

A Bridge between Local GAAP and Solvency II Frameworks to Quantify Capital Requirement for Demographic Risk

Gian Paolo Clemente [1], Francesco Della Corte [2,*] and Nino Savelli [1]

[1] Department of Mathematics for Economic, Financial and Actuarial Sciences, Università Cattolica del Sacro Cuore, 20123 Milano, Italy; gianpaolo.clemente@unicatt.it (G.P.C.); nino.savelli@unicatt.it (N.S.)
[2] Department of Statistical Sciences, Università La Sapienza, 00185 Roma, Italy
* Correspondence: francesco.dellacorte@uniroma1.it

Abstract: The aim of this paper is to provide a stochastic model useful for assessing the capital requirement for demographic risk in a framework coherent with the Solvency II Directive. The model extends to the market consistent context classical methodologies developed in a local accounting framework. The random variable demographic profit, defined in literatue under local accounting principles, is indeed analysed in a Solvency II framework. We provide a unique formulation for different non-participating life insurance contracts and we prove analytically that the valuation of demographic profit can be significantly affected by the financial conditions in the market. Regarding this topic, we implement the Vašíček model to add randomness to risk-free rates. A case study has also been developed considering a portfolio of life insurance contracts. Results prove the effectiveness of the model in highlighting the main drivers of capital requirement evaluation (e.g., the volatility of both mortality rates and risk-free rates), also compared to the local GAAP framework.

Keywords: life insurance; Solvency Capital Requirement; Solvency II; local GAAP; risk theory

Citation: Clemente, Gian Paolo, Francesco Della Corte, and Nino Savelli. 2021. A Bridge between Local GAAP and Solvency II Frameworks to Quantify Capital Requirement for Demographic Risk. *Risks* 9: 175. https://doi.org/10.3390/risks9100175

Academic Editor: Anna Rita Bacinello

Received: 16 August 2021
Accepted: 22 September 2021
Published: 29 September 2021

1. Introduction

Two key innovations, brought by the Solvency II directive in insurance, are the introduction of the market consistent framework for the valuation of assets and liabilities and the definition of risk-based principles for the assessment of the Capital Requirement. In this context, the quantification of losses on an annual time horizon at a given confidence level is a crucial element in determining the requirement. Each company must decide whether to adopt the standard approach or to use its own (partial or full) internal model, which has to be approved by the local supervisory authority. Furthermore, several sources of risk are involved in the valuation process; measuring the dependence between them is also a crucial point.

In this framework, we focus on demographic profit and we provide a stochastic model to quantify the capital requirement for both mortality and longevity risk. In the literature, several papers have dealt with this topic. In particular, Olivieri and Pitacco (2008) design a framework for a market-consistent analysis of the life-annuity portfolio. The authors link the traditional approach to a risk-neutral valuation assessing the cost of capital for longevity risk and measuring the amount of target capital for mortality and longevity risk. Hari et al. (2008) analyse the relevance of longevity risk for the solvency position of annuity portfolios distinguishing between micro and macro-longevity risks.

Stevens et al. (2010) quantify the value of annuity liabilities and of the related longevity risk capital requirement by applying the classical Lee–Carter model to estimate the uncertainty of future survival probabilities. Bauer and Ha (2015) propose an approach for the calculation of the required risk capital based on least-squares regression and Monte Carlo simulations. Savelli and Clemente (2013) provide an approach based on risk theory to evaluate the capital requirement for mortality and longevity risk in a local accounting framework. Boonen (2017) examines the consequences for a life insurance company of a calibration

of longevity and financial risks by using the expected shortfall instead of value-at-risk. Furthermore, the notion of market-consistent valuation of insurance liabilities has been investigated recently by several authors (Pelsser and Stadje 2014; Dhaene et al. 2017) and the analyses have also been extended to a dynamic multi-period setting (Barigou et al. 2019).

Dahl (2004) model mortality intensity as a stochastic process and quantify mortality risk by capturing the importance of time dependency and uncertainty. This paper contributes to the existing literature, proposing a different approach for modelling the capital requirement for mortality and longevity risk. We adapt the well-known gain and loss decomposition (Bacinello 1986) to a Solvency II framework, providing a closed formula for the random variable demographic profit and loss of a life insurance company. We show that this general formula holds for different non-participating life insurance contracts and we analytically split it into several elements in order to emphasize the main key drivers. To the best of our knowledge, a closed formula is not already available in the literature in a market-consistent framework. Additionally, it is noteworthy that, although our aim is not to forecast future mortality rates, the proposed approach is also consistent with the application of mortality models.

In particular, we assume a portfolio of non-participating life insurance policies composed by several cohorts of contracts, where in each cohort all the policyholders have the same characteristics (e.g., age, gender etc.) and the only element of distinction is represented by the sums insured. Hence, policyholders in the same cohort are assumed to be independent and identically distributed (i.i.d.), with the exception of the insured sums. It is noteworthy that the aggregation between different cohorts is not considered here as well as the possible presence of derivative contracts. Therefore, further research will concern the aggregation of several cohorts and portfolios composed of different contracts in order to catch the effects of both dependencies and natural hedging (see, e.g., Cox and Lin 2007).

Through this model, we prove the analytical decomposition of the expected demographic profit/loss, highlighting main drivers. Additionally, we assess the distribution via Monte Carlo simulations and we identify a Solvency Capital Requirement compliant with Solvency II. Furthermore, we assure that the model accurately reflects different sources of profit as requested by the requirements set by the Solvency II Directive (European Parliament and Council 2015, art. 123). In addition, a numerical section is presented to apply the proposed approach to alternative life insurance policies; here, we focus on the risk identified in Shen and Sherris (2018) as idiosyncratic risk.

The remainder of this paper is organized as follows. Section 2 exploits the traditional Homans formula, based on local Generally Accepted Accounting Principles (GAAP), adapting it to a market consistent context. Section 3 focuses on the random variable demographic profit, also providing a decomposition of this random variable useful for profit and loss composition. Section 4 presents the algebra underlying the model and the proof of a recursive formula that supports the results. Section 5 presents some simplified examples to emphasize the main key drivers. In Section 6, we assess our proposal by developing detailed case studies based on a real portfolio composed by different non-participating life insurance contracts. In particular, the main results confirm the effectiveness of the model in measuring the capital requirement and assessing the different components that affect the demographic results. In Section 7, we propose the conclusions of our paper.

2. Technical Profit and Gain/Loss Decomposition in a Solvency II Framework

In this section, we provide a formula for the random variable (r.v.) technical profit of a life insurance company. In particular, we define it in a market consistent framework according to the definition of technical liabilities given by the Solvency II regulation. Furthermore, we prove that a gain and loss decomposition is possible in order to emphasize the main profit components. The decomposition is developed in a similar fashion to the well-known decomposition provided by Homans (Bacinello 1986; Savelli and Clemente 2013) in a local accounting framework.

We start by briefly recalling the r.v. technical profit, that we denote[1] with $\tilde{Y}_{t+1}$, in a local accounting context (Savelli and Clemente 2013; Savelli 1993):

$$\tilde{Y}_{t+1} = [VB_t + \tilde{B}_{t+1} - \tilde{E}_{t+1} - \tilde{S}_{t+1}](1 + \tilde{j}_{t+1}) - [\tilde{X}_{t+1} + \tilde{VB}_{t+1}]. \tag{1}$$

First of all we specify that, consistent with the provisions of Solvency II (European Parliament and Council 2015, 2021), our purpose is to evaluate the capital requirement on an annual time horizon, therefore the stochastic variables will be those evaluated in $t+1$ since the valuation instant coincides with t.

The random variable technical profit $\tilde{Y}_{t+1}$ is defined as the difference of two terms. The first one is the sum of the complete technical provisions VB_t,[2] and the gross earned premiums $\tilde{B}_{t+1}$, net of expenses $\tilde{E}_{t+1}$ and surrenders $\tilde{S}_{t+1}$ accumulated at the actual financial return rate $\tilde{j}_{t+1}$[3]. The second term in Equation (1) is the sum of total claim costs $\tilde{X}_{t+1}$ and the complete technical provisions stored at the end of the year $\tilde{VB}_{t+1}$. It is noteworthy that we consider with the r.v. $\tilde{X}_{t+1}$ different non-participating life insurance policies (i.e., as specified later, this r.v. could be equal to zero or to the total lump sums paid in the case of death or survival according to the kind of benefit covered by the insurance policy).

With the introduction of the Solvency II framework (European Parliament and Council 2021), the previous formula has to be adapted to consider the market consistent valuation of assets and liabilities. Referring only to non-hedgeable liabilities, these are calculated as the sum of Best Estimate and Risk Margin (see Art. 77 of Directive 2009/138/EC). Hence, we can rewrite Equation (1) as:

$$\tilde{Y}^{MCV}_{t+1} = [BE_t + \tilde{B}_{t+1} - \tilde{E}_{t+1} - \tilde{S}_{t+1}](1 + \tilde{j}_{t+1}) - [\tilde{X}_{t+1} + \tilde{BE}_{t+1}]. \tag{2}$$

It should be pointed out that the Risk Margin is not considered since the purpose of this model is to identify a Solvency Capital Requirement consistent with the legislation and, therefore, with the Delegated Acts. Indeed, Delegated Regulation (European Parliament and Council 2015) assumes that the worst case scenario does not change the amount of Risk Margin included in the technical provisions. Therefore, the inclusion of this aforementioned component in Equation (2) when the formula is used for risk capital purposes is not in line with the constraints introduced by the regulation and could inappropriately affect the comparison with the standard formula requirement. Similarly to the well-known results regarding the decomposition of the classical Homans formula, we prove in the Appendix A the five components of the technical profit formula in a stochastic context. Our main interest is to focus on the first and the second components, respectively the demographic and financial profit and loss. Using rate-based expressions[4] instead of amounts (therefore switching from uppercase letters to lowercase ones), we can define the demographic profit (loss) as:

$$\begin{aligned} {}_1\tilde{y}^{MCV}_{t+1} = \{&[be_t^{Rf(t),q(t)} + b_{t+1} \cdot (1 - \alpha^* - \beta^*) - \gamma^*] \cdot (w_t - \tilde{s}_{t+1}) \cdot (1 + j^*) \\ &- (\tilde{x}_{t+1} + \tilde{w}_{t+1} \cdot \tilde{be}_{t+1}^{Rf(\tilde{t}+1),q(\tilde{t+1})}), \} \end{aligned} \tag{3}$$

where $be_t^{Rf(t),q(t)}$ is the rate of best estimate based on the risk-free curve available at time t and realistic demographic assumptions $q(t)$ at time t, b_{t+1} is the premium rate, α^*, β^* and γ^* are expense loading coefficients for acquisition, management and collection costs, respectively. The term $(w_t - \tilde{s}_{t+1})$ is the difference between the amount of the sums insured w_t in time t and surrenders $\tilde{s}_{t+1}$; j^* is the first order financial rate (i.e., the technical rate assumed in the premium assessment). Similarly the reserve at the end of the year is computed as the product of sums insured $\tilde{w}_{t+1}$ and the best estimate rate $\tilde{be}_{t+1}^{Rf(\tilde{t}+1),q(\tilde{t+1})}$ based on financial $Rf(\tilde{t}+1)$ and demographic $q(\tilde{t+1})$ assumptions in force at time $t+1$. It is noteworthy that Equation (3) also allows to analyse the effects of a possible change in the demographic technical base in $t+1$. From a qualitative point of view, demographic risk is defined as the possibility of suffering losses because of a variation in the effective

mortality of the cohort of policyholders. Since we deal with policyholders that have the same characteristics within the same cohort, we assume that the probabilities of death of the entities are the same and the demographic evolution of the single policyholder is independent from the others (i.e., policyholders are i.i.d.). The only difference between them is represented by the insured sum. We point out that, although a change in value of risk-free rates is considered in the evaluation of capital requirement related to interest risk, a model oriented to highlight the valuation concerning the bridge between the Local GAAP Technical Provisions and the market consistent valuation of Solvency II Best Estimate, must consider the effect of risk-free rates component. The best estimates involved in the valuation (see Equation (3)) depend on risk-free rates. Additionally, considering $\tilde{x}_{t+1}$, it is possible to find a capital requirement framework in line with the proposal made in the Quantitative Impact Study n.2, carried out in may 2006 for the preparation of final SCR standard formula, where a closed notation was provided for both mortality and longevity risk.

A peculiar mention must be given also to another profit component, the so-called financial profit, which is necessary to explain some key aspects of the model. It is defined as follows:

$$\begin{aligned} {}_2\tilde{y}_{t+1}^{MCV} = (\tilde{j}_{t+1} - j^*) \cdot [be_t^{Rf(t),q(t)} \cdot w_t + b_{t+1}(1 - \alpha^* - \beta^*) \cdot (w_t - \tilde{s}_{t+1}) + \\ - \gamma^* \cdot w_t - g_t^* \cdot be_t^{Rf(t),q(t)} \cdot \tilde{s}_{t+1}], \end{aligned} \tag{4}$$

where $\tilde{j}_{t+1}$ is the r.v. that describes the rate of return of invested assets and g_t^* is a specific penalization coefficient applied in case of surrender (see Appendix A for details on the formula). As expected, the sign of this component depends on the relation between the effective investment rate and the technical rate guaranteed to the policyholders. For the sake of brevity, the other profit components are reported in Appendix A, in particular that for expenses, for lapses and a residual margin. As proved, the sum of these five components gives back the whole technical profit (see Equation (2)).

3. The Demographic Profit and Its Factorisation

Given the gain and loss decomposition provided in the previous section, we now focus only on the demographic component (see Equation (3)). Indeed, modelling this random variable, we are able to assess the capital requirement for mortality or longevity risk. After some simple manipulations, it is possible to rewrite Equation (3) as follows:

$$\begin{aligned} {}_1\tilde{y}_{t+1}^{MCV} = D_{t+1}^b \cdot [q_{x+t}^* \cdot (w_t - \tilde{s}_{t+1}) - \tilde{z}_{t+1}] + \\ + (be_t^{Rf(t),q} - v_t^b) \cdot (w_t - \tilde{s}_{t+1}) \cdot (1 + j^*) - \tilde{w}_{t+1} \cdot (\tilde{be}_{t+1}^{\tilde{R}f(t+1),q} - v_{t+1}^b), \end{aligned} \tag{5}$$

where D_{t+1}^b is the complete sum-at-risk rate at time $t+1$ and q^* is the first-order annual death probability, v_t^b is the complete reserve rate based on a first order basis. The sum-at-risk are here defined "complete" since complete reserve rate is considered (i.e., including expenses reserves); they can be negative, as in pure endowment and annuities cases. This formula is based on the following relation that describes the evolution of the sums insured over time:

$$\tilde{w}_{t+1} = w_t - \tilde{s}_{t+1} - \tilde{z}_{t+1}, \tag{6}$$

where $\tilde{z}_{t+1}$ is the amount of sums insured eliminated in case of death.[5] In Equation (5), we assume that the best estimates in t and in $t+1$ are calculated on the same realistic demographic assumptions. Therefore, we simplify the notation using q instead of $q(t)$ and $q(t+1)$. Since the assessment is carried out on a one-year time span, it makes sense to consider that, within such a short period of time, the insurer does not change its demographic expectations. However, it is possible to evaluate the additional effect on the demographic profit of a one-year change of the second-order demographic assumptions.[6]

It is worth pointing out that the first term in Equation (5), here denoted as ${}_1\tilde{y}^{LG}_{t+1}$:

$$ {}_1\tilde{y}^{LG}_{t+1} = D^b_{t+1} \cdot [q^*_{x+t} \cdot (w_t - \tilde{s}_{t+1}) - \tilde{z}_{t+1}], \tag{7} $$

represents the demographic profit in a local accounting framework (Savelli and Clemente 2013).

Additionally, it is interesting to separately highlight the effects of risk-free rates volatility and demographic trends. In this regard, we provide the following decomposition:

$$ {}_1\tilde{y}^{MCV}_{t+1} = {}_1\tilde{y}^{LG}_{t+1} + {}_1\tilde{y}^{MCVRf-j*}_{t+1} + {}_1\tilde{y}^{MCVq-q*}_{t+1}, \tag{8} $$

where ${}_1\tilde{y}^{MCVRf-j*}_{t+1}$ is the demographic profit given by the differences between the first order financial rate j^* and the risk-free rate curve. The term ${}_1\tilde{y}^{MCVq-q*}_{t+1}$ instead measures the demographic profit originated by the differences between first-order and second-order death probabilities (q^* and q, respectively). To provide this decomposition and to define the second and the third term in Equation (8), we denote with $epv_t^{j^*,q}$ the expected present value of future cash-flows evaluated at time t and compute by using first-order discount rates j^* and second-order death probabilities q. In other words, this amount differs from $be_t^{Rf(t),q}$ only in terms of discounting factors.

It is easy to show that ${}_1\tilde{y}^{MCVRf-j*}_{t+1}$ is defined as:

$$ \begin{aligned} {}_1\tilde{y}^{MCVRf-j*}_{t+1} =& (w_t - \tilde{s}_{t+1}) \cdot [(be_t^{Rf(t),q} - epv_t^{j^*,q})(1+j^*) - (\tilde{be}_{t+1}^{Rf(\tilde{t}+1),q} - epv_{t+1}^{j^*,q})] \\ &+ (\tilde{be}_{t+1}^{Rf(\tilde{t}+1),q} - epv_{t+1}^{j^*,q}) \cdot \tilde{z}_{t+1}, \end{aligned} \tag{9} $$

and the third component in Equation (8) is:

$$ \begin{aligned} {}_1\tilde{y}^{MCVq-q*}_{t+1} =& (w_t - \tilde{s}_{t+1}) \cdot [(epv_t^{j^*,q} - v_t^b)(1+j^*) - (epv_{t+1}^{j^*,q} - v_{t+1}^b)] + \\ & (epv_{t+1}^{j^*,q} - v_{t+1}^b) \cdot \tilde{z}_{t+1}. \end{aligned} \tag{10} $$

It is interesting to note that ${}_1\tilde{y}^{MCVRf-j*}_{t+1}$ is strictly related to the difference between the best estimate and the expected present value of future cash-flows $epv_t^{j^*,q}$. In particular, we have a positive value if this difference, accumulated at the technical rate j^*, is greater than the analogous difference computed at time $t+1$. It must be noted that the difference $(be_t^{Rf(t),q} - epv_t^{j^*,q})$ only depends on the difference between the risk-free rates at time t and the technical rate j^*. For instance, a sudden and substantial change in value of the risk-free curve entails a jump in $t+1$ greater than the jump in t.

We also recall that we are focusing here only on the demographic profit. Hence, the whole effect of the risk-free rate curve on the technical profit can be assessed by also considering the financial profit. However, this point goes beyond the scope of the paper that is to quantify the capital requirement for mortality or longevity risk.

The term ${}_1\tilde{y}^{MCVq-q*}_{t+1}$ depends instead on the difference between the expected present value $epv_t^{j^*,q}$ and the technical provisions defined according to local accounting rules. Both values are computed with the same discounting rate j^*, but using a different life table (second-order and first-order, respectively). It must be pointed out that the sign of ${}_1\tilde{y}^{MCVq-q*}_{t+1}$ is mainly related to the comparison between the term $(epv_t^{j^*,q} - v_t^b)$, accumulated at the technical rate j^*, and the same difference evaluated at time $t+1$. We have indeed that the last term in Equation (10) usually has a very low weight and hence a low effect on the sign of ${}_1\tilde{y}^{MCVq-q*}_{t+1}$.

Now, we focus on the expected demographic profit (i.e., ${}_1\tilde{y}^{MCV}_{t+1}$) and we prove (see Section 4) that when $t > 1$, we have:

$$ \mathbb{E}\left[{}_1\tilde{y}^{MCV}_{t+1}\right] = \mathbb{E}\left[{}_1\tilde{y}^{MCVRf-j*}_{t+1}\right] \tag{11} $$

since

$$\mathbb{E}\left[{}_1\tilde{y}_{t+1}^{LG}\right] = -\mathbb{E}\left[{}_1\tilde{y}_{t+1}^{MCVq-q*}\right]. \tag{12}$$

This result shows that in case the second-order life table chosen by the insurance company is stable in the period $(t, t+1]$, the sign of the average demographic profit depends mainly on the differences between the risk-free curve and first-order financial rate. In particular, by Equation (9), we can also rewrite the mean as (when $t \geq 1$):

$$\begin{aligned}
&\mathbb{E}\left[{}_1\tilde{y}_{t+1}^{MCV}\right] = \mathbb{E}\left[{}_1\tilde{y}_{t+1}^{MCVRf-j*}\right] \\
&\mathbb{E}\left[{}_1\tilde{y}_{t+1}^{MCV}\right] = w_t \cdot (1+j^*) \cdot \left[b_t + be_t^{Rf(t),q} - \mathbb{E}\left[\tilde{be}_{t+1}^{Rf(\tilde{t}+1),q}\right] \cdot {}_1E_{x+t}^{j^*,q} - \mathbb{E}[\tilde{x}_{t+1}]\right].
\end{aligned} \tag{13}$$

On the basis of Equation (13), it easy to show that (see Section 4):

$$\mathbb{E}\left[{}_1\tilde{y}_{t+1}^{MCV}\right] = 0, \tag{14}$$

if, at time t, the one-year spot rate is equal to j^*.

It is worth pointing out that, at the inception of the contract (i.e., when $t = 0$), by Equation (13) the expected value of the demographic profit also depends on the differences between first-order and second-order life tables.

4. Model Algebra and Underlying Recursive Formula

We report in this section the main results and related proofs needed to support the presented stochastic model.

Theorem 1. *Considering a without-profit life insurance contract, we have that* $\mathbb{E}\left[{}_1\tilde{y}_{t+1}^{LG}\right] = -\mathbb{E}\left[{}_1\tilde{y}_{t+1}^{MCVq-q*}\right]$ *for* $t > 1$.

Proof. The starting point is represented by the sum of Equations (7) and (10). However, we specify that, instead of using the compact notation of Equation (7), we consider the extended definition of demographic profit:

$$\begin{aligned}
{}_1\tilde{y}_{t+1}^{LG} &= [v_t^b + \pi] \cdot (w_t - \tilde{s}_{t+1}) \cdot (1+j^*) - (\tilde{x}_{t+1} + \tilde{w}_{t+1} \cdot v_{t+1}^b) \\
&= D_{t+1}^b \cdot [q_{x+t}^* \cdot (w_t - \tilde{s}_{t+1}) - \tilde{z}_{t+1}],
\end{aligned}$$

where π is the constant pure premium rate obtained as $\pi = \pi_{t+1} = b_{t+1}(1-\alpha^*-\beta^*) - \gamma^*$. The proof regarding the equality between the two equations can be found in (Savelli and Clemente 2013). Hence, we have:

$$\begin{aligned}
{}_1\tilde{y}_{t+1}^{LG} +_1 \tilde{y}_{t+1}^{MCVq-q^*} &= v_t^b \cdot (w_t - \tilde{s}_{t+1}) \cdot (1+j^*) + \pi \cdot (w_t - \tilde{s}_{t+1}) \cdot (1+j^*) \\
&\quad - v_{t+1}^b \cdot \tilde{w}_{t+1} - \tilde{x}_{t+1} + epv_t^{j^*,q} \cdot (w_t - \tilde{s}_{t+1}) \cdot (1+j^*) \\
&\quad - v_t^b \cdot (w_t - \tilde{s}_{t+1}) \cdot (1+j^*) - (epv_{t+1}^{j^*,q} - v_{t+1}^b) \cdot (w_t - \tilde{s}_{t+1} - \tilde{z}_{t+1}).
\end{aligned}$$

By Equation (6), it is possible to rewrite the previous relation as follows:

$$\begin{aligned}
{}_1\tilde{y}_{t+1}^{LG} +_1 \tilde{y}_{t+1}^{MCVq-q^*} &= \left(\pi + epv_t^{j^*,q}\right) \cdot (w_t - \tilde{s}_{t+1}) \cdot (1+j^*) \\
&\quad - \tilde{x}_{t+1} - epv_{t+1}^{j^*,q} \cdot (w_t - \tilde{s}_{t+1} - \tilde{z}_{t+1}) \\
&= (w_t - \tilde{s}_{t+1}) \cdot \left[\left(\pi + epv_t^{j^*,q}\right) \cdot (1+j^*) - epv_{t+1}^{j^*,q}\right] \\
&\quad + epv_{t+1}^{j^*,q} \cdot \tilde{z}_{t+1} - \tilde{x}_{t+1}.
\end{aligned}$$

We now compute the expected value and we consider the case of an endowment policy. The result is easily extendable to pure endowment and term insurance policies, since these contracts can be seen as specific cases of an endowment contract.

$$\mathbb{E}\Big[{}_1\tilde{y}^{LG}_{t+1} + {}_1\tilde{y}^{MCVq-q^*}_{t+1}\Big] =$$
$$\mathbb{E}[w_t - \tilde{s}_t]\Big[\Big(\pi + epv^{j^*,q}_t\Big)\cdot(1+j^*) - epv^{j^*,q}_{t+1}\Big] + epv^{j^*,q}_{t+1}\cdot\mathbb{E}[\tilde{z}_{t+1}] - \mathbb{E}[\tilde{x}_{t+1}].$$

Since $\tilde{x}_{t+1} = \tilde{z}_{t+1}$ for an endowment contract and $\mathbb{E}[\tilde{z}_{t+1}] = q_{x+t}\cdot\mathbb{E}[w_t - \tilde{s}_t]$, we have:

$$\mathbb{E}\Big[{}_1\tilde{y}^{LG}_{t+1} + {}_1\tilde{y}^{MCVq-q^*}_{t+1}\Big] =$$
$$\mathbb{E}[w_t - \tilde{s}_t]\left(\Big(\pi + epv^{j^*,q}_t\Big)\cdot(1+j^*) - epv^{j^*,q}_{t+1}\cdot p_{x+t} - q_{x+t}\right).$$

Focusing on the term in the bracket, we prove that the following recursive equation holds:

$$\Big(\pi + epv^{j^*,q}_t\Big)\cdot(1+j^*) = epv^{j^*,q}_{t+1}\cdot p_{x+t} + q_{x+t}. \tag{15}$$

In the case of a endowment contract with unitary sum insured, we have:

$$\begin{aligned} epv^{j^*,q}_t =& {}_{n-t}p_{x+t}\cdot(1+j^*)^{-(n-t)} + \sum_{h=0}^{n-t-1} {}_{h/1}q_{x+t}\cdot(1+j^*)^{-(h+1)} + \\ &- \pi\sum_{h=0}^{n-t-1} {}_hp_{x+t}\cdot(1+j^*)^{-h} = \\ &{}_{n-t}p_{x+t}\cdot(1+j^*)^{-(n-t)} + \\ &+ (q_{x+t}\cdot(1+j^*)^{-1} + \sum_{h=1}^{n-t-1} {}_{h/1}q_{x+t}\cdot(1+j^*)^{-(h+1)}) + \\ &- \pi\cdot(1 + \sum_{h=1}^{n-t-1} {}_hp_{x+t}\cdot(1+j^*)^{-h}), \end{aligned}$$

which, for $s = h-1$, could be rewritten as:

$$\begin{aligned} epv^{j^*,q}_t =& {}_{n-t}p_{x+t}\cdot(1+j^*)^{-(n-t)} + \\ &+ (q_{x+t}\cdot(1+j^*)^{-1} + \sum_{s=0}^{n-t-2} {}_{(s+1)/1}q_{x+t}\cdot(1+j^*)^{-(s+2)}) + \\ &- \pi\cdot(1 + \sum_{s=0}^{n-t-2} {}_sp_{x+t}\cdot(1+j^*)^{-(s+1)}). \end{aligned}$$

Considering now:

$$\begin{aligned} \frac{epv^{j^*,q}_t}{{}_1E_{x+t}} =& {}_{n-t-1}p_{x+t+1}\cdot(1+j^*)^{-(n-t-1)} + \\ &\left(\frac{q_{x+t}}{{}_1p_{x+t}} + \sum_{s=0}^{n-t-2}\frac{{}_{(s+1)/1}q_{x+t}}{{}_1p_{x+t}}\cdot(1+j^*)^{-(s+1)}\right) + \\ &- \frac{\pi}{{}_1E_{x+t}} - \pi\cdot\sum_{s=0}^{n-t-2} {}_sp_{x+t+1}\cdot(1+j^*)^{-s}, \end{aligned}$$

we have:

$$\frac{epv^{j^*,q}_t}{{}_1E_{x+t}} = epv^{j^*,q}_{t+1} - \frac{\pi}{{}_1E_{x+t}} + \frac{q_{x+t}}{{}_1p_{x+t}}$$

which, with simple algebra, easily follows Equation (15): □

Having proved Equation (11), the final purpose of this section is to consider the demographic risk expressed in Equation (3) and to prove the following theorem:

Theorem 2. *Considering a without-profit endowment insurance contract that pays a lump sum equal to 1 either in the case of death or in the case of survival at the end of the contract and without benefits in the case of lapses, if second-order technical bases at time t and time t + 1 are the same, the following recursive equation holds:*

$$(be_t + \pi)(1 + i_t(0,1)) =_{/1} q_{x+t} + be_{t+1} \cdot_1 p_{x+t}, \tag{16}$$

where $i_t(0,1)$ is the one-year risk-free spot rate in force at time t and be_t and be_{t+1} are the pure best estimate rates computed using realistic demographic and financial assumptions in force at time t and neglecting expenses and expenses loadings.

Proof. We recall here that the definition of the best estimate rate of an endowment policy computed using realistic demographic assumption q and the risk-free rate curve i_t in force at time t.

$$\begin{aligned} be_t =_{n-t} p_{x+t} \cdot \left[\prod_{h=0}^{n-t-1} (1 + i_t(0,h,h+1)) \right]^{-1} + \\ \sum_{k=0}^{n-t-1} {}_{k/1}q_{x+t} \left[\prod_{h=0}^{k} (1 + i_t(0,h,h+1)) \right]^{-1} - \pi \cdot \ddot{a}_{(x+t):(n-t)}, \end{aligned} \tag{17}$$

where $i_t(0,h,h+1)$ is a risk-free forward rate.

The previous formula is also equal to:

$$\begin{aligned} be_t =_{n-t} p_{x+t} \left[\prod_{h=0}^{n-t-1} (1 + i_t(0,h,h+1)) \right]^{-1} +_{/1} q_{x+t} \cdot (1 + i_t(0,1))^{-1} + \\ \sum_{k=1}^{n-t-1} {}_{k/1}q_{x+t} \left[\prod_{h=0}^{k} (1 + i_t(0,h,h+1)) \right]^{-1} - \pi \cdot \sum_{h=1}^{n-t-1} {}_h E_{x+t} - \pi. \end{aligned} \tag{18}$$

From Equation (18), we have that the following relation holds:

$$\begin{aligned} (be_t + \pi) \cdot (1 + i_t(0,1)) -_{/1} q_{x+t} =_{n-t} p_{x+t} \left[\prod_{h=1}^{n-t-1} (1 + i_t(0,h,h+1)) \right]^{-1} \\ + \sum_{s=0}^{n-t-2} \left({}_{(s+1)/1}q_{x+t} \left[\prod_{h=1}^{s+1} (1 + i_t(0,h,h+1)) \right]^{-1} \right) \\ - \pi \cdot \sum_{h=1}^{n-t-1} \left({}_h p_{x+t} \left[\prod_{j=1}^{h} (1 + i_t(0,j,j+1)) \right]^{-1} \right). \end{aligned} \tag{19}$$

Since the estimation of the best estimate at time $t+1$ under the assumption in force at time t is equal to:

$$\begin{aligned} be_{t+1} =& {}_{n-t-1}p_{x+t+1}\left[\prod_{h=1}^{n-t-1}(1+i_t(0,h,h+1))\right]^{-1} + \\ &+ \sum_{k=0}^{n-t-2}\left({}_{k/1}q_{x+t+1}\cdot\left[\prod_{h=1}^{k+1}(1+i_t(0,h,h+1))\right]^{-1}\right) + \\ &- \pi\cdot\ddot{a}_{(x+t+1):(n-t-1)}, \end{aligned} \tag{20}$$

it is noticeable that the right-hand side of Equation (19) is equal to $be_{t+1}\cdot_1 p_{x+t}$. Hence, we have:

$$(be_t+\pi)(1+i_t(0,1)) =_{/1} q_{x+t} + be_{t+1}\cdot_1 p_{x+t}. \tag{21}$$

It is worth pointing out that the proof can be easily adapted to the cases of single premiums, pure endowment or term insurance contracts and flat rates, that have also been analysed in the paper. All of these combinations can be considered as special cases of the one that has been proved. □

The most interesting aspect of this recursive formula concerns the fact that Equation (3) for $t>1$, has an expected value different from 0 when the technical rate j^* differs from the spot rate $i_t(0,1)$. This difference between Equation (3) and Equation (21) will be relevant for the interpretation of the results reported in Sections 5 and 6.

5. The Profit Formation

We focus in this section on the expected demographic profit considering two non-participating life insurance contracts: a pure endowment and a term insurance. We consider these two policies because their combination allows us to obtain other traditional policies issued in the insurance market. As is well-known, an Endowment contract coincides with the sum of a Pure Endowment[7] and a Term Insurance[8] with the same maturity and same sums insured, and an Annuity can be defined as the sum of several Pure Endowments with different maturities and a Term Insurance with variable insured sums is a slight adjustment of the classical Term Insurance. Hence, previous formulas can be used as a basis for evaluating the different kinds of contracts previously mentioned.

We consider a cohort of policyholders, whose main characteristics are summarized in Table 1. We start from a simplified application that allows us to provide additional insights. In particular, for the sake of simplicity, we assume a flat risk free-rates constant over time and we neglect the effect of expenses. Additionally, we are assuming that the risk-free rates are equal to the technical rate j^* guaranteed to the policyholder. We have instead that the insurance company priced contracts assuming first-order death probabilities q^* equal to 85% of the death probabilities given by the ISTAT2016 population life table. In this first analysis, we assume that the observed mortality follows rates given by the ISTAT2016 population life table. In other words, a prudential pricing has been applied by the insurance company and, hence, a demographic profit is expected. In this regard, we compare in Figure 1 how the profit is released over time in either a market-consistent or a local accounting framework.

We emphasize that the stochastic evolution of the cohort implies deviations from 0 of the r.v. demographic profit. The comparison shows how these fluctuations impact differently in a Local GAAP context and in a market consistent context (see Theorem 2). In a local accounting framework (i.e., see ${}_1\tilde{y}^{LG}_{t+1}$, Equation (7)), the expected profit varies over time, depending on the trend of the sum-at-risk, the implicit safety loading and the effects of mortality. As expected, in a market consistent context, because of unlocked technical bases, the expected profit (i.e., ${}_1\tilde{y}^{MCV}_{t+1}$) occurs when the difference between the technical bases and realistic assumptions is revealed, while only the unexpected profit linked to the idiosyncratic risk of the mortality rates occurs over time. In particular, at the inception

of the contract, we notice the effect of the difference between first-order basis (used for premium assessment) and second-order basis (used for the market-consistent valuation of technical provisions). In other words, implicit safety loadings are released as a technical profit at the end of the first year.

Table 1. Model parameters.

Individual age at policy issue	40
Gender	Male
Policy duration	20
Expenses loadings	0%
Risk-free rates	1%
Number of policyholders	15,000
Initial sums insured	1,510,653,999
CV[9]	1.99
I order demographic basis	0.85·ISTAT2016
II order demographic basis	ISTAT2016
Technical rate	1%

From year 2 to the end of the contract, we observe that $\mathbb{E}\left[{}_1\tilde{y}_{t+1}^{MCV}\right]$ is equal to 0. We are indeed assuming that risk-free rates are constant and equal to first-order technical rate j^* and that the realistic assumptions used for best estimate valuation are kept unchanged over time by the company: these results derive from Theorem (1) and Theorem (2) of Section 4.

The same analysis has been also applied to term insurance contracts. In this case, we maintain the same assumptions reported in Table 1, but we assume that premiums have been computed using an ISTAT2014 life table, while insureds die at the same rates used for the pure endowment portfolio; therefore, also in this case we have an implicit safety loading.

It is worth pointing out the higher expected demographic profit with respect to a pure endowment portfolio and a different behaviour at time 1 between regular and single premiums (see Figure 1, top). A higher profit is here realised when a single premium is charged because of greater values of the implicit safety loading.[10]

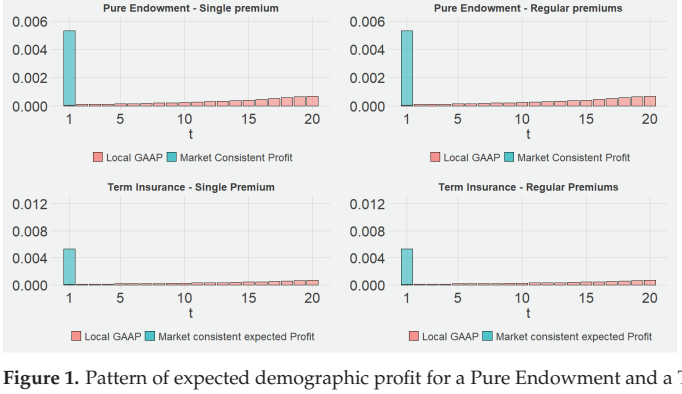

Figure 1. Pattern of expected demographic profit for a Pure Endowment and a Term Insurance.

Previous examples assumed a full coincidence between technical rates and risk-free rates. The advantage is the fact that demographic profit is not affected by the behaviour of financial rates. We analyse now the effects of alternative risk-free rates and we focus only on the expected profit evaluated in a market-consistent framework.

Figure 2, left hand-side, reports the pattern of the expected profit for a pure endowment. In this case, the same assumptions of Table 1 have been considered, but constant spot risk-free rates equal to 2% are assumed. Higher risk-free rates lead to an increase of the initial profit due to a lower technical provision at the end of the year because of higher discounting effects.[11] A lower increase is observed in the case of regular premiums because also future cash-in (premiums) are discounted at higher rates.

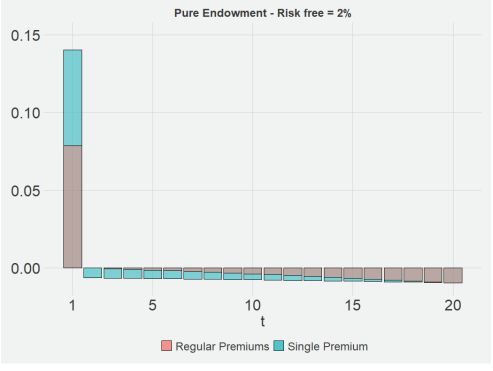

Figure 2. Expected demographic profit in the Pure Endowment.

Following periods, namely for $t > 1$, are instead characterized by expected losses. This behaviour can be explained by Equation (9). As shown in Figure 3, the reserve jump $(be_t^{Rf(t),q} - epv_t^{j^*,q})$ is negative and is accumulated at a rate j^*. This amount is higher than the term $(\tilde{be}_{t+1}^{Rf(t+1),q} - epv_{t+1}^{j^*,q})$. The same result can also be explained by Equation (13), where, under the assumption that the best estimates at time t and $t+1$ are positive, we have an expected loss if j^* is smaller than the spot rate $i(t, t+1)$.

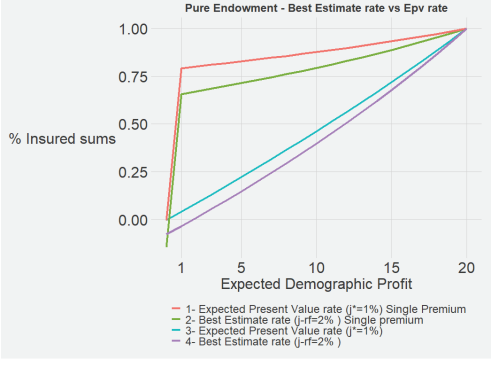

Figure 3. Expected present value and best estimate rates.

It is also interesting to note that in case of a negative best estimate we have an opposite result. In Figure 4, we consider again a pure endowment with the same characteristics but we assume an extraordinarily large flat rate equal to 20%. It could be noticed that, in line with Equation (13), in time periods in which $be_t^{Rf(t),q}$ is negative, a positive expected profit is observed (see $0 \leq t \leq 11$ in Figure 4).

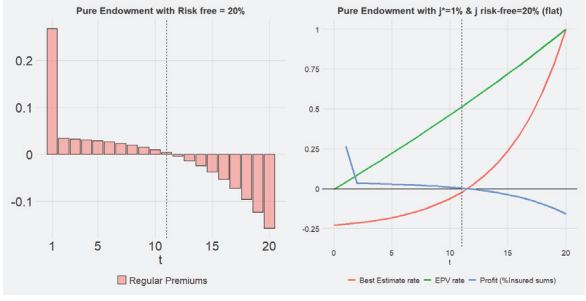

Figure 4. Expected demographic profit in the Pure Endowment with higher risk-free rates.

In Figure 5, we report the behaviour of the expected profit in case of either a regular and a single premium for the term insurance. Policyholder and contract characteristics are the same reported in Table 1 and the risk-free rate is equal to 2%. Results confirm a consistent behaviour independent of the kind of policy considered.

However, because of the lower best estimate rate, the effect of financial rates is less relevant when a term insurance contract is considered.

Finally, in this section, the analysis has been developed assuming a constant risk-free rate for all maturities. However, considering the case of a risk-free curve, similar comments follow from Equations (9) and (13) based on the comparison between the technical rate j^* and the forward rates for each period $(t, t+1)$.

Before presenting the next section, it is emphasized that, for a particularly young insurance company, the strictly one year vision can lead to incorrect and partial results, indeed if the Solvency Capital Requirement were calculated over a three-year time horizon, the results would be the opposite.

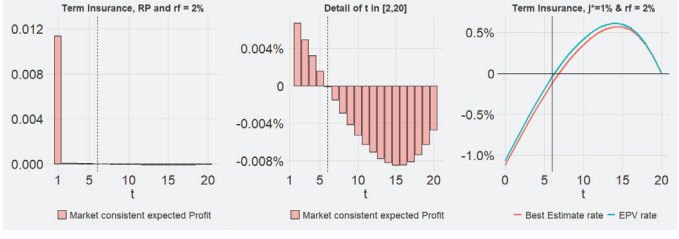

Figure 5. Expected demographic profit in the Term Insurance with higher risk-free rates.

6. The Application of the Model to Non-Participating Life Policies

In this section, we analyse the behaviour of our model in terms of volatility and capital requirement by developing a detailed case study. We consider a portfolio characterized by three non-participating insurance policies: a Pure Endowment, an Endowment and a Term Insurance. To this end, we are able to catch how the different characteristics of the contracts can affect the demographic profit distribution and the related capital requirement.

In Table 2, we summarize the general characteristics (age and contractual duration of the policy) and the expense loadings. For the sake of comparability, we assume that different policies have been underwritten by policyholders with the same characteristics. Furthermore, the sums insured at time 0, w_0, are calculated as the sum of the individual sums insured of each policyholder:

$$w_0 = \sum_{i=1}^{l_0} C_i = l_0 \cdot \bar{C}_0, \tag{22}$$

where l_0 is the number of policyholders in $t = 0$.

Table 2. Model parameters.

Individual age at policy issue	40
Policy duration	20
Premium type	Annual premiums (20)
Acquisition loading	50%
Collection loading	2.5%
Management loading	0.15%
Number of policyholders (l_0)	15,000
Expected value of the single insured sum	100,000
CV of the sums insured	1.99%

The risk-free rate curve used is the one provided by EIOPA for the Euro area (at the end of 2015); we preferred to use a curve calibrated in a quiet period, which does not present particular types of stress. We have chosen the one without volatility adjustment. Demographic technical bases are summarized in Table 3 and are different for each policy because the goal is to highlight specific profit creation considering a realistic rating process.

Consequently, for the Endowment and the Term Insurance with positive sum-at-risk, the pricing is carried out with the ISTAT2014 demographic table. Pure Endowment, characterized by a negative sum-at-risk, has been priced multiplied by the death probabilities, derived by ISTAT2016 life tables, by a coefficient α_t between 0.8 and 0.9 that depends on the age of the policyholder. The effective mortality of all portfolios is instead described by the ISTAT2016 table. We are obviously aware that second-order mortality can be affected by self-selection or medical-selection (e.g., in term insurance products to identify calibrated risks). Similarly, term insurance and endowment policies are usually priced using a different life table. To assure a greater comparison between results we considered in this numerical analysis similar technical bases for different policies. The results can be easily adapted to the case of a higher customization of life tables.

It is also noteworthy that future mortality rates can be obviously obtained using forecasting models (as, for instance, the Lee–Carter model). However, the main comments described in this section also hold in the case of projected second-order life tables.

Table 3. Demgraphic assumptions.

	Pure Endowment	**Endowment**	**Term Insurance**
First order—q*	α_t·ISTAT2016	ISTAT2014	ISTAT2014
Second order—q	ISTAT2016	ISTAT2016	ISTAT2016

The model is applied by means of Monte Carlo simulations. In particular, the number of deaths is simulated in a one-year time horizon by a Binomial distribution with parameters equal to the number of policyholders and the second-order death probability. To consider the variability of the sums insured, we extract the insured capital at the end of the year and the amounts paid in case of death by LogNormal distributions with mean and CV defined in Table 2.

Another key element is the assessment of the Best Estimate rate at the end of the period. It is assumed that, on average, the spot rates at the end of the year will coincide with the forward rates inferable from the risk-free curve of spot rates at the beginning of the year. The volatility of risk-free rates is introduced through the use of a Vasicek model (Vasicek 1977); particularly effective in case of negative risk-free rates for shorter maturities. Hence, the calibration of the Vašíček model is carried out for each policy and at each time point, requiring that the expected value of the best estimate rate, calculated at the end of the time span, coincides with the best estimate rate calculated with the forward rates

implicit in the spot rate curve at the beginning of the time horizon. This method has been selected to eliminate the possibility of arbitrage. In this way, the expected present value in t of the best estimate calculated from $t+1$, is equal to the expected present value in $t+1$ of the best estimate (obviously calculated in $t+1$) since the spot rates in $t+1$ coincide with the forward rates inferable from the spot curve available in t. Given this constraint, valid alternatives, which consider the adjustment of the yield term, are the models proposed in (Ho and Lee 1986; Black et al. 1990). However, it is specified that, since the model is balanced on forward rates, the most important element is the sigma σ multiplier of the infinitesimal increment of the Brownian Motion dW_t as it is the parameter that directly influences the volatility of the risk-free rate curve.

The results of the stochastic model are presented. Two points must be highlighted:

- For each policyholder, 10 million simulations have been made. Therefore, the results are particularly consistent, especially in terms of volatility;[12]
- The total amount of the sums insured at the inception of the policy ($t = 0$) is equal to approximately 1.5 billion euros. It is therefore noted that any Capital Requirement, in terms of magnitude, must be compared with the value just mentioned, although at first glance it may seem particularly high.

First of all, Table 4 shows[13] the results of the simulation model applied at the inception of the contract ($t = 0$) and with a one-year view to the portfolio of Pure Endowment policies.

Table 4. Simulated MCV results—Pure Endowment.

Pure Endowment	t **= 0**	t **= 10**	t **= 19**
$\mathbb{E}\left[{}_1\tilde{y}_{t+1}^{MCV}\right](T)$	150,339,562	−8,882,965	−19,893,883
$\mathbb{E}\left[{}_1\tilde{y}_{t+1}^{MCV}\right]$	150,349,827	−8,760,096	−19,894,122
$\mathbb{E}\left[{}_1\tilde{y}_{t+1}^{MCV}\right]$ on w_t	9.95%	−0.61%	−1.38%
$\sigma({}_1\tilde{y}_{t+1}^{MCV})$	4,345,500	5,937,483	1,821,044
$\gamma({}_1\tilde{y}_{t+1}^{MCV})$	−0.04	−0.02	0.97
SCR	−138,942,272	24,208,313	23,333,458
SCR on w_t	−9.20%	1.62%	1.60%

It should be noted that the initial Best Estimate rate at the time 0^+ is negative (equal to −7.65%). Despite the significant contribution of the implicit safety demographic loading, the largest share of expected profit derives from the difference between the first order financial rate ($j^* = 1\%$) and the discounting spot rate for longer maturities. For instance, the expected survival benefits paid to the policyholder at the end of the coverage are discounted by using a spot rate equal to 1.57%.[14]

Additionally, we have that the capital requirement, computed here using a value at risk at a 99.5% confidence level, is negative. We have indeed that the huge expected profit allows to cover adverse fluctuation of demographic assumption also in the worst case computed at the previously mentioned confidence level. A different situation is instead obtained, assumed to be at times t = 10 and t = 19, respectively. In Table 4 we also report the main characteristics of profit distribution as well as the capital requirement computed on a one-year view at different time periods.

It is interesting to note that, after the first year of contract, where the expected profit at inception is accounted for, the risk-free forward rate higher than the technical rate leads to significant expected losses (in accordance to Equation (13). This effect increases as the year progressively grows because forward rates grow over time. Because of this behaviour we have positive requirements in both periods.

In Table 5, we provide results obtained applying the model in a local accounting framework. It is noteworthy that we observe that the standard deviation in $t = 10$ increases due to the greater volatility of risk-free rates, while in $t = 19$ only the strictly demographic volatility remains, because the only risk-free rate is known. As regards skewness, what happens is similar: in $t = 0$ and $t = 10$ the skewness deriving from the Vašíček model is the main driver, while in $t = 19$ only the skewness of the purely demographic component remains. With reference to the simulated SCR, it should be noted that the previous Solvency 0 and Solvency I regulations indicated 0.3% of positive sum-at-risk as a capital requirement for life underwriting risk without differentiations related to the characteristics of the insurance portfolio.

Table 5. Local GAAP results—Pure Endowment.

Pure Endowment	t **= 0**	t **= 10**	t **= 19**
$\mathbb{E}\left[{}_1\tilde{y}^{LG}_{t+1}\right](T)$	2528	230,554	1,040,705
$\sigma({}_1\tilde{y}^{LG}_{t+1})(T)$	16,455	615,730	1,799,850
$\gamma({}_1\tilde{y}^{LG}_{t+1})(T)$	2.41	1.54	1.09
SCR	19,463	792,091	2,397,872
SCR on w_t	0.01%	0.05%	0.16%

A similar analysis has been developed for an Endowment; we report in Table 6 the main characteristics of the distribution of ${}_1\tilde{y}^{MCV}_{t+1}$ and the SCR ratio according to the three time periods. Table 7 summarizes analogous values computed in a local accounting framework.

Table 6. Simulated MCV results—Endowment.

Endowment	t **= 0**	t **= 10**	t **= 19**
$\mathbb{E}\left[{}_1\tilde{y}^{MCV}_{t+1}\right](T)$	153,901,015	−9,096,636	−20,084,746
$\mathbb{E}\left[{}_1\tilde{y}^{MCV}_{t+1}\right]$	153,905,829	−9,138,027	−20,084,746
$\mathbb{E}\left[{}_1\tilde{y}^{MCV}_{t+1}\right]$ on w_t	10.19%	−0.61%	−1.38%
$\sigma({}_1\tilde{y}^{MCV}_{t+1})$	4,588,717	6,020,325	0
$\gamma({}_1\tilde{y}^{MCV}_{t+1})$	−0.05	−0.02	0
SCR	−141,802,756	24,821,250	20,084,746
SCR on w_t	−9.39%	1.66%	1.38%

Table 7. Local GAAP results—Endowment.

Endowment	t **= 0**	t **= 10**	t **= 19**
$\mathbb{E}\left[{}_1\tilde{y}^{LG}_{t+1}\right](T)$	260,745	395,352	0
$\sigma({}_1\tilde{y}^{LG}_{t+1})(T)$	750,933	595,986	0
$\gamma({}_1\tilde{y}^{LG}_{t+1})(T)$	−2.41	−1.54	0
SCR	3,289,428	2,091,067	0
SCR on w_t	0.22%	0.14%	0%

Endowment contract shows similar results to the pure endowment case in terms of both expected profit and capital requirement ratio. The main differences can be noticed in the last year of the contract ($t = 19$). We have indeed that, given the fact that the payment of benefit is certain, we have no volatility and, hence, the capital requirement is only needed to face expected losses.

As well-known previous contracts are typically chosen for saving purposes and the financial profit is the key issue for an insurance company. Therefore, we investigate the behaviour of the demographic profit in the case of a term insurance, which is typically chosen by policyholders for risk-protection purposes. The main results are reported in Table 8.

Table 8. Simulated MCV results - Term Insurance.

Term Insurance	t **= 0**	t **= 10**	t **= 19**
$\mathbb{E}\left[{}_1\tilde{y}^{MCV}_{t+1}\right](T)$	20,898,387	−271,353	−269,009
$\mathbb{E}\left[{}_1\tilde{y}^{MCV}_{t+1}\right]$	20,891,192	−269,927	−269,285
$\mathbb{E}\left[{}_1\tilde{y}^{MCV}_{t+1}\right]$ on w_t	1.38%	−0.02%	−0.02%
$\sigma({}_1\tilde{y}^{MCV}_{t+1})$	777,012	1,224,059	1,820,823
$\gamma({}_1\tilde{y}^{MCV}_{t+1})$	−2.42	−1.48	−0.97
SCR	−17,219,206	24,821,250	6,769,046
SCR on w_t	−1.14%	0.36%	0.47%

It is interesting to note that the expected gain accounted for in $t = 1$, although strictly greater than the expected losses of the subsequent periods, is lower than those of other policies (e.g., pure endowment, endowment). In this case, the very small volume of mathematical reserves ensures that expected losses and expected profits are very low. The previous comment is also explained by the fact that we are assuming the same first and second-order life tables in term insurance and endowment. On the other hand, despite the volatility of sums insured paid in the case of death, a lower ratio between the capital requirement and the sums insured is observed.

Comparing the results of the Term Insurance with those obtained in a Local GAAP context (see Table 9), we observe that also in this case, the volatility in $t = 0$ and $t = 10$ is mainly driven by the volatility of the Vašíček model, while in $t = 19$ it remains only the volatility of the strictly demographic component. As in the case of the Pure Endowment, it is clearly observed that where the financial component is zero (in $t = 19$ the only spot rate is known), only the purely demographic skewness remains.

Table 9. Local GAAP results—Term Insurance.

Term Insurance	t **= 0**	t **= 10**	t **= 19**
$\mathbb{E}\left[{}_1\tilde{y}^{LG}_{t+1}\right](T)$	266,582	800,159	2,160,710
$\sigma({}_1\tilde{y}^{LG}_{t+1})(T)$	767,745	1,206,226	1,799,850
$\gamma({}_1\tilde{y}^{LG}_{t+1})(T)$	−2.41	−1.54	−1.09
SCR	3,335,518	4,265,074	4,320,054
SCR on w_t	0.22%	0.29%	0.29%

Finally, it should be noted that, despite the different nature of the alternative policies, a similar effect of the implicit forward rates is noticed both in terms of expected gains/losses, and in terms of capital requirement.

7. Conclusions

In this paper, we focus on the evaluation of the capital requirements for both mortality and longevity risk. In particular, we adapt classical actuarial relations to the market consistent framework required by the Solvency II directive. We provide a specific model that is able to catch the characteristics of demographic risk for non-participating life insurance contracts. As is well-known, in a local accounting context, differences between expected and observed mortality rates are a key topic for assessing demographic risk. We show that in a market-consistent framework, the financial component cannot be completely separated from the purely demographic one. We prove indeed that in the case where second-order demographic assumptions are stable over time, the connection between the financial guaranteed rate and the risk-free rate curve becomes the key element for the assessment for one-year demographic risk. Hence, to have a complete view of the insurance position, the main results must then be compared with the financial profit and the capital requirement for market risk too. Therefore, further research should regard an integrated assessment of both demographic and financial risks that could be helpful for defining strategies and future management actions regarding both portfolio characteristics and asset allocation. Finally, further developments will exploit the proposed model and closed formulas to quantify both idiosyncratic and systematic volatility to quantify the Solvency Capital Requirement.

Author Contributions: All authors contributed equally to this manuscript. All authors have read and agreed to the published version of the manuscript.

Funding: This research received no external funding.

Data Availability Statement: Data is contained within the article as they are entirely simulated on the assumptions stated.

Conflicts of Interest: The authors declare no conflict of interest.

Appendix A. Homans' Revised Decomposition

We show here the decomposition of Equation (2) in five components. For the sake of brevity, we limit this appendix to the definition of the five components we found. The proof follows by simple algebra.

$$\tilde{Y}^{MCV}_{t+1} =_1 \tilde{y}^{MCV}_{t+1} +_2 \tilde{y}^{MCV}_{t+1} +_3 \tilde{y}^{MCV}_{t+1} +_4 \tilde{y}^{MCV}_{t+1} +_5 \tilde{y}^{MCV}_{t+1} \tag{A1}$$

It is noteworthy that we focus exclusively on without-profit policies. The reason for this choice lies in the fact that the model aims at isolating the demographic component.

We give now the definition of the five components expressed in rate notation. The first component represents the demographic profit and it is defined as in Equation (3):

$$\begin{aligned} {}_1\tilde{y}^{MCV}_{t+1} = [be^{Rf(t),q(t)}_t + b_{t+1}(1-\alpha^*-\beta^*) - \gamma^*](w_t - \tilde{s}_{t+1})(1+j^*) + \\ - (\tilde{x}_{t+1} + \tilde{be}^{Rf(t+1),q(t+1)}_{t+1}) \end{aligned} \tag{A2}$$

While the second profit component as defined in Equation (4) could be seen as:

$$\begin{aligned} {}_2\tilde{y}_{t+1} =& (\tilde{j}_{t+1} - j^*) \cdot (be^{Rf(t),q(t)}_t \cdot w_t + b_{t+1}(1-\alpha^*-\beta^*)(w_t - \tilde{s}_{t+1}) + \\ & - (\gamma^* w_t) - (g^*_t \cdot be^{Rf(t),q(t)}_t \cdot \tilde{s}_{t+1}) \end{aligned} \tag{A3}$$

The lapse profit, is defined as:

$${}_3\tilde{y}^{MCV}_{t+1} = (be^{Rf(t),q(t)}_t - \gamma^* - g^*_t \cdot be^{Rf(t),q(t)}_t) \cdot (1+j^*) \cdot \tilde{s}_{t+1} \tag{A4}$$

where g^*_t is a penalization coefficient that considers a surrender penalty:

$$g_t^* = \begin{cases} 0 & if\ t < \tau \\ (1+j_s)^{-(m-t)} & if\ t >= \tau \end{cases} \tag{A5}$$

where $\tau > 0$ and $j_s^* < j^*$ are fixed by the undertaking.

The fourth component of profit is the expense one and it is defined in the following way:

$$_4\tilde{y}_{t+1} = (1+j^*)[(\Delta\alpha_{t+1}^* + \Delta\beta_{t+1}^*) \cdot b_{t+1} \cdot (w_t - \tilde{s}_{t+1}) + \Delta\gamma_{t+1}^* \cdot w_t] \tag{A6}$$

where $\Delta\alpha_{t+1}^*$, $\Delta\beta_{t+1}^*$ and $\Delta\gamma_{t+1}^*$ depend on the differences between the first order expense assumptions and the realistic ones.

The last component, is the residual profit:

$$\begin{aligned} _5\tilde{y}_{t+1} = (\tilde{j}_{t+1} - j^*)[(\Delta\alpha_{t+1}^* + \Delta\beta_{t+1}^*) \cdot b_{t+1} \cdot (w_t - \tilde{s}_{t+1}) + \\ + \Delta\gamma_{t+1}^* \cdot w_t] \end{aligned} \tag{A7}$$

Notes

1 From now on, each random variable will be indicated with the tilde.

2 "Complete technical provisions" VB_t indicates the sum of the pure mathematical reserve (expected present value of the benefits net of the expected present value of the premiums) and the expense reserve. Both are calculated on locked and prudential (demographic and financial) bases: hence both demographic and financial bases used are the same as applied in the pricing phase.

3 By "actual financial return rate" we mean the yield obtained by the company, different from the technical rate j^* used in the pricing phase.

4 The rates are calculated on unitary insured sums, so as to be able to distinguish the trends of the main quantities from the monetary amounts of the insured sums.

5 In this context $\tilde{x}_{t+1} = \tilde{z}_t + 1$ for term Insurance and Endowment Policies; $\tilde{x}_{t+1} = 0$ for Pure Endowment policies.

6 The technical bases of the first order are those used in the pricing phase, they are therefore the prudential ones that lead to an expected profit. The second order bases, on the other hand, are the realistic assumptions of the Undertaking: therefore q indicates the best estimate of the probability of death of the individual policyholder while j indicates the best estimate of the return deriving from the investment of premiums and reserves.

7 As is well-known, a Pure Endowment is a policy that, in the face of a single premium or regular (constant) Premiums, entitles to receive a certain insured sum upon maturity, only if the insured is alive on that date. Hence, the best estimate in t is equal to the first part of Equation (17), hence $be_t = {}_{n-t}p_{x+t} \cdot \left[\prod_{h=0}^{n-t-1}(1+i_t(0,h,h+1))\right]^{-1} - \pi \cdot \ddot{a}_{(x+t):(n-t)}$.

8 A Term Insurance is a policy that pays the beneficiary a certain insured sum on a generic policy anniversary t if the policyholder dies in the time span $[t-1, t)$: the best estimate at time t is therefore $\sum_{k=0}^{n-t-1} {}_{k/1}q_{x+t}\left[\prod_{h=0}^{k}(1+i_t(0,h,h+1))\right]^{-1} - \pi \cdot \ddot{a}_{(x+t):(n-t)}$.

9 CV stands for Coefficient of Variation of initial sums insured.

10 λ_t is calculated as $\lambda_t = \dfrac{(q_t^* - q_t)}{q_t}$ and while in the Pure Endowment λ_t was set equal to 15%, using ISTAT2014 entails that when $t = 0$, $\lambda_0 = 24.64\%$, then it increases until $t = 19$, where $\lambda_{19} = 32.34\%$.

11 $\mathbb{E}\left[{}_1\tilde{y}_1^{MCV}\right] = \pi \cdot w_0 \cdot (1+j^*) - \mathbb{E}\left[\tilde{be}_1^{Rf(1),q}\right] \cdot w_0 \cdot {}_1p_{40}$ This formulation is easily obtainable by computing the expected value on Equation (3), when $t = 0$.

12 With an Intel i7 8700K processor (working in parallel—6 Cores, 12 Threads) it requires about 18 min.

13 In all tables, T stands for Theoretical values, i.e., the exact characteristics of the random variables computed using closed formulas.

14 Results are strongly influenced by the risk-free curve used. For instance, using the EIOPA curve for August 2020 we obtain an expected profit in $t = 19$ in Table 4, because of a spot rate equal to 0.69%.

References

Bacinello, Anna Rita. 1986. Portfolio valuation in life insurance. In *Insurance and Risk Theory*. Dordrecht: Springer, pp. 385–99.

Barigou, Karim, Ze Chen, and Jan Dhaene. 2019. Fair dynamic valuation of insurance liabilities: Merging actuarial judgement with market- and time-consistency. *Insurance: Mathematics and Economics* 88: 19–29. [CrossRef]
Bauer, Daniel, and Hongjun Ha. 2015. A least-squares monte carlo approach to the calculation of capital requirements. Paper presented at World Risk and Insurance Economics Congress, Munich, Germany, August 6, pp. 2–6.
Black, Fischer, Emanuel Derman, and William Toy. 1990. A one-factor model of interest rates and its application to treasury bond options. *Financial Analysts Journal* 46: 33–39. [CrossRef]
Boonen, Tim J. 2017. Solvency ii solvency capital requirement for life insurance companies based on expected shortfall. *European Actuarial Journal* 7: 405–34. [CrossRef] [PubMed]
Cox, Samuel H., and Yijia Lin. 2007. Natural hedging of life and annuity mortality risks. *North American Actuarial Journal* 11: 1–15. [CrossRef]
Dahl, Mikkel. 2004. Stochastic mortality in life insurance: Market reserves and mortality-linked insurance contracts. *Insurance: Mathematics and Economics* 35: 113–36. [CrossRef]
Dhaene, Jan, Ben Stassen, Karim Barigou, Daniël Linders, and Ze Chen. 2017. Fair valuation of insurance liabilities: Merging actuarial judgement and market-consistency. *Insurance: Mathematics and Economics* 76: 14–27. [CrossRef]
European Parliament and Council. 2015. *Commission Delegated Regulation (EU) 2015/35*. Strasbourg: European Parliament and Council.
European Parliament and Council. 2021. *Directive 2009/138/EC*. Strasbourg: European Parliament and Council.
Hari, Norbert, Anja De Waegenaere, Bertrand Melenberg, and Theo E. Nijman. 2008. Longevity risk in portfolios of pension annuities. *Insurance: Mathematics and Economics* 42: 505–19. [CrossRef]
Ho, Thomas SY, and Sang-Bin Lee. 1986. Term structure movements and pricing interest rate contingent claims. *The Journal of Finance* 41: 1011–29. [CrossRef]
Olivieri, Annamaria, and Ermanno Pitacco. 2008. Assessing the cost of capital for longevity risk. *Insurance: Mathematics and Economics* 42: 1013–21. [CrossRef]
Pelsser, Antoon, and Mitja Stadje. 2014. Time-consistent and market-consistent evaluations. *Mathematical Finance: An International Journal of Mathematics, Statistics and Financial Economics* 24: 25–65. [CrossRef]
Savelli, Nino. 1993. *Un Modello di Teoria del Rischio per la Valutazione della Solvibilità di una Compagnia di Assicurazioni Sulla Vita*. Rome: LINT.
Savelli, Nino, and Gian Paolo Clemente. 2013. A risk-theory model to assess the capital requirement for mortality and longevity risk. *Journal of Interdisciplinary Mathematics* 16: 397–429. [CrossRef]
Shen, Yang, and Michael Sherris. 2018. Lifetime asset allocation with idiosyncratic and systematic mortality risks. *Scandinavian Actuarial Journal* 2018: 294–327. [CrossRef]
Stevens, Ralph, Anja De Waegenaere, and Bertrand Melenberg. 2010. *Calculating Capital Requirements for Longevity Risk in Life Insurance Products: Using an Internal Model in Line with Solvency II*. Technical Report. Tilburg: Tilburg University.
Vasicek, Oldrich. An equilibrium characterization of the term structure. 1977. *Journal of Financial Economics* 5: 177–88. [CrossRef]

risks

MDPI

Article

Modeling the Future Value Distribution of a Life Insurance Portfolio

Massimo Costabile [1,*,†] and Fabio Viviano [2,3,†]

[1] Department of Economics, Statistics and Finance, University of Calabria, Ponte Bucci Cubo 0 C, 87036 Rende, CS, Italy
[2] Department of Economics and Statistics, University of Udine, Via Tomadini 30/A, 33100 Udine, Italy; viviano.fabio@spes.uniud.it
[3] Department of Economics, Business, Mathematics and Statistics "B. de Finetti", University of Trieste, Piazzale Europa 1, 34127 Trieste, Italy
* Correspondence: massimo.costabile@unical.it
† These authors contributed equally to this work.

Abstract: This paper addresses the problem of approximating the future value distribution of a large and heterogeneous life insurance portfolio which would play a relevant role, for instance, for solvency capital requirement valuations. Based on a metamodel, we first select a subset of *representative policies* in the portfolio. Then, by using Monte Carlo simulations, we obtain a rough estimate of the policies' values at the chosen future date and finally we approximate the distribution of a single policy and of the entire portfolio by means of two different approaches, the ordinary least-squares method and a regression method based on the class of generalized beta distribution of the second kind. Extensive numerical experiments are provided to assess the performance of the proposed models.

Keywords: GB2; LSMC; metamodel; regression models; Solvency II

JEL Classification: G22

Citation: Costabile, Massimo, and Fabio Viviano. 2021. Modelling the Future Value Distribution of a Life Insurance Portfolio. *Risks* 9: 177. https://doi.org/10.3390/risks9100177

Academic Editor: Mercedes Ayuso

Received: 19 August 2021
Accepted: 27 September 2021
Published: 2 October 2021

1. Introduction

In many relevant situations, life insurers face the necessity to determine the distribution of the value of their portfolio of policies at a certain future date. This happens, for example, when regulators need to maintain solvency capital requirements in order to continue to conduct business, as stated in the Solvency II directive or in the Swiss Solvency Test. In particular, Article 101(3) of the European directive requires that the Solvency Capital Requirement "shall correspond to the Value-at-Risk of the basic own funds of an insurance or reinsurance undertaking subject to a confidence level of 99.5% over a one-year period" (see European Parliament and European Council 2009). As a consequence, insurers are obliged to assess the value of assets and liabilities at a future date, the so-called risk horizon, in order to derive their full loss distributions. To achieve this, the relevant risk factors must be projected at the risk horizon and then, conditional on the realized values, a market consistent valuation of the insurer's assets and liabilities is required. This has led insurance and reinsurance companies to face a computationally intensive problem. Indeed, due to the complex structure of the insurer's liabilities, in general, closed form formulas are not available and a straightforward approach, common among insurers, is to obtain an estimate through nested Monte Carlo simulations. Unfortunately, this approach is extremely time consuming and becomes readily unmanageable from a computational point of view. In this regard, one possible alternative method proposed in the literature to reduce the computational effort and to preserve the accuracy of the desired estimates is the Least-Squares Monte Carlo (LSMC) method, firstly introduced by Carrière (1996), Tilley (1993), and Longstaff and Schwartz (2001) in the context of American-type Option Pricing. Application of the LSMC method for valuing solvency capital requirements in the

insurance business was proposed in Cathcart and Morrison (2009) and Bauer et al. (2010). Moreover, Floryszczak et al. (2016) and Krah et al. (2018) illustrate a practical implementation of the LSMC in this particular context. The above-mentioned papers, proposed in the actuarial literature, share the common feature of evaluating capital requirements for a single policy.

In the case of an entire portfolio of policies, the nested simulation approach is even more difficult to implement due to the huge computational effort needed. For instance, assuming 10,000 outer trajectories simulated from the current time to the risk horizon for each one of the v risk factors, and then 2500 inner paths for each outer, with a monthly discretization for 20 years, and considering an insurance portfolio composed of 10,000 contracts, the total number of cash-flow projections needed would be $10{,}000 \times v \times 2500 \times 12 \times 20 \times 10{,}000 = v \times 6 \times 10^{13}$, which is very hard to manage.

In order to keep the computational complexity of the evaluation problem at a reasonable level, we propose a metamodeling approach. Metamodeling, introduced in system engineering (see Barton 2015), can be defined as "the practice of using a model to describe another model as an instance" (see Allemang and Hendler 2011). This approach has also been widely used in the actuarial literature to estimate the price and Greeks of large portfolios of life insurance policies. For instance, Gan (2013) developed a metamodel based on data clustering and machine learning to price large portfolios of variable annuities, while Gan and Lin (2015) tackled a similar problem by developing a functional data approach. In addition, Gan (2015) compares the data clustering approach and Latin hypercube sampling to select representative variable annuities. Finally, Gan and Valdez (2018) proposes a metamodel to estimate partial Greeks of variable annuities with dependence.

In the present paper, the metamodel we propose to approximate the future value distribution of a life insurance portfolio is constructed in different steps:

1. Select a subset of representative policies by means of conditional Latin hypercube sampling;
2. Project the risk factors from the evaluation date to the risk horizon by means of outer simulations;
3. Compute a rough estimate of each representative policy by means of a very limited (say two) number of inner simulations;
4. Create a regression model to approximate the distribution of the value of representative policies;
5. Use the regression model to estimate the future value distribution of the entire portfolio.

We propose two different approaches to develop the regression model in steps 4 and 5. The first approach relies upon the well-established Ordinary Least Squares (OLS) method for approximating the conditional distribution of each representative policy at the risk horizon, and then a second OLS regression is applied to estimate the future value distribution of the entire portfolio. Roughly speaking, we may say that the LSMC method is applied to estimate the distribution of the value of each representative policy at the risk horizon, and then this information is extended to the entire portfolio by means of a simple OLS regression. We call this approach the LSMC method.

The second approach exploits the class of generalized beta of the second kind (GB2) distributions to model the conditional distribution of each representative policy value at the risk horizon and also to estimate the future value distribution of the entire portfolio. We underline that the GB2 regression model has been used in Gan and Valdez (2018) for modeling the fair current market values of guarantees embedded in a large variable annuity portfolio starting from a set of representative policies. Extensive numerical experiments have been conducted in order to assess the performance of the proposed models. The remainder of the paper is structured as follows. Section 2 provides the evaluation framework and Section 3 introduces the metamodeling approach. Section 4 illustrates some numerical results, and finally, in Section 5, conclusions are drawn.

2. The Evaluation Framework

We consider a life insurance portfolio with M contracts underwritten by different policyholders (males and females) of different ages at the inception date $t = 0$. We take into account different types of life insurance policies which differ from each other in terms of maturity, policyholders' ages, and sex. In particular, we consider unit-linked products, term life insurance and immediate life annuities. We assume that the unit-linked product pays, upon reaching maturity, and assuming the survival of the insured, the maximum value between the minimum guaranteed benefit and the value of a specific reference asset. The immediate life annuity is assumed to pay 10% of the level of a given reference asset continuously whilst the insured is alive; finally, the term insurance contract pays the total value of the asset upon the death of the policyholder before maturity. Regarding all the possible policy configurations, see Table 1.

Table 1. This table shows the parameters used to generate the life insurance portfolio.

Feature	Value
Policyholder age	{55, . . ., 65}
Sex	{Male, Female}
Maturity	{10, 15, 20, 25, 30}
Product type	{Unit-linked, Term Insurance, Life Annuity}

Since our task is to approximate the portfolio value distribution at the risk horizon starting from a set of representative policies, we use the Conditional Latin Hypercube Sampling (CLHS) method (see Minasny and McBratney 2006). Indeed, this approach has already been applied to select subsets of representative policies providing reliable results, e.g., see Gan and Valdez (2018). Therefore, in order to select a set of s representative contracts, we apply the CLHS method to the design matrix $\mathbf{X}$, which contains all the features characterizing each specific policy, i.e., types, maturity, sex and age of the policyholder. Note that the categorical variables are treated as dummy variables.

In order to project the cash-flows generated by the contracts over time, we need to simulate the possible evolution of the risk factors. In this regard, we consider a computational framework where mortality, interest rate and the reference asset are taken into account. Despite insurance companies being exposed to systematic and non-systematic mortality risks, in our setting we consider only the first component for computational purposes due to the big dimension of the portfolio that will be considered.

Let $(\Omega, \mathbb{F}, \mathbb{P})$ be a filtered probability space large enough to support a process X in $\mathbb{R}^k$, representing the evolution of financial variables, and a process Y in $\mathbb{R}^d$, representing the evolution of mortality. The filtration $\mathbb{F} = (\mathcal{F}_t)_{t\geq 0}$ represents the flow of information available as time passes by; this includes knowledge of the evolution of all state variables up to each time t and of whether the policyholder has died by then. Specifically, we define $\mathcal{F}_t$ as the σ-algebra generated by $\mathcal{G}_t \cup \mathcal{H}_t$, where

$$\mathcal{G}_t = \sigma(Z_s : 0 \leq s \leq t), \quad \mathcal{H}_t = \sigma\Big(\mathbb{I}_{\{\varsigma \leq s\}} : 0 \leq s \leq t\Big),$$

and where $Z = (X, Y)$ is the joint state variables process in $\mathbb{R}^{k+d}$. Thus, we have $\mathbb{F} = \mathbb{G} \vee \mathbb{H}$, with $\mathbb{G} = \mathbb{G}^X \vee \mathbb{G}^Y$ and with $\mathbb{H} = (\mathcal{H}_t)_{t\geq 0}$ being the smallest filtration with respect to which ς is a stopping time and interpreted as the remaining lifetime of an insured. For more detail of modeling mortality under the intensity-based framework, see Biffis (2005).

Under the physical probability measure, $\mathbb{P}$, we assume that the financial risk factors (reference asset value S, and interest rate r) dynamics are described by the following stochastic differential equations

$$\begin{aligned} dS(t) &= S(t)(r(t) + \lambda)dt + S(t)\sigma_S dW^{1,\mathbb{P}}(t), \\ S(0) &= S_0, \end{aligned} \tag{1}$$

where λ is the risk premium, σ_S is a positive constant, $W^{1,\mathbb{P}}(t)$ is a standard Wiener process, and $r(t)$ is the risk-free interest rate, which is assumed to follow the dynamics

$$\begin{aligned} dr(t) &= \alpha(\theta - r(t))dt + \sigma_r dW^{2,\mathbb{P}}(t), \\ r(0) &= r_0. \end{aligned} \tag{2}$$

Here, $W^{2,\mathbb{P}}(t)$ is a standard Wiener process, and the coefficients α, θ, σ_r are positive constants representing the speed of mean reversion, the long-term interest rate, and the interest rate volatility, respectively. Further, we assume that the two Wiener processes, $W^{1,\mathbb{P}}(t)$ and $W^{2,\mathbb{P}}(t)$, are correlated with the correlation coefficient ρ.

In the absence of arbitrage opportunities, an equivalent martingale measure $\mathbb{Q}$ exists, under which all financial security prices are martingales after deflation by the money market account. We refer the readers to Biffis (2005) for more detail. Under the risk-neutral probability measure, $\mathbb{Q}$, the dynamics in Equations (1) and (2) can be re-written as

$$dS(t) = S(t)r(t)dt + S(t)\sigma_S dW^{1,\mathbb{Q}}(t),$$

and

$$dr(t) = \alpha\Big(\theta - \frac{\sigma_r}{\alpha}\gamma - r(t)\Big)dt + \sigma_r dW^{2,\mathbb{Q}}(t),$$

where γ is the market price of risk. Note that $W^{1,\mathbb{Q}}(t)$ and $W^{2,\mathbb{Q}}(t)$ are two correlated standard Wiener processes with the coefficient of correlation ρ under $\mathbb{Q}$.

Concerning mortality, following Fung et al. (2014), we assume that the force of mortality, $\mu_{x+t}(t)$, under the physical probability measure $\mathbb{P}$ for an individual aged x at time $t = 0$, evolves accordingly to the following one-factor, non-mean-reverting and time-homogeneous affine process:

$$\begin{aligned} d\mu_{x+t}(t) &= [a + b\mu_{x+t}(t)]dt + \sigma_\mu \sqrt{\mu_{x+t}(t)} dW^{3,\mathbb{P}}(t), \\ \mu_x(0) &> 0, \end{aligned} \tag{3}$$

where $a \neq 0, b > 0, \sigma_\mu > 0$ represent the volatility of the mortality intensity and $W^{3,\mathbb{P}}(t)$ is a standard Wiener process which is assumed to be independent with respect to $W^{1,\mathbb{P}}(t)$ and $W^{2,\mathbb{P}}(t)$. As pointed out by Fung et al. (2014), the important advantages of the mortality model defined in Equation (3) are its tractability since analytical expressions are available to evaluate survival probabilities, and also its simplicity since the model dynamics can be easily simulated. Furthermore, this model guarantees that, under specific conditions, the force of mortality is strictly positive (i.e., if $a \geq \sigma_\mu^2/2$).

The dynamics in Equation (3) under $\mathbb{Q}$ can be defined as

$$\begin{aligned} d\mu_{x+t}(t) &= \big[a + (b - \delta\sigma_\mu)\mu_{x+t}(t)\big]dt + \sigma_\mu \sqrt{\mu_{x+t}(t)} dW^{3,\mathbb{Q}}(t), \\ \mu_x(0) &> 0, \end{aligned}$$

where $W^{3,\mathbb{Q}}(t)$ is a standard Wiener process under the risk-neutral measure and δ is the market price of the systematic mortality risk.

Note that the parameters in the stochastic mortality model are estimated by calibrating the implied survival curve to the one obtained from the Italian population data of year 2016

(assumed to be $t = 0$) collected from the Human Mortality Database (see Fung et al. 2014). The calibration procedure was conducted for all policyholder ages and genders reported in Table 1.

Finally, it is worth noting that, due to the flexibility of the methodology that will be proposed, different and/or more complex dynamics to describe the evolution of the risk factors may be assumed with respect to the ones assumed above.

3. Problem and Methodology

Under the framework defined in Section 2, we need to evaluate the streams of payments embedded in each policy inside the insurance portfolio. Before discussing the methodology, let us recall some results provided by Biffis (2005) related to the time-τ fair values of the most common payoffs embedded in typical life insurance products, i.e., survival and death benefits.

Proposition 1. *(Survival benefit.) Let C be a bounded $\mathbb{G}$-adapted process. Then, the time-τ fair value $\mathrm{SB}_\tau(C_T; T)$ of the time-T survival benefit of amount C_T, with $0 \le \tau \le T$, is given by:*

$$SB_\tau(C_T; T) = \mathbb{E}\Big[\mathrm{e}^{-\int_\tau^T r_s \mathrm{d}s}\mathbb{I}_{\{\varsigma > T\}} C_T \mid \mathcal{F}_\tau\Big] = \mathbb{I}_{\{\varsigma>\tau\}}\mathbb{E}\Big[\mathrm{e}^{-\int_\tau^T (r_s+\mu_s)\mathrm{d}s} C_T \mid \mathcal{G}_\tau\Big].$$

In particular, if C is $\mathbb{G}^X$-adapted, the following holds:

$$\mathrm{SB}_\tau(C_T; T) = \mathbb{I}_{\{\varsigma>\tau\}}\mathbb{E}\Big[\mathrm{e}^{-\int_\tau^T r_s \mathrm{d}s} C_T \mid \mathcal{G}^X_\tau\Big]\mathbb{E}\Big[\mathrm{e}^{-\int_\tau^T \mu_s \mathrm{d}s} \mid \mathcal{G}^Y_\tau\Big].$$

Proposition 2. *(Death benefit.) Let C be a bounded $\mathbb{G}-$predictable process. Then, the time-t fair value $\mathrm{DB}_\tau(C_\varsigma; T)$ of the death benefit of amount C_ς, payable in case the insured dies before time T, with $0 \le \tau \le T$, is given by*

$$\mathrm{DB}_\tau(C_\varsigma; T) = \mathbb{E}\Big[\mathrm{e}^{-\int_\tau^\varsigma r_s \mathrm{d}s} C_\varsigma \mathbb{I}_{\{\tau<\varsigma\le T\}} \mid \mathcal{F}_\tau\Big] = \mathbb{I}_{\{\varsigma>\tau\}}\int_\tau^T \mathbb{E}\Big[\mathrm{e}^{-\int_\tau^u (r_s+\mu_s)\mathrm{d}s}\mu_u C_u \mid \mathcal{G}_\tau\Big]\mathrm{d}u.$$

In particular, if C is $\mathbb{G}^X$-predictable, the following holds

$$\mathrm{DB}_\tau(C_\varsigma; T) = \mathbb{I}_{\{\varsigma>\tau\}}\int_\tau^T \mathbb{E}\Big[\mathrm{e}^{-\int_\tau^u r_s \mathrm{d}s} C_u \mid \mathcal{G}^X_\tau\Big]\mathbb{E}\Big[\mathrm{e}^{-\int_\tau^u \mu_s \mathrm{d}s}\mu_u \mid \mathcal{G}^Y_\tau\Big]\mathrm{d}u.$$

We refer the readers to Biffis (2005) for the corresponding proofs and further details. Therefore, as we can see from Propositions 1 and 2, evaluating life insurance policies at future times implies solving conditional expectations for which often analytical formulas do not exist. Due to this, simulation-based approaches are extensively used (see Boyer and Stentoft 2013), among which we mention the nested simulations method where a high number of inner simulations branch out from another huge set of outer scenarios. However, the simulations within simulations approach is computationally challenging, especially when several policies are considered, as in our case. Therefore, in the following, we are going to discuss two methodologies to evaluate the streams of payments embedded in each policy inside the insurance portfolio. For this purpose, we project the relevant risk factors affecting the policy (i.e., S, r, and μ) under the physical probability measure from time $t = 0$ up to the risk horizon τ, and then for each outer scenario another set of inner trajectories is simulated under the risk-neutral measure.

In order to avoid the huge computational cost of a pure nested model, as in the LSMC approach, we simulate n possible outer trajectories of the risk factors and then for each of them we further simulate $\bar{n} \ll n$ inner paths. Following this approach, let $\mathbf{Z}^i$ be an $n \times v$ matrix, where the row vector $\mathbf{z}^i_k$ contains the kth outer scenario of the v risk factors affecting the value of the ith representative policy. For each vector $\mathbf{z}^i_k$ and for time $\tau < t \le T$, we simulate $\bar{n}$ trajectories under the risk-neutral probability measure. To simplify the notation,

we focus on the ith representative policy, and we denote $\mathbf{z}_{j,t}^{k}$ the vector containing the time-t values of the risk factors along the jth inner trajectory corresponding to the kth outer scenario. Moreover, we label $\mathbf{Y}$ a $n \times s$ matrix where the element y_{ik} represents the value of the ith policy corresponding to the kth outer scenario obtained by averaging across the few inner simulations. Formally,

$$y_{ik} = \frac{1}{\bar{n}} \sum_{j=1}^{\bar{n}} \sum_{\tau < t \leq T_i} \Phi_t^i \left(\mathbf{z}_{j,t}^{k} \right) \quad i = 1, \ldots, s, \text{ and } k = 1, \ldots, n, \tag{4}$$

where $\Phi_t^i(\cdot)$s represent the discounted cash-flows at time t of the ith policy with maturity T_i.

In this way, we obtain a first (rough) estimate of each representative policy value distribution at the future time τ. The next step is to obtain a more accurate estimate of the distribution of the time-τ value of each representative policy and then to infer the distribution of the time-τ value of the entire portfolio. We achieve this by applying two different approaches, an OLS as in the least-squares Monte Carlo method and a GB2 model.

3.1. The LSMC Method

The least-squares Monte Carlo method applied to the problem of computing the distribution of the insurer's liabilities at a certain future date is based on the idea that the bias deriving from the few inner simulations can be reduced by approximating the involved conditional expectations with a linear combination of basis functions depending on some covariates, whose coefficients are estimated through an ordinary least-squares procedure (see Bauer et al. 2010 for further details).

A straightforward application of the LSMC approach would be to apply the method on each policy inside the insurance portfolio. However, this kind of strategy would be quite computationally expensive due to the big dimensions of an insurance portfolio. Due to this, we propose applying the LSMC method first on just a set of representative policies and then through an OLS regression extend it to the entire portfolio.

Hence, according to the LSMC method, we assume that the conditional ith representative policy value, $\widehat{y}_{ik}$, can be expressed as a linear combination of basis functions depending on the covariate matrix $\mathbf{z}_k^i$ as follows:

$$\widehat{y}_{ik} = \sum_{j=1}^{L} \hat{\beta}_j^i e_j \left(\mathbf{z}_k^i \right) \qquad i = 1, \ldots, s \text{ and } k = 1, \ldots, n, \tag{5}$$

where $e_j(\cdot)$ is the jth basis function in the regression, L is the number of basis functions, and $\hat{\beta}_j^i$s represent the coefficients estimated through

$$\left(\hat{\beta}_1^i, \ldots, \hat{\beta}_L^i \right) = \underset{\beta_1, \ldots, \beta_L}{\operatorname{argmin}} \left[\sum_{k=1}^{n} \left(y_{ik} - \sum_{j=1}^{L} \beta_j^i e_j \left(\mathbf{z}_k^i \right) \right)^2 \right].$$

In this way, we obtain an $n \times s$ matrix $\widehat{\mathbf{Y}}$ where each row vector $\widehat{\mathbf{y}}_k$ contains the values of each representative policy corresponding to the kth outer scenario.

Now, in order to approximate the distribution of the value of the entire portfolio, we construct an OLS regression model for each outer scenario. In this regard, we denote with $\mathbf{X}$ an $M \times (w+1)$ matrix, where the row vector $\mathbf{x}_i$ contains the w covariates (*gender, product type, age, and maturity*) characterizing the ith contract in the portfolio plus an intercept term (M is the total number of contracts inside the insurance portfolio). Moreover, let $\bar{\mathbf{X}}$ be the $s \times (w+1)$ matrix describing the structure of the representative insurance portfolio. Hence, $\bar{\mathbf{x}}_i$ contains the w covariates characterizing the ith representative contract plus an intercept term.

Therefore, we regress each row vector $\widehat{\mathbf{y}}_k$ ($k = 1, \ldots, n$) on the covariate matrix $\bar{\mathbf{X}}$, and once the coefficients are estimated, we extend them to the remaining policies by

exploiting the matrix $\mathbf{X}$. In this way, we obtain the value of the ith contract corresponding to the kth outer scenario, which is denoted by $\widehat{v}_{ik}$. Formally,

$$\widehat{v}_{ik} = \mathbf{x}_i \hat{\boldsymbol{\beta}}_k' \qquad i = 1, \ldots, M \text{ and } k = 1, \ldots, n, \tag{6}$$

where

$$\hat{\boldsymbol{\beta}}_k' = \left(\bar{\mathbf{X}}'\bar{\mathbf{X}}\right)^{-1}\bar{\mathbf{X}}'\bar{\mathbf{y}}_k'.$$

Finally, the entire portfolio value distribution is obtained by adding up all the policy values in Equation (6) corresponding to each outer scenario.

3.2. The GB2 Model

A GB2 model appears to provide a flexible family of distributions as it nests a range of standard distributions as special or limiting cases, such as the log-normal, the generalized-gamma, the Burr type III, the Burr type XII and many other (see McDonald 1984). Moreover, it has been used in several actuarial applications (e.g., see Gan and Valdez 2018) to model the fair market value of a portfolio made up of life insurance policies. A GB2 random variable can be constructed from a transformed ratio of two gamma random variables. The density function of a GB2 random variable, Y, is given by

$$f(y) = \frac{|a|}{bB(p,q)}\left(\frac{y}{b}\right)^{ap-1}\left[1+\left(\frac{y}{b}\right)^{a}\right]^{-p-q}, \quad y > 0, \tag{7}$$

where $a \neq 0, p > 0, q > 0$ are shape parameters, $b > 0$ is the scale parameter, $B(\cdot)$ is the Beta function, and its expectation equals:

$$\mathbb{E}[Y] = b \cdot \frac{B\left(p+\frac{1}{a}, q-\frac{1}{a}\right)}{B(p,q)}, \tag{8}$$

which exists if $-p < \frac{1}{a} < q$.

In order to approximate the value of the portfolio, at first we approximate the time-τ value of each representative policy, and then we use this information to approximate the distribution of the value of the entire insurance portfolio at the risk horizon. To achieve this, we construct two different GB2 regression models which exploit the generated information at the risk horizon $\big($i.e. $S(\tau), r(\tau),$ and $\mu(\tau)\big)$, and then the features characterizing uniquely each policy, respectively.

Specifically, since the policy values y_{ik} obtained from Equation (4) are not accurate due to the few inner trajectories on which they are based on, we aim at reducing the bias by estimating the involved conditional expectation through a GB2 regression model. In this regard, we assume that the ith policy value at time τ conditioned on a specific outer scenario is a GB2 random variable with parameters (a_i, p_i, q_i, b_i). In particular, we make the $b-$ parameter depend on some independent covariates (i.e., the value at time τ of the risk factors which affect the policy of interest). Note that several approaches to incorporate covariates in the GB2 regression model exist as well as different re-parametrization (see Beirlant et al. 2004; Frees and Valdez 2008). However, as noticed by Sun et al. (2008) and Frees et al. (2016), incorporating them into the scale parameter, b, facilitates the interpretability of the model; indeed, as can be seen in Equation (8), the expectation will change proportionally with respect to b, allowing one to interpret the regression coefficients as proportional changes.

Hence, $b\left(\mathbf{Z}^i\right) = \exp\left(\mathbf{Z}^i\boldsymbol{\beta}_i'\right)$, where $\boldsymbol{\beta}_i = (\beta_{i;0}, \beta_{i;1}, \ldots, \beta_{i;v})$ are the corresponding coefficients attached to each risk-factor. Note that the matrix $\mathbf{Z}^i$ now includes an intercept term.

We can use the maximum likelihood method to estimate the parameters. Since we incorporate covariates through the scale parameter, we can write the log-likelihood function of the model as

$$l(a_i, p_i, q_i, \boldsymbol{\beta}_i) = n \ln \frac{|a_i|}{B(p_i, q_i)} - a_i p_i \sum_{k=1}^{n} \mathbf{z}_k^i \boldsymbol{\beta}_i' + (a_i p_i - 1) \sum_{k=1}^{n} \ln(y_{ik}) - (p_i + q_i) \sum_{k=1}^{n} \ln \left[1 + \left(\frac{y_{ik}}{\exp(\mathbf{z}_k^i \boldsymbol{\beta}_i')} \right)^{a_i} \right], \quad (9)$$

where $i = 1,\ldots s$, n is the number of the generated outer scenarios and y_{ik} denotes the value of the ith policy corresponding to the kth outer scenario.

Once we estimate the parameters for the GB2 model, we use the expectation for predicting the value of the policy at time τ. Since we incorporate covariates through the scale parameter, we can estimate it as

$$\widehat{y}_{ik} = \frac{\exp\left(\mathbf{z}_k^i \widehat{\boldsymbol{\beta}}_i'\right) B\left(\hat{p}_i + \frac{1}{\hat{a}_i}, \hat{q}_i - \frac{1}{\hat{a}_i}\right)}{B(\hat{p}_i, \hat{q}_i)}, \quad i = 1, 2, \ldots, s \text{ and } k = 1, \ldots, n, \quad (10)$$

where $\mathbf{z}_k^i$ is the vector containing the kth outer scenario of the risk factors affecting the ith representative policy.

Once we obtain an estimate of the distribution of each representative policy at time τ, we extend this information to the remaining policies. As already carried out for the OLS model, we are going to exploit both the matrices $\bar{\mathbf{X}}$ and $\mathbf{X}$ on which we now construct a new GB2 regression model.

Therefore, let $\widehat{\mathbf{Y}}$ be the $n \times s$ matrix whose elements $\widehat{y}_{ik}$ denote the value of the ith representative policy corresponding to the kth outer scenario obtained through Equation (10).

Now, we construct a GB2 regression model in order to infer, starting from the set of representative policies, the distribution of the entire portfolio. Hence, recalling the pdf defined in Equation (7), we define the following log-likelihood function as:

$$l(a_k, p_k, q_k, \boldsymbol{\beta}_k) = s \ln \frac{|a_k|}{B(p_k, q_k)} - a_k p_k \sum_{i=1}^{s} \bar{\mathbf{x}}_i \boldsymbol{\beta}_k' + (a_k p_k - 1) \sum_{i=1}^{s} \ln(\widehat{y}_{ik}) - (p_k + q_k) \sum_{i=1}^{s} \ln \left[1 + \left(\frac{\widehat{y}_{ik}}{\exp(\bar{\mathbf{x}}_i \boldsymbol{\beta}_k')} \right)^{a_k} \right], \quad (11)$$

where s is the number of the representative policies and $\bar{\mathbf{x}}_i$ is the row vector containing the information of the ith representative contract.

Once again, after we estimate the parameters through the maximum likelihood approach, we can then derive the distribution at the risk horizon for all the policies inside the insurance portfolio as

$$\widehat{v}_{ik} = \frac{\exp\left(\mathbf{x}_i \widehat{\boldsymbol{\beta}}_k'\right) B\left(\hat{p}_k + \frac{1}{\hat{a}_k}, \hat{q}_k - \frac{1}{\hat{a}_k}\right)}{B(\hat{p}_k, \hat{q}_k)}, \quad i = 1, 2, \ldots, M \text{ and } k = 1, \ldots, n, \quad (12)$$

where $\widehat{v}_{ik}$ is the value of the ith contract corresponding to the kth outer scenario.

Finally, the entire portfolio value distribution is again obtained by adding up all the policy values corresponding to each outer scenario.

Note that the log-likelihood functions in Equations (9) and (11) may have multiple local maxima and since an analytic solution does not exist, we need to rely on a numerical procedure to estimate the involved parameters. We adopt the same multistage optimization algorithm described in Gan and Valdez (2018).

4. Numerical Results

In this section, we present some numerical results obtained by exploiting the previously defined models. In particular, we consider a life insurance portfolio with M = 10,000 contracts, and we focus on approximating its value distribution at the future time $\tau = 1$ year. These policies can be of three different types: a unit-linked pure endowment contract with a minimum maturity guarantee $G = 100$ payable upon the survival of the policyholder at the maturity date T, term life insurance policy which pays the value of a reference asset in case of death before maturity T, and an immediate life annuity contract

with continuous survival benefits equal to the 10% of a reference asset value up to the entire life of the insured person. We consider different policyholders, both males and females, with different ages x at time $t = 0$, which is also assumed to be the inception time of each policy. These characteristics are reported in Table 1. We assume that the insurance benefits depend upon a reference asset with the initial value S_0.

In Tables A1 and A2 given in Appendix A, we report the values of the involved parameters in Equations (1)–(3). In particular, concerning mortality, we have calibrated the survival curve implied by Equation (3) on the Italian males and females mortality data in the year 2016 obtained from the Human Mortality Database for each age $x \in \{55, \ldots, 65\}$, and we assumed a longevity risk premium $\delta = 0$.

We conduct this numerical experiment by varying both the number of outer simulations, n, and the number of representative policies, s. In particular, we adopt a monthly Euler's discretization setting in order to project $n \in \{1000, 5000, 10000\}$ outer trajectories of each risk factor under the $\mathbb{P}$-measure, and then for each outer scenario we further simulate $\bar{n} = 2$ inner trajectories under the risk-neutral probability measure. With this simulation set, we are able to obtain a first rough estimate of $\mathbf{Y}$ on which we construct the LSMC and GB2 models discussed in Sections 3.1 and 3.2, respectively. Note that, concerning the LSMC method, we exploit as basis functions Hermite polynomials of orders 1 and 2, which are denoted, respectively, as LSMC_1 and LSMC_2 hereafter.

To determine the number of representative contracts s, we start from the informal rule proposed by Loeppky et al. (2009), which provide reasons and evidence supporting that the sample size should be about 10 times the input dimension. In our case, the dimension of covariates in the design matrix $\mathbf{X}$ is 5 (including the binary dummy variables converted from the categorical variables), and so we choose $s = 50$ as the initial number of representative contracts. However, we investigate the models' performances by setting $s = 75$ and $s = 100$.

Finally, the results are compared with a solid benchmark obtained through a nested simulations approach based on 10,000 $\times$ 2500 simulations. This allows us to conclude on the reliability of the proposed methodologies and to compare them in terms of computational demand.

Figure 1 shows the Quantile-Quantile (Q-Q) plots of the portfolio value at time $\tau = 1$ obtained by the nested simulations algorithm (assumed to be the theoretical one) and those predicted by the GB2 regression model and the LSMC models based on n = 10,000 outer simulations and by varying the number of representative contracts $s \in \{50, 75, 100\}$. In this regard, we can see from Figure 1 that the proposed methodologies provide a good approximation except for the right tail of the distribution. In particular, concerning the GB2 regression model, we can see that the higher the number of representative contracts, the better the approximation.

For a comprehensive analysis, we perform multiple runs of each proposed method; in particular, the following analysis is based on 50 runs.

In Tables 2–4, we report the Mean Absolute Percentage Error (MAPE) relative to different quantities obtained by performing 50 runs of the proposed methodologies with a fixed number of outer scenarios (n = 10,000) and by varying the number of representative contracts ($s \in \{50, 75, 100\}$).

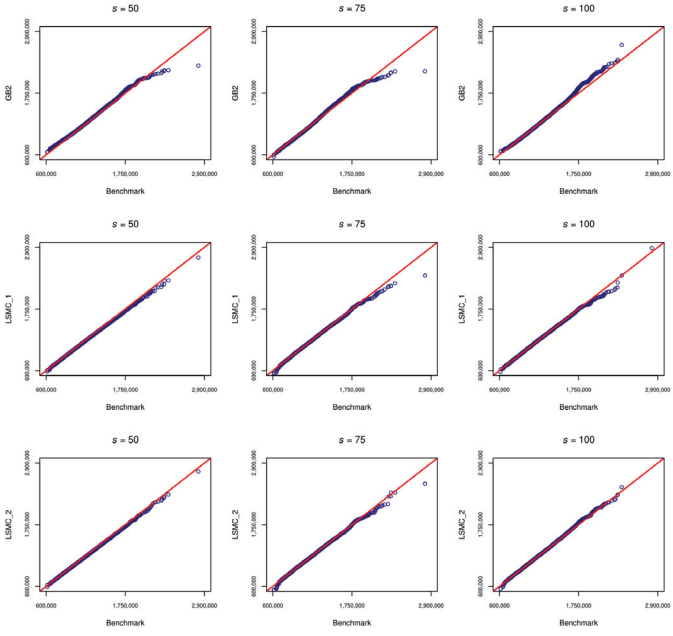

Figure 1. Q-Q plots relative to the future value distribution of the insurance portfolio. The theoretical distribution is assumed to be the one obtained by nested simulations based on 10,000 $\times$ 2500 trajectories. The first row refers to the GB2 regression model based on 10,000 outer scenarios and by varying the number of representative contracts, $s \in \{50, 75, 100\}$. The second and third rows refer to the LSMC method with Hermite polynomials of orders 1 and 2 based on 10,000 outer scenarios and by varying the number of representative contracts, $s \in \{50, 75, 100\}$.

Table 2. This table reports the MAPE of the estimates obtained by running 50 times the GB2 and LSMC methods with n = 10,000 and $s = 50$. The benchmark values are based on a nested simulations algorithm with 10,000 $\times$2500 trajectories applied to the entire portfolio.

	5th Perc.	10th Perc.	Median	Mean	90th Perc.	95th Perc.	99th Perc.	99.5th Perc.
GB2	2.812%	2.180%	1.798%	2.594%	3.832%	4.016%	6.154%	4.375%
LSMC_1	3.238%	3.000%	2.399%	2.557%	2.398%	2.174%	2.436%	2.722%
LSMC_2	2.762%	2.754%	2.567%	2.557%	2.436%	2.114%	2.356%	2.841%

Table 3. This table reports the MAPE of the estimates obtained by running 50 times the GB2 and LSMC methods with n = 10,000 and $s = 75$. The benchmark values are based on a nested simulations algorithm with 10,000 $\times$ 2500 trajectories applied to the entire portfolio.

	5th Perc.	10th Perc.	Median	Mean	90th Perc.	95th Perc.	99th Perc.	99.5th Perc.
GB2	1.971%	1.782%	0.806%	0.542%	3.605%	3.949%	6.094%	3.867%
LSMC_1	2.500%	1.338%	1.530%	1.392%	1.251%	1.657%	0.941%	1.678%
LSMC_2	1.828%	1.047%	1.756%	1.392%	1.307%	1.485%	1.842%	2.142%

Table 4. This table reports the MAPE of the estimates obtained by running 50 times the GB2 and LSMC methods with n = 10,000 and $s = 100$. The benchmark values are based on a nested simulations algorithm with 10,000 × 2500 trajectories applied to the entire portfolio.

	5th Perc.	10th Perc.	Median	Mean	90th Perc.	95th Perc.	99th Perc.	99.5th Perc.
GB2	1.986%	1.745%	0.519%	0.347%	1.129%	1.313%	2.856%	1.944%
LSMC_1	1.629%	1.504%	0.440%	0.627%	0.764%	0.824%	0.958%	2.561%
LSMC_2	1.148%	1.145%	0.578%	0.627%	0.762%	0.986%	2.101%	2.334%

If we compare Tables 2–4, it is evident that increasing the number of representative contracts s leads to a better approximation of the mean and of the other considered measures of position. Moreover, it seems that the GB2 model, at least for a low number of representative contracts, is not able to adequately model the right tail of the distribution.

In Table 5, we report the Mean Percentage Error (MPE) and MAPE relative to the mean estimates obtained by running the GB2 and LSMC methods 50 times with different numbers of outer simulations, n, and representative contracts, s.

Table 5. This table reports the MPE and MAPE of the mean estimates obtained by running 50 times the GB2 and LSMC methods and varying the number of outer simulations (Outer) and that of representative contracts s. The benchmark value is based on a nested simulations algorithm with 10,000 × 2500 trajectories applied to the entire portfolio.

		s = 50		s = 75		s = 100	
Outer	**Method**	**MPE**	**MAPE**	**MPE**	**MAPE**	**MPE**	**MAPE**
1000	GB2	3.612%	3.612%	0.163%	0.983%	−0.240%	0.923%
	LSMC_1	−3.475%	3.475%	−2.104%	2.221%	−1.017%	1.364%
	LSMC_2	−3.475%	3.475%	−2.104%	2.221%	−1.017%	1.364%
5000	GB2	2.981%	2.981%	0.715%	0.747%	−0.301%	0.474%
	LSMC_1	−2.840%	2.840%	−1.533%	1.533%	−1.029%	1.092%
	LSMC_2	−2.840%	2.840%	−1.533%	1.533%	−1.029%	1.092%
10,000	GB2	2.594%	2.594%	0.491%	0.542%	0.179%	0.347%
	LSMC_1	−2.557%	2.557%	−1.392%	1.392%	−0.490%	0.627%
	LSMC_2	−2.557%	2.557%	−1.392%	1.392%	−0.490%	0.627%

Looking at Table 5, we can see that for a fixed number of outer scenarios and for each applied method, the accuracy of the mean estimates increases with the number of representative contracts s. Moreover, it is evident that in most of the considered configurations, the GB2 model outperforms the LSMC methods. Furthermore, if we look at the last column of Table 5 ($s = 100$), for instance, we can see that the higher the number of outer scenarios, the better the approximation. Finally, we can see that increasing the number of basis functions up to degree two in the LSMC method does not improve the accuracy of the mean estimates. This is probably due to the few outer simulated trajectories (at most 10,000 paths), which is not sufficient to appreciate the improvement which is usually expected. In the left-hand side of Figure A1 given in Appendix B, we report the corresponding box-plots from which it is possible to see that, in each of the considered configurations, the LSMC method systematically underestimates the quantity of interest.

Concerning the estimate of the 99.5th percentile of the distribution, which would be of interest for valuing solvency capital requirements, Table 6 reports the MPE and MAPE relative to 50 estimates obtained by varying both the number of simulations and the number of representative contracts.

Table 6. This table reports the MPE and MAPE of the 99.5th percentile estimates obtained by running the GB2 and LSMC methods 50 times and varying the number of outer simulations (Outer) and that of representative contracts s. The benchmark value is based on a nested simulations algorithm with 10,000 × 2500 trajectories applied to the entire portfolio.

		s = 50		s = 75		s = 100	
Outer	**Method**	**MPE**	**MAPE**	**MPE**	**MAPE**	**MPE**	**MAPE**
1000	GB2	3.936%	6.570%	−1.512%	5.453%	1.410%	4.494%
	LSMC_1	−2.664%	3.715%	−6.308%	6.478%	−2.961%	4.253%
	LSMC_2	−0.252%	6.487%	−4.211%	7.150%	−1.438%	5.517%
5000	GB2	4.110%	4.723%	3.813%	4.018%	0.081%	2.653%
	LSMC	−2.908%	3.001%	−4.708%	4.722%	−1.659%	2.006%
	LSMC_2	−1.787%	3.484%	−3.118%	4.017%	−0.462%	3.110%
10,000	GB2	4.157%	4.375%	3.737%	3.867%	0.421%	1.944%
	LSMC_1	−2.643%	2.722%	−1.560%	1.678%	−2.522%	2.561%
	LSMC_2	−2.259%	2.841%	−0.131%	2.142%	−1.007%	2.334%

From Table 6, we can detect a similar behaviour as the one previously discussed. Specifically, we can see that, concerning the GB2 model, an increase in the number of representative contracts (for fixed n) leads to an improvement of the resulting estimates. On the contrary, for the LSMC method, there is no clear pattern. Indeed, as we can see, increasing the number of representative contracts (for a fixed n) does not lead to a clear improvement in the results. Moreover, increasing the number of basis functions as well as the number of outer simulations does not increase the accuracy of the estimates (see also the right side of Figure A1 in Appendix B). As in the case of the mean estimate, this could be due to the small number of outer simulations, and so we may conclude that passing from 1000 to 10,000 trajectories is still not sufficient to exploit more basis functions. Once again, if we look at the case of n = 10,000 and s = 100, the GB2 model outperforms the LSMC approach.

Now, let us examine the speed of the proposed algorithms with respect to the benchmark. Table 7 shows the runtime of GB2 and LSMC expressed as a percentage of the time required by the nested simulation method based on 10,000 outers and 2500 inners. Note that we conducted all experiments using `R` on a computer equipped with an Intel® Core(TM) i7-1065G7 CPU 1.50 GHz processor with 12 GB of RAM and Windows 10 Home operating system.

Table 7. Percentage of the runtime required by the GB2 and LSMC methods with respect to the nested simulations approach. Note that the computational demand to construct the benchmark with a nested simulations approach based on 10,000 × 2500 scenarios applied to the entire portfolio is about 187,200 s.

Method	n = 1000			n = 5000			n = 10,000		
	s = 50	s = 75	s = 100	s = 50	s = 75	s = 100	s = 50	s = 75	s = 100
GB2	0.069%	0.078%	0.098%	0.337%	0.380%	0.501%	0.660%	0.832%	1.021%
LSMC_1	0.005%	0.006%	0.007%	0.012%	0.018%	0.019%	0.036%	0.045%	0.047%
LSMC_2	0.005%	0.006%	0.007%	0.013%	0.019%	0.020%	0.037%	0.046%	0.047%

As we can see from Table 7, by applying the proposed methodologies, we have drastically reduced the computational time required instead by a nested simulations approach. Moreover, as expected, the LSMC method presented in Section 3.1 outperforms the GB2 model in terms of time in each of the proposed configurations. However, this is due to the existence of a closed form formula for the estimation of the involved parameters. Indeed, as stated in Section 3.2, the estimation procedure for the GB2 model is based on a multistage optimization algorithm due to the complexity of the likelihood functions, which

may have multiple local maxima. Regardless, if compared with the simulations within simulations method, the GB2 model proved to be an accurate and efficient alternative.

Full LSMC

To provide an exhaustive analysis, we consider a straightforward application of the LSMC method. Hence, we apply the LSMC method on each contract composing the insurance portfolio without considering any set of representative policies. The results are then compared with those already shown in the previous section both in terms of accuracy and computational demand. Just as an example, we construct the LSMC model by exploiting as set of basis functions Hermite polynomials with order 1 based on 10,000 $\times$ 2 simulations (LSMC_Full). Table 8 reports the MPE and MAPE relative to the 5th-percentile, the mean, and the 99.5th percentile estimates obtained by performing 50 runs of the proposed methods. Further, we report the results relative to the GB2 model (GB2) and LSMC method with Hermite polynomials of order 1 (LSMC_1) and order 2 (LSMC_2) based on 10,000 $\times$ 2 simulations and $s = 100$ representative policies.

Table 8. This table reports the MPE and MAPE relative to the 5th percentile, the mean, and the 99.5th percentile estimates obtained by applying different methodologies. GB2 stands for the GB2 regression model based on n = 10,000 outer scenarios and $s = 100$ representative policies; LSMC_1 refers to the LSMC method based on n = 10,000 outer scenarios and $s = 100$ representative policies with Hermite polynomials of order 1; LSMC_2 refers to the LSMC method based on n = 10,000 outer scenarios and $s = 100$ representative policies with Hermite polynomials of order 2; LSMC_Full refers to the LSMC method based on n = 10,000 outer scenarios and constructed on each contract in the insurance portfolio. The results are compared with the corresponding benchmark value based on nested simulations with 10000 $\times$ 2500 trajectories applied to the entire portfolio.

Method	5th Perc.		Mean		99.5th Perc.	
	MPE	MAPE	MPE	MAPE	MPE	MAPE
GB2	−1.986%	1.986%	0.179%	0.347%	0.421%	1.944%
LSMC_1	−1.472%	1.629%	−0.490%	0.627%	−2.522%	2.561%
LSMC_2	−0.742%	1.148%	−0.490%	0.627%	−1.007%	2.334%
LSMC_Full	−0.501%	1.032%	−0.084%	0.461%	−0.420%	1.070%

As is shown in Table 8, the errors relative to the LSMC_Full approach are lower than those of the other proposed methods since the estimates are based on the entire insurance portfolio, i.e., this approach does not suffer of any uncertainty related to the missingness of policies in its estimation procedure. Figure A2 given in Appendix B reports the box-plots on which the quantities in Table 8 are based on.

Finally, we compare these methods in terms of time. In Table 9, we report the computational time required by the algorithms. We can see that the naive application of the LSMC approach is more computationally expensive with respect to the GB2 and LSMC models based on a set of representative policies.

Table 9. Runtime, in seconds, of GB2 model and LSMC methods based on 10,000 $\times$ 2 simulations and $s = 100$ representative contracts (GB2, LSMC_1, LSMC_2). LSMC_Full refers to the LSMC method applied to each contract in the insurance portfolio.

Method	Time
GB2	1911.445
LSMC_1	87.824
LSMC_2	88.290
LSMC_Full	7847.960

5. Conclusions

In this paper, we addressed the problem of approximating the value of a life insurance portfolio at a future time by proposing two different methodologies able to avoid the time-consuming nested simulations approach. The first approach can be thought of as extension of the well-known LSMC method, while the second is based on the GB2 distribution, which is widely used to approximate the fair value of portfolios of life insurance policies. To validate the proposal, we have considered a solid benchmark obtained by nested simulations, and we compared the two proposed methodologies both in terms of accuracy and efficiency. The analysis has been carried out by considering an ever increasing number of simulations and representative policies, from which it turned out that, generally, both the methodologies are able to provide increasingly accurate results. Moreover, the LSMC method proved to be faster in computational terms but also less accurate than the GB2 model. Furthermore, the proposed methodologies have been compared with a straightforward application of the LSMC method (i.e., without considering any subset of representative policies), which turned out to be more accurate but computationally more expensive.

Extensive numerical results have shown that the proposed methods represent viable alternatives to the full nested Monte Carlo model. Therefore, the proposed metamodeling approach may help insurance and reinsurance undertakings to reduce the computational budget needed, for instance, in the context of evaluating solvency capital requirements. In this regard, it can be used to evaluate the future cash-flows (inflows and outflows) generated by the entire portfolio by considering at first only a subset of policies, and then extend to the remaining ones. Indeed, this represents the main issue for deriving the full loss distribution on which the Value-at-Risk measure should be obtained, as prescribed by the European Solvency II directive.

Author Contributions: Both authors contributed equally to this manuscript. Both authors have read and agreed to the published version of the manuscript.

Funding: This research received no external funding.

Conflicts of Interest: The authors declare no conflict of interest.

Appendix A. Parameter Values

Table A1 shows the parameter values assumed for the dynamics of the reference asset and interest rates defined in Equations (1) and (2).

Table A1. Parameters of the reference asset value process, S, and interest rate stochastic process, r.

S_0	σ_S	λ	r_0	α	θ	σ_r	γ	ρ
100	0.20	0.00	0.04	0.10	0.02	0.02	0.00	0.00

Table A2 shows the estimated parameters of the mortality model defined in Equation (3) obtained by fitting the corresponding survival curve on that implied by the Italian males and females mortality data in year 2016 obtained from the Human Mortality Database for each age $x \in \{55, \ldots, 65\}$.

Table A2. Estimated parameters of the stochastic mortality model for Italian male (left) and female (right) aged $x \in \{55, \ldots, 65\}$ in 2016.

Age	Male			Female		
	$\hat{a}$	$\hat{b}$	$\hat{\sigma}_\mu$	$\hat{a}$	$\hat{b}$	$\hat{\sigma}_\mu$
55	0.00040	0.0881	0.00157	0.00010	0.10017	0.00100
56	0.00700	0.0705	0.00262	0.00001	0.11110	0.00100
57	0.00001	0.1051	0.00100	0.00001	0.11060	0.00100
58	0.00001	0.1045	0.00390	0.00009	0.10740	0.00850
59	0.00040	0.0832	0.00100	0.00001	0.11570	0.00100
60	0.00060	0.0743	0.00100	0.00042	0.08362	0.00669
61	0.00030	0.0907	0.00100	0.00044	0.08505	0.00100
62	0.00010	0.1033	0.00710	0.00001	0.11990	0.00100
63	0.00012	0.1063	0.00750	0.00040	0.09704	0.00182
64	0.00008	0.1112	0.00810	0.00039	0.09860	0.00376
65	0.00020	0.1075	0.00123	0.00049	0.09558	0.00720

Appendix B. Further Results

Figure A1 reports the boxplot relative to the mean (left) and the 99.5th percentile (right) estimates obtained by running 50 times the GB2 and LSMC methods varying both the number of outer scenarios, n, and that of the representative policies, s. In this regard, we can see that the variability of the estimates decreases as the number of outer scenarios and the number of representative contracts increases.

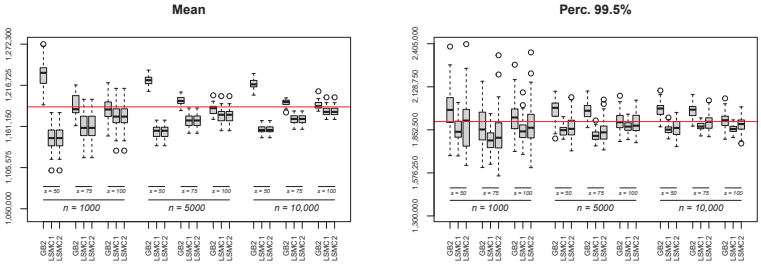

Figure A1. Boxplots relative to the mean (**left**) and the 99.5th percentile (**right**) estimates obtained by running the GB2 and LSMC methods 50 times and varying the number of outer simulations n and that of representative contracts s. The red line refers to the benchmark value based on a nested simulations algorithm with 10,000 $\times$ 2500 trajectories applied to the entire portfolio.

Figure A2 compares the straightforward application of the LSMC approach with respect to the proposed methodologies providing the boxplots relative to the mean and the 99.5th percentile estimates.

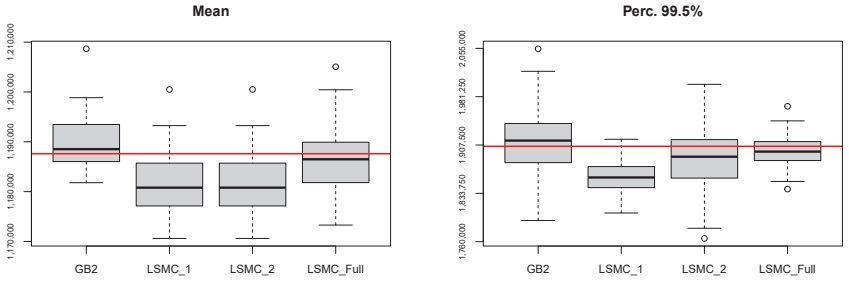

Figure A2. Boxplots relative to the mean and the 99.5th percentile estimates obtained by running the proposed methodologies 50 times. GB2 stands for the GB2 regression model based on 10,000 outer scenarios and $s = 100$ representative policies; LSMC_1 refers to the LSMC method based on 10,000 outer scenarios and $s = 100$ representative policies with Hermite polynomials of order 1; LSMC_2 refers to the LSMC method based on 10,000 outer scenarios and $s = 100$ representative policies with Hermite polynomials of order 2; LSMC_Full refers to the LSMC method based on 10,000 outer scenarios and constructed on each contract in the insurance portfolio. The red line refers to the benchmark value based on a nested simulations algorithm with $10{,}000 \times 2500$ trajectories applied to the entire portfolio.

References

Allemang, Dean, and Jim Hendler. 2011. *Semantic Web for the Working Ontologist: Effective Modeling in RDFS and OWL*, 2nd ed. San Francisco: Morgan Kaufmann Publishers Inc.

Barton, Russel R. 2015. Tutorial: Simulation metamodeling. Paper presented at 2015 Winter Simulation Conference (WSC), Huntington Beach, CA, USA, December 6–9.

Bauer, Daniel, Daniela Bergmann, and Andreas Reuss. 2010. Solvency II and Nested Simulations-a Least-Squares Monte Carlo Approach. Working Paper. Georgia State University and Ulm University. Available online: http://citeseerx.ist.psu.edu/viewdoc/summary?doi=10.1.1.466.1983 (accessed on 17 August 2021).

Beirlant, Jan, Yuri Goegebeur, Johan Segers, and Jozef L. Teugels. 2004. *Statistics of Extremes: Theory and Applications*. Chichester: Wiley.

Biffis, Enrico. 2005. Affine processes for dynamic mortality and actuarial valuations. *Insurance: Mathematics and Economics* 37: 443–68. [CrossRef]

Boyer, M. Martin, and Lars Stentoft. 2013. If we can simulate it, we can insure it: An application to longevity risk management. *Insurance: Mathematics and Economics* 52: 35–45. [CrossRef]

Carrière, Jacques F. 1996. Valuation of the early-exercise price for options using simulations and nonparametric regression. *Insurance: Mathematics and Economics* 19: 19–30. [CrossRef]

Cathcart, Mark, and Steven Morrison. 2009. Variable annuity economic capital: The least-squares Monte Carlo approach. *Life & Pensions* 2: 44–48.

European Parliament, and European Council. 2009. *Directive 2009/138/EC on the Taking-Up and Pursuit of the Business of Insurance and Reinsurance (Solvency II)*. Brussels: European Council.

Floryszczak, Anthony, Olivier Le Courtois, and Mohamed Majri. 2016. Inside the Solvency II black box: Net Asset Values and Solvency Capital Requirements with a least-squares Monte-Carlo approach. *Insurance: Mathematics and Economics* 71: 15–26.

Frees, Edward W., and Emiliano A. Valdez. 2008. Hierarchical Insurance Claims Modeling. *Journal of the American Statistical Association* 103: 1457–69. [CrossRef]

Frees, Edward W., Gee Lee, and Lu Yang. 2016. Multivariate Frequency-Severity Regression Models in Insurance. *Risks* 4: 4. [CrossRef]

Fung, Man Chung, Katja Ignatieva, and Michael Sherris. 2014. Systematic mortality risk: An analysis of guaranteed lifetime withdrawal benefits in variable annuities. *Insurance: Mathematics and Economics* 58: 103–15. [CrossRef]

Gan, Guojun, and Emiliano A. Valdez. 2018. Regression modeling for the valuation of large variable annuity portfolios. *North American Actuarial Journal* 22: 40–54. [CrossRef]

Gan, Guojun, and X. Sheldon Lin. 2015. Valuation of large variable annuity portfolios under nested simulation: A functional data approach. *Insurance: Mathematics and Economics* 62: 138–50. [CrossRef]

Gan, Guojun. 2013. Application of data clustering and machine learning in variable annuity valuation. *Insurance: Mathematics and Economics* 53: 795–801.

Gan, Guojun. 2015. Application of metamodeling to the valuation of large variable annuity portfolios. Paper presented at 2015 Winter Simulation Conference (WSC), Huntington Beach, CA, USA, December 6–9.

Krah, Anne-Sophie, Zoran Nikolić, and Ralf Korn. 2018. A least-squares Monte Carlo framework in proxy modeling of life insurance companies. *Risks* 2: 62. [CrossRef]

Loeppky, Jason L., Jerome Sacks, and William J. Welch. 2009. Choosing the sample size of a computer experiment: A practical guide. *Technometrics* 51: 366–76. [CrossRef]
Longstaff, Francis A., and Eduardo S. Schwartz. 2001. Valuing American options by simulations: A simple least-squares approach. *The Review of Financial Studies* 1: 113–47. [CrossRef]
McDonald, James B. 1984. Some generalized functions for the size distribution of income. *Econometrica* 52: 647–63. [CrossRef]
Minasny, Budiman, and Alex B. McBratney. 2006. A conditioned Latin hypercube method for sampling in the presence of ancillary information. *Computers & Geosciences* 32: 1378–88.
Sun, Jiafeng, Edward W. Frees, and Marjorie A. Rosenberg. 2008. Heavy-tailed longitudinal data modeling using copulas. *Insurance: Mathematics and Economics* 42: 817–30. [CrossRef]
Tilley, James A. 1993. Valuing American options in a path simulation model. *Transactions of Society of Actuaries* 45: 499–520.

risks

MDPI

Article

Designing Annuities with Flexibility Opportunities in an Uncertain Mortality Scenario

Annamaria Olivieri

Department of Economics and Management, University of Parma, Via J. F. Kennedy 6, 43125 Parma, Italy; annamaria.olivieri@unipr.it.com; Tel.: +39-0521032387

Abstract: We consider annuity designs in which the benefit amount is allowed to fluctuate (up or down), based on a given mortality/longevity experience. This way, guarantees are relaxed in respect of traditional annuity arrangements. On the other hand, while the annuitant is exposed to the risk of a future reduction of the benefit amount because of higher longevity, he/she can immediately take advantage of a lower premium loading, as well as of a future increase of the benefit amount in the case of higher mortality. Flexibility in the annuity design could be welcomed by individuals, as the conservative features of traditional products partly explain their lack of attractiveness in most markets. To further contribute to the flexibility of the product, we suggest a pricing structure based on periodic fees applied to the policy fund, instead of the usual upfront loading at issue. Periodic fees are more suitable to support a revision of the arrangement after issue, which is currently not allowed in traditional annuity products. We show that periodic fees can be introduced by identifying a discount factor to be used for pricing and reserving. We assume stochastic mortality, and we compare alternative mortality/longevity linking solutions, by assessing the periodic fees and other quantities.

Keywords: mortality/longevity-linked annuities; aggregate longevity/mortality risk; longevity guarantee; periodic longevity fee

JEL Classification: G22

Citation: Olivieri, Annamaria. 2021. Designing Annuities with Flexibility Opportunities in an Uncertain Mortality Scenario. *Risks* 9: 189. https://doi.org/10.3390/risks9110189

Academic Editor: Mercedes Ayuso

Received: 31 August 2021
Accepted: 19 October 2021
Published: 22 October 2021

1. Introduction

The need for individuals to take autonomous decisions regarding their post-retirement income is widely recognized. Such a need has become more urgent after the adoption of Defined Contribution principles (in place of Defined Benefit) in Pillar I and II pension systems of many countries, as individuals are thus exposed to significant financial and longevity risks when in retirement. Among the private arrangements providing a post-retirement income, traditional life annuities are perhaps the most protective form for individuals, thanks to the longevity and financial guarantees they provide. This suggestion is supported by the classical result by (Yaari 1965), which identifies annuities as the optimal choice for a retiree. However, guarantees of traditional annuities expose the provider to major risks, furthermore over a long-term time horizon; this is why guarantees are matched by a conservative structure of benefits and investments, with loadings judged to be very high. These are some of the reasons explaining the so-called annuity puzzle, i.e., the fact that individuals are not attracted by life annuities and markets remain underdeveloped (see, for example, (Davidoff et al. 2005) and, for a recent contribution and updated list of references, (Peijnenburg et al. 2016)).

The current pandemic may suggest that planning the post-retirement income is no longer a topical issue. On the contrary, longevity remains a matter not to be disregarded, neither by individuals nor by providers. While it is clear that the COVID-19 pandemic is currently causing a mortality shock, different scenarios about the future mortality are possible, including an increase in the life expectancy of the survivors (see, for example, Cairns et al. 2020; Milevsky 2020). Furthermore, social security could be in greater difficulty

in the near future, due to the economic crises that have occurred in the latest years. It is, therefore, still relevant to consider situations where a significant part of the post-retirement income will have to be covered with private resources. Individuals will have to decide whether to self-annuitize their money, retaining all risks, or transfer all or part of the risks to providers, who then in turn have to develop cost-effective and attractive solutions.

In a scenario characterized by longevity but also by mortality shocks (which in the current pandemics are particularly severe at high ages), it is convenient to redefine longevity guarantees, so as to make them cheaper and more appealing both for individuals and providers. In particular, if the benefit amount is contingent on an appropriate mortality/longevity experience, possible profits and losses originated by unanticipated mortality/longevity are (at least partially) shared between individuals and providers, resulting in lower loadings, but also providing the opportunity to design a more flexible product structure.

Mortality/longevity-linked annuity benefits have been addressed in several contributions in the latest decade; see, in particular, (Bravo and de Freitas 2018; Chen and Rach 2019; Chen et al. 2019; Denuit et al. 2011; Milevsky and Salisbury 2015; Richter and Weber 2011; Weinert and Gründl 2021). Some forms already exist in the market; for example, in Danish deferred group annuities the benefit amount is increased by a bonus if the actual investment performance exceeds the guaranteed return or if the mortality experience is higher than expected (see Andersen and Skjodt 2007). While alternative linking coefficients have been examined in the literature, the problems mainly discussed are the fair valuation of the contract, as well as optimality issues for the individual, in an expected utility framework. The idea of linking a post-retirement income benefit to a mortality/longevity experience has not been developed for the first time in the latest decade, however. Conversely, such an idea is very old, dating back to the 17th century, when the so-called tontine investments were conceived. However, tontine annuities were originally designed not for protecting against the longevity risk, but for speculative purposes; see (McKever 2009) and (Milevsky 2014) for historical notes. Recently, mortality/longevity-linking structures have been adopted within pooled arrangements; while the best known are Group-Self Annuitization pools (see, for example, Piggott et al. 2005; Qiao and Sherris 2012), other schemes are investigated in (Stamos 2008), (Donnelly et al. 2013) and (Donnelly 2015), to cite some contributions. Pooled arrangements are self-insured: no guarantee is provided; individuals pool together their money, trying to take advantage of pooling effects. Self-insured solutions are cheaper than annuities, but individuals retain all risks, as members of the pool. In contrast, some forms of guarantees should be kept in mortality/longevity-linked annuities. A general description of linking coefficients, including as particular cases most of the solutions analysed in the literature both for insured and self-insured arrangements, is developed by (Olivieri and Pitacco 2020a).

As mentioned above, annuities are usually viewed as a very conservative product by individuals, as they represent an inflexible and illiquid asset, they imply an irreversible decision at issue, they do not satisfy bequest needs or they meet bequest preferences only partially, if a death benefit is included (see Pitacco 2016). Innovation can be pursued in various respects. Making the benefit amount contingent on mortality/longevity is undoubtedly an important innovation. In particular, it favours the adoption of not excessively prudential assumptions about future mortality, otherwise necessary given that annuities extend over a very long time-horizon. Bequest preferences can be met by introducing death benefits. While this is customary in annuities (as mentioned above), with death benefits payable up to some (not very high) age, Bernhardt and Donnelly (2019) introduce bequest in pooled arrangements. Several opportunities for innovation can be obtained when combining different benefits, such as the just mentioned case of annuities and death benefits. Particularly interesting in this regard is the combination of different forms of annuities; Chen et al. (2019, 2020) and Chen and Rach (2019) consider the case of fixed annuity benefits combined with mortality/longevity linked-benefits.

Another line of innovation can be developed in respect of the structure of the fees. It is traditional for life annuities to define and charge the premium loading at issue, when the individual transfers their money to the provider. Such a pricing structure concurs to the inflexibility of the product, as on one hand pricing assumptions are fully chosen at issue, on the other the provider is required to pre-define the management over time of the upfront loadings. Conversely, periodic fees can pave the way for greater product flexibility, for example making it easier to switch to different forms of benefits after issue, or making it possible to revise the pricing assumptions. In this latter regard, we note that while the possibility of revising pricing assumptions can be viewed with suspicion by individuals, any change will not necessarily be to the advantage of the provider (rather, it may be favourable to the individual); in principle, any change in pricing assumptions will be limited by the policy conditions underwritten at issue. Periodic fees are a natural choice when periodic premiums are paid, i.e., usually in the case of endowments. In a mortality/longevity linking framework, Hanbali et al. (2019) focus in particular on the case of pure endowments, by assuming level premiums (subject to possible adjustments in time). Periodic fees are common in variable annuities, independent of the time-profile of the premium stream. Here, guarantees are priced by charging a periodic fee to the policy account value, with the possibility for the policyholder to waive the guarantee at any time (except for agreed time windows), with a consequent interruption of the relevant fee charge; for a general overview, see (Bacinello et al. 2011). In a recent contribution by (Chen et al. 2021) periodic fees are introduced in a tontine scheme, and are expressed as a proportion of the benefit amount; the size of the fee that makes the individual indifferent between choosing a fixed-benefit or a tontine annuity is in particular examined, identifying this way the range of acceptable fee levels in tontine arrangements.

In this paper, we consider mortality/longevity-linked annuities, that include guarantees in the form of barriers for the benefit amount. We further develop Olivieri and Pitacco (2020a, 2020b), by introducing periodic fees instead of an upfront fee at issue. Periodic fees are charged to the policy fund value and their level is assessed based on the losses and profits retained by the provider, which in turn depend on the linking coefficient and the barriers for the benefit amount. The metric we use to assess the required fees is the business value for the provider; this quantity, defined as the present value of future profits net of the cost of capital, is suitable as a joint summary of the losses and profits retained by the provider. We show that the periodic fee identifies a discount factor to be used for pricing and reserving. We then define the individual reserve, and split it into two components, one covering the value of future benefits and one the value of future fees; such an information can be useful in some applications.

The remainder of the paper is organized as follows. In Section 2, we describe the model, in particular the mortality/longevity-linking annuity benefits examined in the paper (Section 2.1), the structure of periodic fees and the corresponding discount factor (Section 2.2), the individual reserve and its components (Section 2.3), the business value to the provider (Section 2.4); finally, we discuss how to assess the required fees, based on an assessment of the business value (Section 2.5). Some numerical findings are illustrated in Section 3, more specifically in Section 3.3, after having sketched the stochastic mortality model adopted (Section 3.1) and provided details about the arrangements analysed in the numerical implementation (Section 3.2). Finally, Section 4 concludes the paper, with some final comments.

2. Model Setup

2.1. Mortality/Longevity-Linked Annuity Benefits

We consider a discrete-time annuity immediate in arrears, i.e., with payments at the end of the year. For simplicity, one cohort only is addressed, homogeneous in all respects. The entry time is 0 and the entry age is x. In this paper, we focus on mortality/longevity risk only, while we disregard other risks. For this reason, a deterministic financial setting is adopted.

We follow the general linking structure described in (Olivieri and Pitacco 2020a), to which we refer for a detailed discussion about the rationale and actuarial technique backing the annuity benefit adjustment. We consider the following two alternative mortality/longevity-linked annuity benefits:

$$b_t = b_{t-1} \cdot \frac{p_{x+t-1}(0)}{\widetilde{p}_{x+t-1}} \; ; \tag{1}$$

$$b_t = b_0 \cdot \frac{1 + a_{x+t}(0)}{1 + a_{x+t}(t)} \; , \tag{2}$$

where b_0 is chosen at time 0 in both cases. The meaning of the quantities in Equations (1) and (2) is as follows: $p_{x+t-1}(0)$ denotes the annual survival probability at age $x+t-1$ provided by a best-estimate mortality assumption (i.e., life table) at time 0; $\widetilde{p}_{x+t-1}$ represents the proportion of survivors (or longevity index) observed in a chosen population; $a_{x+t}(0), a_{x+t}(t)$ denote the actuarial value at age $x+t$ of a unitary discrete-time annuity in arrears, based on the best-estimate mortality assumptions (namely, life tables), respectively, at time 0 and t. An interpretation about the two adjustments coefficients follows below.

In Equation (1), which we will call linking by means of the survival probability, the benefit amount is adjusted based on the comparison between the survival rate realized in a given population, $\widetilde{p}_{x+t-1}$, and a benchmark, $p_{x+t-1}(0)$, chosen at time 0. An increase (decrease) of the benefit amount follows from $p_{x+t-1}(0) > \widetilde{p}_{x+t-1}$ ($p_{x+t-1}(0) < \widetilde{p}_{x+t-1}$), i.e., in the case of higher realized mortality (longevity) than predicted by the benchmark. We note that, for an annuity business, a profit (loss) is typically reported by the provider in the case of higher mortality (longevity); thus, the benefit adjustment in (1) serves to mitigate such a profit (loss), partially transferring it to the individuals. The strength of the mitigation effect depends, however, on the population in which $\widetilde{p}_{x+t-1}$ is measured (as well as on other policy conditions, such as any barriers set for the benefit amount).

As far as the population is concerned, the choice is between the provider's pool or a reference population. While the provider's pool usually shows a small size and is thus subject to major random fluctuations, large reference populations are more appropriate, so that deviations between $\widetilde{p}_{x+t-1}$ and $p_{x+t-1}(0)$ can be mainly attributed to an unanticipated underlying mortality/longevity trend. Random fluctuations represent a traditional risk for insurers (and annuity providers), and the relating risk management actions should be arranged using the well-known pooling arguments. Conversely, mortality/longevity-linking benefits are recommended to cope with unanticipated mortality/longevity trends. In the following, we then assume that $\widetilde{p}_{x+t-1}$ is measured on a large population. We finally note that any possible difference between the mortality/longevity in the provider's pool and the reference population may be due not only to random fluctuations, but also to different underlying trends. A basis risk follows for the provider, which we do not address in this paper.

It is interesting to note that rule (1) is equivalent to the following:

$$b_t = b_0 \cdot \frac{{}_tp_x(0)}{{}_t\widetilde{p}_x} \; , \tag{3}$$

where ${}_tp_x(0)$ is the survival probability from age x to age $x+t$ provided by the best-estimate mortality assumption at time 0, while ${}_t\widetilde{p}_x$ is the proportion of survivors from age x to age $x+t$ in the reference population. Equation (3) shows an important feature, which does not emerge explicitly from Equation (1): the adjustment coefficient should be applied to the benefit amount defined at the time the benchmark is referred to, namely time 0 in this case. In other words, there must be a consistency between the time-frame involved by the adjustment coefficient and the reference time of the quantity to which such a coefficient is applied.

Coming to the benefit adjustment in Equation (2), which we will call linking by means of the actuarial value of the annuity, we first note that $a_{x+t}(h) = \sum_{s=1}^{\omega-(x+t)} (1+i)^{-s}$.

${}_sp_{x+t}(h)$, where i is a chosen discount rate, ${}_sp_{x+t}(h)$ the survival probability (from age $x+t$ to age $x+t+s$) based on best-estimate assumptions at time h, and ω the maximum attainable age (that we assume to be deterministic). The ratio $\frac{1+a_{x+t}(0)}{1+a_{x+t}(t)}$ then involves a comparison between possibly different mortality assumptions (or life tables) adopted to assess the actuarial value of a unitary annuity, at time 0 and time t. The actuarial value in the numerator, in particular, is a benchmark. If higher (lower) mortality is forecasted at time t, then $a_{x+t}(0) > a_{x+t}(t)$ ($a_{x+t}(0) < a_{x+t}(t)$), implying an increase (reduction) of the benefit amount. Updated mortality/longevity assumptions in the actuarial value of the annuity can result in a profit (loss) for the provider, which is (partially) mitigated by the benefit adjustment. We note that, in line with what commented above for the linking by means of the survival probabilities, having set the benchmark at time 0, the benefit adjustment is applied to the benefit amount at the same time.

Both in the linking by means of the survival probability and by means of the actuarial value of the annuity, explicit guarantees can be introduced, for example, by setting bounds for the benefit amount or the benefit adjustment. Furthermore, it is also reasonable to accept a maximum age to apply the benefit adjustment (say, age 95), in order to avoid that the individual is exposed to the risk of benefit reductions at very advanced ages.

2.2. Policy Fund and Periodic Fees

In this section, we describe the main setting for periodic fees. As with other annuity products, each individual only pays an initial capital S at entry time 0, and then will cash the annuity benefit annually, until death. Unlike the usual setting for annuities, where the premium loading is charged entirely to the initial capital at time 0, we assume that periodic fees are charged to the policy fund at the beginning of each year. This is similar to what happens in variable annuities. In our discussion, we disregard expenses; the fee (whether it is obtained as a single initial or a periodic loading) is justified by the logic of the safety loading, i.e., by the fact that the arrangement incorporates guarantees whose cost is charged to the individual. When expenses are also addressed, periodic expenses can be added to the periodic fee, while an upfront loading to cover initial expenses could be included.

In this paper, we are mainly concerned with identifying appropriate pricing and reserving logics when fees are periodic. Any possible revision after issue of the fee level requires criteria that we do not address in this paper. In what follows, we assume that the periodic fee level is chosen at time 0, and kept fixed over the whole policy duration; some comments about the possible revision of the fee level after issue will be made later, in Section 3.3.

As stated in Section 2.1, in this paper we consider a pool consisting of one cohort only, homogeneous in all respects (entry age, risk class, benefit amount). With N_{x+t} we denote the number of individuals in the pool at time t (age $x+t$). At time 0, $N_x = n_x$ known, while N_{x+t} is random because of the mortality in the cohort.

Let A_t denote the individual fund (or policy fund) for a policy in-force at time t. No death benefit is paid out by the provider, so that upon death the policy fund is released to the pool (as a form of mortality credit). The dynamics of the policy fund is then described by the following balance equation:

$$A_t \cdot N_{x+t} = A_{t-1} \cdot N_{x+t-1} \cdot (1-\xi) \cdot (1+i) - b_t \cdot N_{x+t}\,, \tag{4}$$

where: ξ is the proportional premium loading (or fee) that is charged to each policy fund at the beginning of each year and i is the (deterministic) return on investments. At time 0, $A_0 = S$.

The policy fund is random because of the mortality in the pool and the path of the benefit amount; in a more general setting, random financial returns can also be addressed.

Solving backwards Equation (4) (note that $A_{\omega-x} = 0$), we find:

$$A_0 = \sum_{s=1}^{\omega-x} b_s \cdot ((1-\xi)\cdot(1+i))^{-s} \cdot \frac{N_{x+s}}{n_x} \,. \tag{5}$$

Equation (5) shows that the periodic fee ξ identifies a discount factor, to be used for pricing. However, in order to quantify ξ, we still need a valuation principle. While we know that $A_0 = S$, the expression on the right hand side of Equation (5) is still random, as both the sequences b_s and N_{x+s} are random. Furthermore, there are two unknowns in Equation (5), namely b_0 and ξ. We further discuss this problem in Section 2.5, after having introduced some quantities. We point out, however, that the approach we suggest to assess the periodic fee will not directly make use of Equation (5); the discussion just developed allows us to say that the periodic fee identifies a discount factor to be used for pricing purposes (as well as for reserving; see Section 2.3).

We note that, if policy conditions admit, the periodic fee could be updated after issue first extending Equation (5) and then implementing an appropriate valuation principle. As already mentioned, in this paper we do not develop the discussion in this respect.

2.3. Individual Reserve and Components

In order to define the individual reserve, we make the following comments. As is well-known, the individual reserve corresponds to the best-estimate value of liabilities plus a risk margin. We assume that the risk margin can be measured through the periodic fee, which (as noted in Section 2.2) identifies a discount factor. We further assume that, to be consistent, the best-estimate assumptions should be those defined when the periodic fee was assessed, i.e., at time 0 in this paper. Consider a policy in-force at time t. The individual reserve is defined as follows:

$$V_t = b_t \cdot \sum_{s=1}^{\omega-(x+t)} ((1-\xi)\cdot(1+i))^{-s} \cdot {}_sp_{x+t}(0) \,. \tag{6}$$

It is useful to note that no future update of the benefit amount is explicitly considered in the definition of the individual reserve, as the periodic fee already includes in the reserve an allowance for the future benefit adjustments.

For shortness, we denote the sum in Equation (6) as $a_{x+t}(0;\xi)$, where the symbol ξ refers to the fact that discounting is based also on the periodic fee (conversely, the notation $a_{x+t}(0)$ will be kept to denote the expression commented in Section 2.1, i.e., when discounting is based on the interest rate only).

It could be useful to split the individual reserve into components. A possible splitting is the following:

$$V_t = b_t \cdot a_{x+t}(0;\xi) = b_t \cdot a_{x+t}(0) + b_t \cdot (a_{x+t}(0;\xi) - a_{x+t}(0)) \,. \tag{7}$$

The first quantity, $V_t^{[\text{ben}]} = b_t \cdot a_{x+t}(0)$ is the best-estimate value of future benefits, while the second, $V_t^{[\text{fee}]} = b_t \cdot (a_{x+t}(0;\xi) - a_{x+t}(0))$, can be interpreted as the part of the individual reserve accounting for fees. This decomposition could be useful first to identify the risk margin included in the individual reserve. It could be further useful in the case of a switch to a different benefit structure, as the provider could only use $V_t^{[\text{ben}]}$ to determine the new benefit level or, in the case of revision of the fee, the revision itself could be limited to the component $V_t^{[\text{fee}]}$. These aspects are not further developed in this paper.

2.4. Pool Fund, Present Value of Future Benefits, Present Value of Future Profits and Business Value

We now address quantities defined in the provider's perspective. Each individual in the pool pays the initial capital S at time 0, and will cash the annual amount b_t at time $t, t = 1, 2, \ldots$, until death. The following quantity describes what we call the pool fund, i.e.,

the remaining money at time t of the total amount of initial capital, net of the benefits paid so far and including interest on investments:

$$F_t = F_{t-1} \cdot (1+i) - b_t \cdot N_{x+t}\,, \tag{8}$$

with $F_0 = S \cdot n_x$. Periodic fees do not enter the assessment of the pool fund; indeed, as individuals transfer money to the pool only at time 0, periodic fees do not originate a real periodic cash flow. Rather, they consist in a loading which is charged annually to the policy funds of the survivors, as expressed by Equation (4).

The difference between the pool fund and the pool reserve, namely

$$SP_t = F_t - V_t \cdot N_{x+t}\,, \tag{9}$$

expresses the surplus cumulated by the provider in the time-interval $(0,t)$. If we consider the surplus cumulated over the whole pool duration $(0,\omega-x)$, we find:

$$SP_{\omega-x} = S \cdot n_x \cdot (1+i)^{\omega-x} - \sum_{s=1}^{\omega-x} b_s \cdot (1+i)^{\omega-x-s} \cdot N_{x+s} \tag{10}$$

$$= n_x \cdot (1+i)^{\omega-x} \cdot \left(S - \sum_{s=1}^{\omega-x} b_s \cdot (1+i)^{-s} \cdot \frac{N_{x+s}}{n_x} \right), \tag{11}$$

where: $\mathrm{PVFB}_0 = \sum_{s=1}^{\omega-x} b_s \cdot (1+i)^{-s} \cdot \frac{N_{x+s}}{n_x}$ represents the Present Value of Future Benefits (PVFB) at time 0, expressed per policy issued. The quantity $\mathrm{PVFP}_0 = S - \mathrm{PVFB}_0$ then represents the total profit, usually called Present Value of Future Profits (PVFP) at time 0, expressed per policy issued.

The PVFB and the PVFP are quantities of great interest for the assessment of the business value. Their definition can easily be extended to times after issue. If n_{x+t} is the number of policies in-force (i.e., in the portfolio) at time t, then

$$\mathrm{PVFB}_t = \sum_{s=1}^{\omega-(x+t)} b_{t+s} \cdot (1+i)^{-s} \cdot \frac{N_{x+t+s}}{n_{x+t}} \tag{12}$$

expresses the PVFB at time t per policy in-force at that time, while PVFP at time t can be assessed as follows:

$$\mathrm{PVFP}_t = V_t - \mathrm{PVFB}_t\,. \tag{13}$$

Alternative valuation assumptions can be adopted in the assessment of PVFB, PVFP, in particular with regard to mortality. The proportions $\frac{N_{x+t+s}}{n_{x+t}}$ in (12) lead to an entity-specific assessment , as the size of the total amount of future payments to be made by the provider (namely, the amounts $b_{t+s} \cdot N_{x+t+s}$) is measured with the number of survivors in the pool, which in their turn results from the mortality in the pool itself. Entity-specific assessments are convenient, for example, to perform a realistic valuation of provider's liabilities. The adoption of the proportion of survivors in the reference population, ${}_s\widetilde{p}_{x+t}$, in place of $\frac{N_{x+t+s}}{n_{x+t}}$ is to be preferred in market-consistent assessments, such as those involved by pricing issues. In this case, mortality/longevity risks to which the provider is exposed (e.g., because of a small pool size or a pool composition affected by adverse-selection), but could be offset by appropriate market transactions, should be excluded from the valuation. Since we are discussing the setting of appropriate fees, in this paper we follow a market-consistent logic, and we disregard risks specific to the provider. In particular, we do not consider different mortality situations between the provider's pool and the reference population, so that we accept $\frac{N_{x+t+s}}{n_{x+t}} = {}_s\widetilde{p}_{x+t}$ at any age.

For further details about the assessment of PVFB and PVFP in more general situations, we refer to Olivieri and Pitacco (2020a, 2020b).

We now assess the business value for the provider, which is the part of PVFP net of the cost of capital that the provider is required to hold to manage the business (for references and an application to traditional annuities, see Blackburn et al. 2017). We assess the cost of capital in a market-consistent style, i.e., as frictional costs net of the value of the limited liability put option. The limited liability put option takes a positive value when, because of the possible depletion of capital, the provider may fail to meet (at least in part) its obligations. We assume that the provider can always obtain the extra capital necessary to fulfil all obligations, in the case the amount initially allocated to the pool becomes insufficient. In this case, the limited liability put option takes a null value. Frictional costs (which arise mainly because of agency costs) are usually assessed as a proportion ρ of the capital held on top of the pool reserve. We assume that such a capital is in the amount required by regulation; we denote with RC_t the capital required at time t per policy in-force at that time. The annual frictional cost per policy in-force at the beginning of the year is then:

$$\mathrm{FC}_t = \rho \cdot \mathrm{RC}_{t-1}. \tag{14}$$

The present value of frictional costs at time t, per policy in-force, is obtained as follows:

$$\mathrm{PVFC}_t = \sum_{s=1}^{\omega-(x+t)} \mathrm{FC}_{t+s} \cdot (1+i)^{-s} \cdot {}_s\widetilde{p}_{x+t}\,. \tag{15}$$

We assess RC_t following the Solvency 2 principles, which require an amount of capital so to avoid default with 99.5% probability, allowing only for risks non-diversifiable on the market. A long-term time horizon in which to assess possible defaults seems the most logical choice in respect of longevity risk, due to its long-term nature. We obtain the required capital at time t per policy in-force from the following condition:

$$\Pr(\mathrm{RC}_t + V_t < \mathrm{PVFB}_t) = 0.005\,. \tag{16}$$

Finally, we define the business value at time t, per policy in-force, as follows:

$$\mathrm{BV}_t = \mathrm{PVFP}_t - \mathrm{PVFC}_t\,. \tag{17}$$

2.5. Setting the Periodic Fee

As is well-known (see, for example, Duffie 2001), the market price of a security is given by the present value of its expected cash flows, where the present value is assessed with the risk-free rate and the expected value is obtained with a suitably risk-adjusted probability measure. When the market is incomplete, as is the case for example of insurance and pension markets, there are infinite suitable probability measures, among which the provider has to choose one to price the annuity contract. This approach apparently contrasts with the traditional insurance pricing model, which first employs best-estimate assumptions, and then adds an implicit or explicit safety loading. The safety loading, in particular, represents the expected profit to the provider and its size should be justified by the risks taken by the provider itself. What is common to both approaches is that the expected profit to the provider is 0 under the chosen valuation assumptions; however, a reward for the retained risks is included, either through the risk-adjustment of the probabilities or the safety loading.

Mortality/longevity-linked annuities certainly require an innovative pricing approach, as they imply a new concept of longevity guarantee, as we have commented in Sections 1 and 2.1. It could be convenient to match somehow market principles with the traditional model. To this aim, we note that of the various quantities described so far, there is one explicitly affected both by expected profits and the risks borne by the provider, which is the business value. Risks, in particular, affect the business value via frictional costs, as they are proportional to the required capital, whose size in turn depends on the potential losses

reported by the provider, apart from the largest losses as identified by the accepted default probability.

We extend the 0 expected profit principle to the business value. Adopting the periodic fee structure described in Section 2.2, at time 0 we assess the periodic fee ξ so that

$$\mathbb{E}[\mathrm{BV}_0] = 0\,. \tag{18}$$

Such an equation can be solved once a (stochastic) mortality model describing the mortality/longevity of the reference population has been chosen. In Section 3.1, we briefly describe the model that we have adopted in the numerical implementation.

We now address some computational issues. First we note that Equation (18) reasonably requires stochastic simulation, although this depends on the mortality model (however, one can hardly count on closed formulae). Second, as already noted (see Section 2.2), given S, there are two unknowns in the relevant equations, namely b_0 and ξ, which among other things are related, as the higher is ξ, the lower is b_0, and vice versa. Whatever is the approach adopted (market-based, traditional or the one we are discussing), there is one degree of freedom, in respect of which we proceed as follows. First we set $\xi = 0$ and assess b_0 solving Equation (6), for $t = 0$ (having $V_0 = S$, at that time). We denote such an initial benefit amount as b_0^*; in practice, $b_0^* = \frac{S}{a_x(0)}$. Then we assess the expected business value, under b_0^*; we use the notation $\mathrm{BV}_0^* = \mathbb{E}[\mathrm{BV}_0; b_0^*]$; if such a quantity is $\neq 0$ (reasonably, it takes a negative value), we adjust (typically, we reduce) the initial benefit amount, so to reach a value 0 for the business value. In practice, we set $V_0^{[\mathrm{fee}]} = -\mathrm{BV}_0^*$ and we find $b_0 = \frac{S - V_0^{[\mathrm{fee}]}}{a_x(0)}$ (see Equation (7)). Finally, we find the periodic fee ξ by solving at time $t = 0$ Equation (6) (which has now only one unknown) in respect of ξ (here, we can use a routine for the internal rate of return). We point out that once b_0 and ξ have been set, we cannot exclude that $\mathbb{E}[\mathrm{BV}_0] \neq 0$. This is because the components of BV_0 are not necessarily proportional to b_0 and usually they are not proportional to ξ. Equation (18) is used to set the fee in a consistent way in the various situations (in particular, working with different mortality/longevity-linking coefficients), but (as we will see in the numerical implementation in Section 3) the fee thus determined can still entail value creation for the provider.

3. Results

3.1. Mortality Model

A stochastic mortality model is required to simulate the survival rates realized in the reference population and in the pool, as well as to obtain updated best-estimate assumptions at every time, consistently with the simulated experience. After the seminal paper by (Lee and Carter 1992), a very prolific research has developed on the stochastic modelling of mortality. Several models are described in the literature; most of them are suitable to obtain accurate projections at the initial time, but can present computational complexity when processing future best-estimate assumptions. Here we adopt a model discussed in (Olivieri and Pitacco 2009), which fits the evaluation needs mentioned above, and is computationally tractable. Below, we recall the main features of the model, referring to (Olivieri and Pitacco 2009) for details.

We refer to a given cohort and denote with $\widetilde{q}_{x+t} = 1 - \widetilde{p}_{x+t}$ the random mortality rate at age $x + t$. We define $\widetilde{q}_{x+t}$ as follows:

$$\widetilde{q}_{x+t} = q_{x+t}(0) \cdot Z_{x+t}\,, \tag{19}$$

where: $q_{x+t}(0) = 1 - p_{x+t}(0)$ is the mortality rate based on best-estimate assumptions at time 0; Z_{x+t} is a (positive) random coefficient (ensuring $0 \leq \widetilde{q}_{x+t} \leq 1$) which measures the deviation of the observed mortality rate compared to the best-estimate one at time 0. We assume:

$$Z_{x+t} \sim \text{Gamma}(\alpha_{x+t}, \beta_{x+t}) \; ; \tag{20}$$

a Gamma distribution also follows for $\widetilde{q}_{x+t}$, with parameters obtained from those in (20). If the Poisson distribution is accepted for the annual number of deaths reported by the cohort, conditional on a given value for the mortality rate, then the unconditional distribution of the annual number of deaths is described by a negative binomial (or Poisson-Gamma) law. We point out that while the Poisson distribution describes random fluctuations in mortality, the Gamma (i.e., the coefficient Z_{x+t}, whatever is its probability distribution) describes aggregate deviations.

The parameters of (20) are first chosen at time 0 , when the cohort starts being observed; thus, $\alpha_{x+t} = \bar{\alpha}_0$ and $\beta_{x+t} = \bar{\beta}_0$ at time 0, where $\bar{\alpha}_0, \bar{\beta}_0$ are given values. Then, year after year the parameters are updated, through an inferential procedure based on the information carried by the observed annual number of deaths. In particular, after h years of observation, once the numbers of deaths $d_x, d_{x+1}, \ldots, d_{x+h-1}$ and the number of survivors $n_x, n_{x+1} = n_x - d_x, \ldots, n_{x+h-1} = n_{x+h-2} - d_{x+h-2}$ have been reported, the initial $\bar{\alpha}_0, \bar{\beta}_0$ are replaced with the following values: $\bar{\alpha}_h = \bar{\alpha}_0 + d_x + d_{x+1} + \cdots + d_{x+h-1}$, $\bar{\beta}_h = \bar{\beta}_0 + n_x \cdot q_x(0) + n_{x+1} \cdot q_{x+1}(0) + \cdots + n_{x+h-1} \cdot q_{x+h-1}(0)$. Updating the parameters $\alpha_{x+t}, \beta_{x+t}$ introduces an implicit correlation among the coefficients Z_{x+t}'s, which is something one expects when an underlying longevity trend drives mortality. Nevertheless, fluctuations in the number of deaths in the opposite direction in respect of the prevailing trend are still admitted at any time. We point out that updating the parameters of the probability distribution of Z_{x+t} allows to update the current best-estimate assumptions, as well as the projection of the future number of survivors in the cohort. Details of the inferential procedure are described in (Olivieri and Pitacco 2009).

In the numerical implementation, we consider a cohort initial age $x = 65$. We set $\bar{\alpha}_0 = \bar{\beta}_0$, so to have $\mathbb{E}_0[Z_{x+t}] = 1$, $\mathbb{E}_0[\widetilde{q}_{x+t}] = q_{x+t}(0)$ (we specify in the subscript of the symbol $\mathbb{E}$ the time at which the expected value is assessed, thus meaning that the state of information about mortality is specified at that time). Based on the information gained from the observed number of deaths up to time h, the best-estimate mortality rate is reassessed as $q_{x+t}(h) = \frac{\bar{\alpha}_h}{\bar{\beta}_h} \cdot q_{x+t}(0)$, where $\frac{\bar{\alpha}_h}{\bar{\beta}_h} \lesseqgtr 1$, depending the realized mortality path. The best-estimate mortality rates $q_{x+t}(0)$ are modelled through a Gompertz law with parameters as in (Bacinello et al. 2018). The remaining expected lifetime at age 65 is almost 20 years at time 0; to avoid distortions from major random fluctuations at the highest ages, the cohort is examined up to age 100 (any payments beyond that age is disregarded). The values $\bar{\alpha}_0 = \bar{\beta}_0 = 100$ $\bar{\alpha}_0 = \bar{\beta}_0 = 1000$ are alternatively adopted; if $\bar{\alpha}_0 = \bar{\beta}_0 = 100$, the coefficient of variation of Z_{x+t} at time 0 is 0.1, while it is 0.0316 if $\bar{\alpha}_0 = \bar{\beta}_0 = 1000$. Given the meaning of Z_{x+t}, the former choice of $\bar{\alpha}_0, \bar{\beta}_0$ then depicts a situation with a higher dispersion in aggregate mortality than the latter choice. To distinguish the two alternative scenarios, shortly we will refer to the choice $\bar{\alpha}_0 = \bar{\beta}_0 = 100$ as to a scenario with major aggregate deviations; the term moderate aggregate deviations will be used instead to refer to the choice $\bar{\alpha}_0 = \bar{\beta}_0 = 1000$ (it is useful to stress that the adjectives 'moderate' and 'major' do not have an absolute meaning here, but they are used in comparative terms between the two situations).

3.2. Benefit Arrangements

We examine the following arrangements:

1. Fixed benefit : $b_t = b_0$ for all times t.
2. Linking by means of the survival probability, with benefit amount defined by Equation (3).
3. Linking by means of the actuarial value of a unitary annuity, with benefit amount defined by Equation (2).

Arrangement 1 represents a standard case, to which arrangements with a mortality/longevity linking can be compared. For arrangements 2 and 3, barriers to the benefit

amount are adopted, both on an annual and a global basis. Year by year, we require $0.9 \cdot b_{t-1} \leq b_t \leq 1.1 \cdot b_{t-1}$, so to avoid strong variations in the benefit amount from one year to the next. In respect of the possible total variation of the benefit amount we consider two cases, implying a different proportion of the risk sharing between the provider and the individual. Specifically, we require alternatively:

- Case (a): $0.75 \cdot b_0 \leq b_t \leq 1.25 \cdot b_0$;
- Case (b): $0.9 \cdot b_0 \leq b_t \leq 1.1 \cdot b_0$.

Finally, we admit that the benefit amount can be updated up to age 95; beyond that age, the benefit amount keeps flat, at the latest updated level.

As mentioned earlier, we disregard financial risk and we adopt a deterministic setting in this regard. Our aim is to make a comparison of the periodic fees and other quantities for the alternative linking solutions. These comparisons are not affected by the interest rate level, when it is deterministic. Thus, we simplify and take $i = 0$, supported in this choice by the low level of interest rates in recent years.

3.3. Implementation and Discussion

In the implementation discussed in this section, the main purpose is to compare the periodic fees required for alternative annuity designs. Some of the quantities described in Section 2 are additionally quoted, in particular the components of the individual reserve, the present value of future profits and the business value. Rather than the absolute values we have obtained for the various quantities, it is the comparison between them that is significant. While absolute values are affected by the various choices made, in particular with regard to the mortality model and the interest rate, their comparison allows a better understanding of what the various linking mechanisms imply, in respect of alternative choices. All assessments have been developed simulating the number of survivors in the reference population; the same proportion of survivors than those of the reference population has been adopted for the pool. The information gained from the mortality observed in the reference population has also been used to update the best-estimate mortality assumptions after issue. The initial capital paid by each individual is $S = 100$ monetary units.

Table 1 quotes the periodic fee, assessed as described in Section 2.5, for alternative arrangements. The proportion ρ of frictional costs has been set to 2%, following market practice (see Blackburn et al. 2017). Tables 2 and 3 list the expected value, the 0.01- and the 0.99-quantiles of the benefit amounts for some times t and for the various arrangements. It is convenient to analyse these three tables jointly, as the time-profile of the benefit amounts helps understanding the size of the fee, while the latter explains the differences among the initial benefit amounts b_0 under the different arrangements.

The arrangement with fixed benefits can be used as a reference case. It requires the highest fees, due to the absence of any form of risk sharing between the provider and the individual. In comparison, mortality/longevity-linking arrangements require lower fees, as they imply, in particular, possible reductions of the benefit amount. When interpreting the results, it should be remembered that when the benefit is linked to a mortality/longevity experience, either by means of the survival probability or the actuarial value of the annuity, the benefit is allowed both to decrease (and this implies a sharing of losses due to higher longevity) and increase (in this case, profits due to higher mortality are shared). The size of the fee is affected by the extent of the possible reduction in losses to the provider, but also by that of profits.

Overall, it seems that the fee is much affected by the loss sharing effect. This emerges, for example, when comparing the cases (a) and (b) for the linking by means of the survival probability; indeed, narrower barriers for the benefit amount imply in particular a reduced participation to possible losses.

The importance of the magnitude of possible losses as a key to interpreting the level of the required fee also emerges when comparing (for any given arrangement) a scenario with moderate deviations in aggregate mortality to one with major deviations. Higher fees are required under the latter scenario. In this regard, it is useful to note that deviations are admitted in terms both of higher and lower mortality rates. Under a scenario with major deviations, higher fees are required; this suggests that the fee itself is in particular affected by the possibility to share the possible losses occurring because of lower mortality rates.

When comparing the fees required for arrangement where benefits are linked by means of the survival probability in the different cases, a univocal behaviour emerges. The same does not happen for arrangements where benefits are linked by means of the actuarial value of the annuity; in this latter case, it seems that the trade-off between profits and losses assumes a different balance depending on the parameters accepted for the benefit barriers and the mortality scenario. For example, ξ takes the same value in a scenario of moderate aggregate deviations, independent of the barriers we have tested for the benefit amount (clearly, a different choice for such barriers could result in a different value for the required fee). From Table 2 we see also that the expected benefit amount and the 0.01- and 0.99-quantiles coincide (apart from roundings) in the two cases (a) and (b).

In principle, the coefficient linking the benefits to the survival rate implies a different time-profile of the adjustments when compared to the coefficient linking the benefit to the actuarial value of the annuity. This is shown, for example, by the quantiles of the benefit amounts quoted in Tables 2 and 3. For a given mortality scenario, the coefficient linking the benefits to the actuarial value of the annuity implies a larger benefit adjustment in earlier times than the coefficient linking the benefit to the survival probability; on the other hand, lower adjustments are then required later in time by the former coefficient. This effect can be explained by the time-horizon referred to by the quantities in the adjustment coefficient; if we compare (3) with (2), we can realize that the actuarial value of the annuity refers to a longer time-horizon than the survival probability in the early years of the annuity (i.e., when t is small); the opposite happens when t is high. The time-profile of the adjustments has an impact on the size of the cash flows, and then on the proportion of the total profits and losses retained by the provider, as well as on the fee.

Table 1. Periodic fee ξ (to be charged each year to the policy fund value).

Arrangement	Moderate Aggregate Deviations	Major Aggregate Deviations
Fixed benefits	0.069%	0.242%
Benefits linked to surv. prob., case (a)	0.003%	0.025%
Benefits linked to act. value, case (a)	0.013%	0.033%
Benefits linked to surv. prob., case (b)	0.006%	0.093%
Benefits linked to act. value, case (b)	0.013%	0.019%

Table 2. Benefit amount b_t (expected value and 0.01- and 0.99-quantiles) for selected times. Moderate aggregate deviations.

Time t	Fixed benefits	Benefits Linked to Surv. Prob., Case (a)			Benefits Linked to Act. Value, Case (a)		
		Exp. value	0.01-quant.	0.99-quant.	Exp. value	0.01-quant.	0.99-quant.
0	5.199	5.242			5.236		
5	5.199	5.242	5.213	5.272	5.236	5.069	5.408
10	5.199	5.242	5.168	5.320	5.236	5.052	5.426
15	5.199	5.242	5.097	5.398	5.236	5.037	5.443
20	5.199	5.243	4.984	5.526	5.236	5.029	5.454
25	5.199	5.246	4.805	5.741	5.236	5.037	5.447
30	5.199	5.253	4.527	6.114	5.236	5.093	5.388
Time t		**Benefits Linked to Surv. Prob., Case (b)**			**Benefits Linked to Act. Value, Case (b)**		
		Exp. value	**0.01-quant.**	**0.99-quant.**	**Exp. value**	**0.01-quant.**	**0.99-quant.**
0		5.240			5.236		
5		5.240	5.211	5.270	5.236	5.069	5.408
10		5.240	5.166	5.318	5.236	5.052	5.426
15		5.240	5.095	5.396	5.236	5.037	5.443
20		5.241	4.982	5.524	5.236	5.029	5.454
25		5.243	4.804	5.739	5.236	5.037	5.447
30		5.244	4.716	5.764	5.236	5.093	5.388

Table 3. Benefit amount b_t (expected value and 0.01- and 0.99-quantiles) for selected times. Major aggregate deviations.

Time t	Fixed benefits	Benefits Linked to Surv. Prob., Case (a)			Benefits Linked to Act. Value, Case (a)		
		Exp. value	0.01-quant.	0.99-quant.	Exp. value	0.01-quant.	0.99-quant.
0	5.090	5.228			5.223		
5	5.090	5.228	5.143	5.326	5.221	4.717	5.784
10	5.090	5.228	5.011	5.487	5.222	4.671	5.846
15	5.090	5.231	4.806	5.757	5.223	4.629	5.905
20	5.090	5.240	4.494	6.223	5.224	4.607	5.946
25	5.090	5.253	4.030	6.534	5.225	4.635	5.929
30	5.090	5.247	3.921	6.534	5.226	4.804	5.736
Time t		**Benefits Linked to Surv. Prob., Case (b)**			**Benefits Linked to Act. Value, Case (b)**		
		Exp. value	**0.01-quant.**	**0.99-quant.**	**Exp. value**	**0.01-quant.**	**0.99-quant.**
0		5.184			5.231		
5		5.185	5.101	5.282	5.229	4.725	5.755
10		5.185	4.970	5.442	5.229	4.708	5.755
15		5.187	4.767	5.703	5.229	4.708	5.755
20		5.185	4.666	5.703	5.229	4.708	5.755
25		5.179	4.666	5.703	5.231	4.708	5.755
30		5.175	4.666	5.703	5.233	4.812	5.745

Table 4 quotes the initial fee π equivalent to the periodic fees in Table 1, obtained from the following condition:

$$S = b_0 \cdot a_x(0) \cdot (1 + \pi) \,. \tag{21}$$

We note that Equation (21) represents the standard approach to premium loading for annuities. As for the periodic fee, a valuation principle is required, or an explicit choice of π, given that Equation (21) has two unknowns (namely, b_0 and π). Here, we assess π consistently with what performed for ξ, i.e., solving Equation (18).

The fees quoted in Table 4 can be compared as discussed for Table 1. When comparing Table 4 with Table 1, we obtain an assessment of the overall loading implied by a given periodic fee. Among the advantages of periodic fees when compared to an upfront loading, we mention the fact that their structure is similar to that of other products, in particular financial investments; then, periodic fees can represent a solution in which individuals are more confident, being more familiar with such a pricing structure. Furthermore, as already mentioned, the application of periodic fees makes it easier to change the guarantee at some point in time, since in the event of a switch from a benefit structure to another the provider can stop applying the current fee and determine the new level according to the new underwritten guarantee, similarly to what happens (for example) in variable annuities. We also note that periodic fees may allow a revision of the pricing basis after issue, if justified by the emerging scenario and if admitted by policy conditions. In this respect, it is necessary to predefine appropriate triggers identifying situations where a revision of the fee is justified. Triggers could, for example, be related to a mortality/longevity index, or a measure of value to the provider, or the default probability of the provider. This topic deserves a specific research, and is not further developed in this paper.

Table 4. Equivalent initial fee π (to be charged to the initial capital).

Arrangement	Moderate Aggregate Deviations	Major Aggregate Deviations
Fixed benefits	0.845%	2.933%
Benefits linked to surv. prob., case (a)	0.038%	0.311%
Benefits linked to act. value, case (a)	0.155%	0.400%
Benefits linked to surv. prob., case (b)	0.076%	1.132%
Benefits linked to act. value, case (b)	0.155%	0.236%

Table 5 lists the individual reserve V_t and its components, namely $V_t^{[\text{ben}]}$ and $V_t^{[\text{fee}]}$, for a sample of times and a sample of linking arrangements. First we note that at time 0 the proportion $\frac{V_t^{[\text{fee}]}}{V_t}$ corresponds to the equivalent initial fee π; then, such a proportion decreases in time, as it is quite natural, given that the time-horizon of the obligation of the provider gradually reduces. In the table we only include some arrangements and only a scenario of moderate aggregate deviations, as other situations suggest similar comments.

Table 5. Individual reserve V_t and components $V_t^{[\text{ben}]}$, $V_t^{[\text{fee}]}$, at selected times t. Moderate aggregate deviations.

Fixed Benefits				
Time t	**Age $x+t$**	V_t	$\frac{V_t^{[\text{ben}]}}{V_t}$	$\frac{V_t^{[\text{fee}]}}{V_t}$
0	65	100.000	99.155%	0.845%
5	70	80.512	99.286%	0.714%
10	75	62.970	99.410%	0.590%
15	80	47.576	99.525%	0.475%
20	85	34.378	99.632%	0.368%
25	90	23.095	99.736%	0.264%
30	95	12.387	99.847%	0.153%
Benefits Linked to Surv. Prob., Case (a)				
Time t	**Age $x+t$**	V_t	$\frac{V_t^{[\text{ben}]}}{V_t}$	$\frac{V_t^{[\text{fee}]}}{V_t}$
0	65	100.000	99.962%	0.038%
5	70	80.614	99.968%	0.032%
10	75	63.126	99.974%	0.026%
15	80	47.750	99.979%	0.021%
20	85	34.545	99.984%	0.016%
25	90	23.242	99.988%	0.012%
30	95	12.496	99.993%	0.007%
Benefits Linked to Act. Value, Case (a)				
Time t	**Age $x+t$**	V_t	$\frac{V_t^{[\text{ben}]}}{V_t}$	$\frac{V_t^{[\text{fee}]}}{V_t}$
0	65	100.000	99.845%	0.155%
5	70	80.597	99.869%	0.131%
10	75	63.102	99.892%	0.108%
15	80	47.721	99.913%	0.087%
20	85	34.515	99.933%	0.067%
25	90	23.207	99.952%	0.048%
30	95	12.458	99.972%	0.028%

In Table 6, we quote the expected value of the Present Value of Future Profits and the Business Value at time 0, per policy issued, for the various arrangements examined so far. We first note that the magnitude of $\mathbb{E}[\text{PVFP}_0]$ is in line with that of the overall loading (see Table 4). Indeed, a large part of the profit is originated by the loading. As is well-known, large loadings impact negatively on the demand; while PVFP_0 measures the profit per policy issued, the total profit gained by the provider also depends on the pool size. This should not be disregarded when performing a profit test of the business with the purpose of identifying a cost-effective solution that may prove attractive to the individual.

As to the business value, first we note that it is not 0. As commented in Section 2.5, condition (18) is a notional reference, which is useful to set the fee consistently in different situations; not necessarily such a condition leads to a situation of a 0 expected value for the business value, as it emerges from Table 6. In such a table, the business value is quoted as a proportion of the present value of future profits. We see that such a proportion is different, depending both on the arrangement and the scenario. In view of practical implementations, the fee obtained under condition (18) could be taken as the minimum acceptable fee for the provider. An additional loading could be suggested by further assessments; for example, instead of condition (18), reference to the tail of BV_0 could be made, by setting an accepted level for the probability of incurring into a negative business value, or setting a target value for the expected business value. In any case, clearly, the loading must prove to be acceptable for individuals. Investigating this aspect is outside the scope of this paper.

Table 6. Present Value of Future Profits and Business Value (expected values), at time 0.

Arrangement	**Moderate Aggregate Deviations**		**Major Aggregate Deviations**	
	$PVFP_0^{[pool]}$	$\frac{BV_0^{[pool]}}{PVFP_0^{[pool]}}$	$PVFP_0^{[pool]}$	$\frac{BV_0^{[pool]}}{PVFP_0^{[pool]}}$
Fixed benefits	0.820	25.160%	2.713	29.071%
Benefits linked to surv. prob., case (a)	0.034	52.960%	0.341	28.146%
Benefits linked to act. value, case (a)	0.151	42.137%	0.387	23.347%
Benefits linked to surv. prob., case (b)	0.076	17.690%	1.140	24.734%
Benefits linked to act. value, case (b)	0.151	42.137%	0.246	9.468%

We finally note that the annual profits, the present value of future profits and the business value can be affected by basis risk in mortality, i.e., by a different mortality in the pool than in the reference population; however, such an aspect is not included in the assessments summarized in this section.

4. Conclusions

In this paper, we investigate annuity designs in which the benefit amount is adjusted in time in relation to a given mortality/longevity experience, compared to a chosen benchmark. Such designs imply a new definition of the longevity guarantee, which deserves attention, given that individuals prove to be dissatisfied with traditional annuities, but need to obtain longevity protection in the private market.

In this paper, in particular, we are concerned with a pricing structure which is innovative for an annuity product. Instead of the traditional upfront single loading, we consider periodic fees, which seem more versatile to introduce opportunities of flexibility into the product. We consider a periodic fee charged year by year to the policy fund value, and we show that this identifies a discount factor, to be used for pricing and reserving. Trying to match traditional with market pricing rules, we assess the periodic fee using a condition expressed in terms of business value. This way, the fees incorporate an allowance for both the expected profit and the risk retained by the provider.

Future steps in the research may concern an assessment of individual preferences in respect of the alternative linking solutions. The business value for the provider could be further examined, by addressing the demand function, as well as the limited liability put option. The implications of switching between alternative linking rules or guarantees require a specific study, as well as the possibility of updating the periodic fee after issue. Addressing a pool consisting of multiple cohorts or heterogeneous in other respects is also significant, in particular to detect possible smoothing effects if the linking coefficient accounts for the mortality experienced over different cohorts. An explicit pricing of the guarantees is a topic to further develop. In this regard, modelling guarantees as financial options offers the possibility to test pricing models developed in that field. Matching the mortality/longevity with a financial linking should also be considered, as most annuities in the market are participating in respect of the return on investments.

Funding: This research received no external funding.

Institutional Review Board Statement: Not applicable.

Informed Consent Statement: Not applicable.

Data Availability Statement: Data is contained within the paper, as they are entirely simulated on the assumptions stated.

Acknowledgments: The author wish to thank the anonymous referees for their constructive comments and suggestions.

Conflicts of Interest: The author declares no conflict of interest.

References

Andersen, Carsten, and Peter Skjodt. 2007. Pension institutions and annuities in Denmark. *Policy Research Working Paper, The World Bank*. Washington, DC: World Bank.

Bacinello, Anna Rita, Pietro Millossovich, and An Chen. 2018. The impact of longevity and investment risk on a portfolio of life insurance liabilities. *European Actuarial Journal* 8: 257–90. [CrossRef]

Bacinello, Anna Rita, Pietro Millossovich, Annamaria Olivieri, and Ermanno Pitacco. 2011. Variable annuities: A unifying valuation approach. *Insurance: Mathematics and Economics* 49: 285–97. [CrossRef]

Bernhardt, Thomas, and Catherine Donnelly. 2019. Modern tontine with bequest: Innovation in pooled annuity products. *Insurance: Mathematics and Economics* 86: 168–88. [CrossRef]

Blackburn, Craig, Katja Hanewald, Annamaria Olivieri, and Michael Sherris. 2017. Longevity risk management and shareholder value for a life annuity business. *ASTIN Bulletin* 47: 43–77. [CrossRef]

Bravo, Jorge Miguel, and Najat El Mekkaoui de Freitas. 2018. Valuation of longevity-linked life annuities. *Insurance: Mathematics and Economics* 78: 212–29. [CrossRef]

Cairns, Andrew J. G., David P. Blake, Amy Kessler, and Marsha Kessler. 2020. The Impact of COVID-19 on Future Higher-Age Mortality. May 19. Available online: https://ssrn.com/abstract=3606988 (accessed on 3 August 2021). [CrossRef].

Chen, An, and Manuel Rach. 2019. Options on tontines: An innovative way of combining tontines and annuities. *Insurance: Mathematics and Economics* 89: 182–92.

Chen, An, Manuel Rach, and Thorsten Sehner. 2020. On the optimal combination of annuities and tontines. *Astin Bulletin* 50: 95–129. [CrossRef]

Chen, An, Montserrat Guillen, and Manuel Rach. 2021. Fees in tontines. *Insurance: Mathematics and Economics* 100: 89–106.

Chen, An, Peter Hieber, and Jakob K. Klein. 2019. Tonuity: A novel individual-oriented retirement plan. *ASTIN Bulletin* 49: 5–30. [CrossRef]

Davidoff, Thomas, Jeffrey R. Brown, and Peter A. Diamond. 2005. Annuities and Individual Welfare. *American Economic Review* 95: 1573–90. [CrossRef]

Denuit, Michel, Steven Haberman, and Arthur Renshaw. 2011. Longevity-indexed life annuities. *North American Actuarial Journal* 15: 97–111. [CrossRef]

Donnelly, Catherine. 2015. Actuarial fairness and solidarity in pooled annuity funds. *ASTIN Bulletin* 45: 49–74. [CrossRef]

Donnelly, Catherine, Montserrat Guillén, and Jens Perch Nielsen. 2013. Exchanging uncertain mortality for a cost. *Insurance: Mathematics and Economics* 52: 65–76. [CrossRef]

Duffie, Darrell. 2001. *Dynamic Asset Pricing Theory*, 3rd ed. Princeton: Princeton University Press.

Hanbali, Hamza, Michel Denuit, Jan Dhaene, and Julien Truffin. 2019. A dynamic equivalence principle for systematic longevity risk management. *Insurance: Mathematics and Economics* 86: 158–67. [CrossRef]

Lee, Ronald, and Lawrence Carter. 1992. Modelling and forecasting US mortality. *Journal of the American Statistical Association* 87: 659–75.

McKever, Kent. 2009. A short history of tontines. *Fordham Journal of Corporate and Financial Law* 15: 491–521.

Milevsky, Moshe A. 2014. Portfolio choice and longevity risk in the late Seventeenth century: A re-examination of the first English tontine. *Financial History Review* 21: 225–58. [CrossRef]

Milevsky, Moshe A. 2020. Is COVID-19 a Parallel Shock to the Term Structure of Mortality? Available online: https://moshemilevsky.com/wp-content/uploads/2020/05/MILEVSKY_20MAY2020_AMAZON.pdf (accessed on 3 August 2021).

Milevsky, Moshe A., and Thomas S. Salisbury. 2015. Optimal retirement income tontines. *Insurance: Mathematics and Economics* 64: 91–105. [CrossRef]

Olivieri, Annamaria, and Ermanno Pitacco. 2009. Stochastic mortality: The impact on target capital. *ASTIN Bulletin* 39: 541–63. [CrossRef]

Olivieri, Annamaria, and Ermanno Pitacco. 2020a. Linking annuity benefits to the longevity experience: Alternative solutions. *Annals of Actuarial Science* 14: 316–37. [CrossRef]

Olivieri, Annamaria, and Ermanno Pitacco. 2020b. Longevity-Linked Annuities: How to Preserve Value Creation against Longevity Risk. In *Life Insurance in Europe*. Edited by M. Borda, S. Grima and I. Kwiecień. Financial and Monetary Policy Studies. Berlin: Springer, vol. 50, pp. 103–26.

Peijnenburg, Kim, Theo Nijman, and Bas J. M. Werker. 2016. The Annuity Puzzle Remains a Puzzle. *Journal of Economic Dynamics and Control* 70: 18–35. [CrossRef]

Piggott, John, Emiliano A. Valdez, and Bettina Detzel. 2005. The simple analytics of a pooled annuity fund. *The Journal of Risk and Insurance* 72: 497–520. [CrossRef]

Pitacco, Ermanno. 2016. Guarantee structures in life annuities: A comparative analysis. *The Geneva Papers on Risk and Insurance—Issues and Practice* 41: 78–97. [CrossRef]
Qiao, Chao, and Michael Sherris. 2013. Managing systematic mortality risk with group self-pooling and annuitization schemes. *The Journal of Risk and Insurance* 80: 949–74.
Richter, Andreas, and Frederik Weber. 2011. Mortality-Indexed annuities. Managing longevity risk via product design. *North American Actuarial Journal* 15: 212–36. [CrossRef]
Stamos, Michael Z. 2008. Optimal consumption and portfolio choice for pooled annuity funds. *Insurance: Mathematics and Economics* 43: 56–68. [CrossRef]
Weinert, Jan Hendrik, and Helmut Gründl. 2021. The modern tontine. *European Actuarial Journal* 11: 49–86. [CrossRef]
Yaari, Menahem E. 1965. Uncertain lifetime, life insurance, and the theory of the consumer. *The Review of Economic Studies* 32: 137–50. [CrossRef]

risks

MDPI

Article

Disruption of Life Insurance Profitability in the Aftermath of the COVID-19 Pandemic

Maria Carannante [1,*,†], Valeria D'Amato [1,†], Paola Fersini [2,†], Salvatore Forte [3,†] and Giuseppe Melisi [4,†]

[1] Department of Pharmacy, University of Salerno, Via Giovanni Paolo II, 132, 84084 Fisciano, Italy; vdamato@unisa.it
[2] Department of Business and Management, Luiss Guido Carli, Viale Romania, 32, 00197 Rome, Italy; pfersini@luiss.it
[3] Faculty of Law, Giustino Fortunato University, Via Raffaele Delcogliano, 82100 Benevento, Italy; s.forte@unifortunato.eu
[4] Department of Law, Economics, Management and Quantitative Methods, University of Sannio, Piazza Guerrazzi, 82100 Benevento, Italy; gimelisi@unisannio.it
* Correspondence: mcarannante@unisa.it
† These authors contributed equally to this work.

Abstract: Life insurance profitability depends on reliable mortality risk projections and pricing. While the COVID-19 pandemic has caused disruptions around the world, this is a temporary mortality shock likely to dissipate. In this paper, we investigate the long-run impact of COVID-19 on life insurance profitability. Due to the long-run dynamics of the mortality characterised by a decreasing effect of the COVID-19 mortality acceleration, we suggest proactive mortality risk management by implementing prompt premium adjustments, in order to increase the resilience of the business.

Keywords: SCR; profitability; annuity; mortality projections

Citation: Carannante, Maria, Valeria D'Amato, Paola Fersini, Salvatore Forte, and Giuseppe Melisi. 2022. Disruption of Life Insurance Profitability in the Aftermath of the COVID-19 Pandemic. *Risks* 10: 40. https://doi.org/10.3390/risks10020040

Academic Editors: Anna Rita Bacinello and Nadine Gatzert

Received: 8 November 2021
Accepted: 3 February 2022
Published: 11 February 2022

Publisher's Note: MDPI stays neutral with regard to jurisdictional claims in published maps and institutional affiliations.

1. Introduction

Aside from the social and health consequences of COVID-19, the pandemic has led to economic and market shocks. Interest rates and equity markets have declined, credit spreads have widened, and volatility has increased. The additional volatility in global markets affecting the value of equity, fixed investments, and low interest rate income has led to the need to implement unconventional monetary policy measures, such as negative rates, large asset purchase programmes, forward guidance, and targeted liquidity provision measures (ECB 2021). Likewise, the impact of COVID-19 on the insurance industry risks is becoming severe.

Insurance companies are required to investigate the potential disruption across the business caused by the pandemic. Indeed, the pandemic is likely to disrupt investments, finance, capital, underwriting, claims, and actuarial functions in several business areas. Over the next few months, due to the increasing uncertainty around new business and underwriting, the appetite for new insurance products may decline, as consumers face increasing temporary or permanent unemployment, potential loss of income, and general market volatility. Cash flow expectations over the next years also depend on global equity markets that have seen reduced investment returns. "The insurance sector must deal with challenging market conditions and maintain operations, while at the same time protecting employees and policyholders" (EIOPA 2020a). The decline in asset liquidity and the increase in overdue liabilities may cause a decrease in assets relative to liabilities (EIOPA 2020b).

According to Karlsson (2020), the pandemic may have seriously affected the operation of European insurance companies, by representing a serious threat for the solvency stability. Understanding how the COVID-19 pandemic has affected insurance companies is crucial especially in light of the "double-hit" scenario characterised by a resurgence of the virus,

reported by previous stress test exercises by Moody's Analytics (2020). The insurance industry's profitability is linked to operational and financial management both of them suffering the effect of the pandemic. The future financial cash flows could be affected by the uncertainty and pessimism due to the pandemic, the spillover effect of the overall decline in the market, leading to investors' herd behaviour to negative abnormal returns. Conversely, in Farooq et al. (2021), the authors take also into account a possible opposite effect of the COVID-19 outbreak of the increasing demand for insurance contracts and premiums. From the operational management point of view, insurers are responding to the widening pandemic on multiple fronts as health insurance, non-life and life offices, some classes of business being most exposed to coronavirus and adversely impacted. Some business classes are more exposed to the COVID-19 outbreak than the others. The portfolio concentration of higher risk business classes seriously threatens the insurance companies, by suggesting more well-diversified portfolios.

In particular, the health insurance premiums continued to grow steadily after the outbreak as pointed out in Wang et al. (2020) and Nguyen and Vo (2020). In particular, in correspondence to the profound shock to the health care systems due to the surge of COVID-19, major commercial health insurance companies increased operating income from decreased care utilization: for instance UnitedHealth Group, CVS Health Care Benefits Segment, Anthem, and Humana all saw operating earnings over 200% of their 2019 amount, much of which has been attributed to delays in routine care (Bryan and Tsai 2021).

Focusing exclusively on aspects related to non-life insurance, the insurers tried to adapt the policies to the new challenges exposed by the crisis in response to the COVID-19, specifically by providing the business interruption (BI) insurance, the crisis having been reaffirmed the importance of business continuity planning. With regard to property and casualty (P&C), the impact on business and coverage has been profound, estimated at USD 80 to USD 100 billion in the case of business interruption (BI) coverage, a critical area of concern under COVID-19 (Marsh 2021). In general, according to an interesting study by Gründl et al. (2020), the insurance industry alone will not be able to provide sufficient coverage for business interruption losses like those occurring during the COVID-19 crisis, as the markup of a hypothetical insurance contract in the top 20% of the realised price markups of NatCat insurance would lead an expected shortfall of the loss distribution which is about 100 times higher. In the automobile insurance field, reductions in driving and accident claims led to premium refunds early during the pandemic by causing well-documented premium changes (Scism 2020).

The uncertain mortality and morbidity events related to COVID-19 are also affecting the life insurance and annuity business. Mortality improvements over the past several years have been muted, likely to continue mainly as a combined effect of the temporary mortality shock due to the pandemic. Indeed, the debate is ongoing on how temporarily stressed mortality rates change post-COVID-19 mortality rates (Andresson and Lindholm 2021) and the mortality term structure (Milesky 2021; Spiegelhalter 2020).

The scarce literature on the topic enlightens that life insurance companies have been forced to significantly adjust life insurance premiums or offerings to account for the increased mortality risk (Pułanska 2021).

Harris et al. (2021) suggest minimal observable premium adjustments through February 2021. They find evidence that premiums raised "for unhealthy older smokers, and policies offered to individuals age 75 and above were differentially removed from the market". Overall, small adjustments in the life business offering correspond to increases in mortality risk perceived from insurers as modest in the short run, by implicitly assuming no effects in the long-run perspective. To the best of our knowledge, in light of the mortality stress temporariness, the academic literature has not extensively focused on the possible changes in profitability margins for life insurance companies.

The novelty of our research properly consists in examining the long-run impact of COVID-19 on life insurance profitability. We suggest connecting the profitability analysis

to the temporary excess of deaths due to the COVID-19 which will be softened in the long run by the structural improvements of longevity projections (Carannante et al. 2021b).

Actuarial assumptions and forecasting are crucial for an effective mortality risk management strategy and preserving the expected cash flows over the coming years. Understanding the impact of future structural improvement scenarios, as well as increased short-term mortality combined with heightened attention to social and health care improvements in the longer term will allow life insurance offices to maintain profitability. In other words, proactive mortality risk management, which requires revising mortality assumptions to make timely decisions in reserves and forecasting, will enable the insurance industry to build resilience and tackle the immediate challenge of positioning the business for the future. The remainder of the paper is structured as follows. In Section 2, we introduce the issue of profitability, define profit resilience in life insurance, and how to quantify it with particular reference to annuity contracts. Section 3 details the numerical applications, focusing on the mortality, financial, and cash flow aspects. Section 4 concludes.

2. Profit Resilience in Annuity

We analyse the expected profit of a variable immediate annuity contract.

The general actuarial model used for the evaluation of the insurance contract and to estimate the future cash flows belongs to the life insurance methodologies, which represent the actuarial practice in many countries, according to a time-discrete approach, which, see Olivieri and Pitacco (2015).

The contract under consideration is an immediate single premium annuity with a revalued instalment for an individual of age x at time 0 in which the contract is underwritten. Obviously, since it is an immediate annuity, the single premium is the only possible alternative. In this case, in order to implement the profit-sharing mechanism that prevails in the Italian market, we implement an actuarial model with cliquet guarantees with annual returns recognised to policyholders depending only on the most recent performance of an investment portfolio. The contract valuation can the be reduced to that of a sequence of one-year forward-start options, see Bacinello (2001, 2003a, 2003b).

To assess the effects depending on age, we consider policyholders aged 20, 40, and 60. In the case of an annuity, the instalment is constant and the pure premium for an individual at age x is given by:

$$P_x \;=\; R \cdot \sum_{t=1}^{\omega-x-1} \frac{l_{x+t}}{l_x} \cdot (1+i)^{-t} \tag{1}$$

where:
P_x is the pure premium based on the first-order mortality basis table;
R is the constant instalment paid by the insurance company during the policyholder's life with a value agreed at contract time;
l_x is the number of policyholders at age x deduced by the first-order mortality basis table used to compute the pure premium;
i is the technical rate;
ω is the extreme age, thus $\omega - 1$ is the last age for a policyholder and $l_\omega = 0$.

Since we consider a variable annuity, the pure premium is defined as:

$$P_x \;=\; R_0 \cdot \sum_{t=1}^{\omega-x-1} \frac{l_{x+t}}{l_x} \cdot (1+i)^{-t} \tag{2}$$

where:
R_0 is the first instalment defined at contract time.

The following instalments are variable based on segregated fund returns with the following formula:

$$R_t = R_{t-1} \cdot (1 + r_t) \tag{3}$$

where:
R_t is the instalment at time t if the policyholder is alive;
R_{t-1} is the instalment at time $t-1$ if the policyholder is alive;
r_t is the downgraded rate of return used to vary the rate based on the segregated fund return rate using the following formula:

$$r_t = \max\left(\frac{g_t - i - mt}{1+i},\ mg\right) \tag{4}$$

where:
g_t is the segregated fund return rate for the period $(t-1, t)$ recognised at time t;
mt is the rate retained by the insurance company on the segregated fund return;
mg is the minimum guaranteed rate of the segregated fund.

Once the pure premium and method of variation of the instalment are determined, the expenses loaded premium at age x can be calculated:

$$PT_x = \frac{P_x \cdot (1+\alpha)}{(1-\beta)} \tag{5}$$

where:
α is the loading rate of the annuity payment;
β is the loading rate of the administrative costs.

The expected profit is defined as:

$$E(U)_{x,k} = PT_{x,k} - BE_{x,k} - CoC_{x,k} \tag{6}$$

where:
$E(U)_{x,k}$ is the present expected profit at time k when the contract is purchased by an individual at age x;
$PT_{x,k}$ is the expenses loaded premium at time k for a policyholder at age x; $BE_{x,k}$ is the best estimate of the contract liability a time k for a policyholder at age x according to Solvency II principles, by considering the financial options and guarantees to include in the insurance contract;
$CoC_{x,k}$ is the cost of capital due to the allocation of the capital requirement under Solvency II for a contract sold a time k for a policyholder at age x.
Cost of capital, $CoC_{x,k}$, is determined according to Solvency II requirements:

$$CoC_{x,k} = \partial \cdot \sum_{l=1}^{m} \frac{C \cdot SCR_{x,k+l-1}}{\left(1 + i_{rf}(k, k+l)\right)^t} \tag{7}$$

where:
∂ is the cost of capital rate increase;
$i_{rf}(k, k+l)$ is the risk-free rate for the time horizon $(k, k+l)$;
C is the cost of capital rate, that is, the unrealised extra-return compared to the risk-free rate;
$SCR_{x,k+l-1}$ is the solvency capital requirement for the time horizon $k+l-1$ and a policyholder of age x;
m is the number of years when the risk expires in terms of capital requirements.

To determine $CoC_{x,k}$, we consider the EIOPA (2014) standard formula with particular reference to the market, longevity, expense, and operational risks. To note is that in determining $RORAC$, the overall SCR is considered, while in determining CoC only non-hedgeable risks are considered.

Furthermore, important to note is that $BE_{x,k}$ is equal to the present expected value of the liability if considering a reliable technical basis, depending on the mortality table. We assume that the realistic projected mortality table is obtained using the stochastic mortality model considering the scenario without the effects of the COVID-19 pandemic, and the scenario with an acceleration of mortality due to COVID-19 (Carannante et al. 2021a, 2021b); a reliable administrative expenses assumption, that is, an annual cost per contract; the risk-free rate maturity structure for discounting contract cash outflows; a stochastic model to determine g_t, that is, the segregated fund return rate for the period $(t-1, t)$ recognised at time t, which allows determining the variation of the annuity instalment R_t, using the Vasicek model.

The Vasicek model is largely used to evaluate the short-term evolution of a return rate, using a stochastic differential equation according to which shocks fluctuate around a long-term value as a function of volatility (for further details, see Vasicek (1977)):

$$dr_t = (\alpha + \beta r_t)dt + \sigma dZ_t \tag{8}$$

where:
r_t is the short-term interest rate at time t;
α is the mean-reverting force of the shocks;
β is the long-term interest rate mean;
σ is the market volatility;
Z_t is a Wiener process.

3. Numerical Application

The application is developed by analysing several different aspects of the definition of an immediate annuity contract. The first concerns the demographic scenario that evaluates the evolution over time of mortality considering the effects of the pandemic. Second, for the financial aspect, we observe the interest rate trend on which the variation of annuity instalment will be based. Third, the cash-flow analysis allows evaluating the differences in the premium in the function of the use of baseline or accelerated mortality tables. The last is the profitability analysis that allows quantifying the extra profit due to the adjustment of the mortality table.

3.1. Demographic Scenario

The first step in evaluating profitability is to determine the demographic technical basis, that is, the individual death probabilities. In this sense, we use a stochastic model capable of projecting the probabilities of life over time. The model defines the probabilities of death with respect to two scenarios.

The baseline scenario assumes the absence of the COVID-19 pandemic, and the projections of survival probabilities are obtained through the Renshaw and Haberman (2003) estimation using the data on deaths collected in the Human Mortality Database,[1] with reference to the entire Italian population, considering the historical series from 1950 to 2017 for all ages from 0 to 100.

The alternative scenario considers the COVID-19 pandemic as a mortality acceleration factor estimated through a multiplicative model, that is, the projections of the accelerated probability of death obtained from the product between the probabilities of the basic scenario model and the multiplicative factor that depends on age x and time t.

Cairns et al. (2020) define the multiplicative factor as a negative exponential function as follows:

$$\pi(x,t) = \frac{\alpha(x)}{\rho(x,t)} exp\left(\frac{-t}{12\rho(x,t)}\right) \tag{9}$$

where:
$\alpha(x)$ is the expected proportion of deaths by COVID-19 at age x;
$\rho(x,t)$ is the expected loss of years of life expectancy at age x and time t.

The α and ρ parameters in Formula (9) are computed from the COVID-19 deaths data and the all-causes mortality data of the Italian population for the year 2020. The data are collected weekly by the Italian Health Institute[2] (ISS) and the Italian Statistical[3] (ISTAT). $\alpha(x)$ is calculated as the ratio of the number of deaths due to COVID-19 infection and the total of deaths for the age x, while $\rho(x,t)$ is calculated as the product of the life expectancy at age x and time t and the proportion of deaths due to COVID-19 at age x on the total mortality due to COVID-19. $\pi(x,t)$ is calculated as a negative exponential function, aggregating the data in a monthly granularity, and it is used as a multiplicative coefficient to recalibrate the mortality projection obtained by the Renshaw–Haberman model. Figure 1 shows the death projections by age for 2021 per 100,000 population, distinguishing between deaths due to COVID-19 and all other causes. To make the data easier to read, we report them in logarithmic scale:

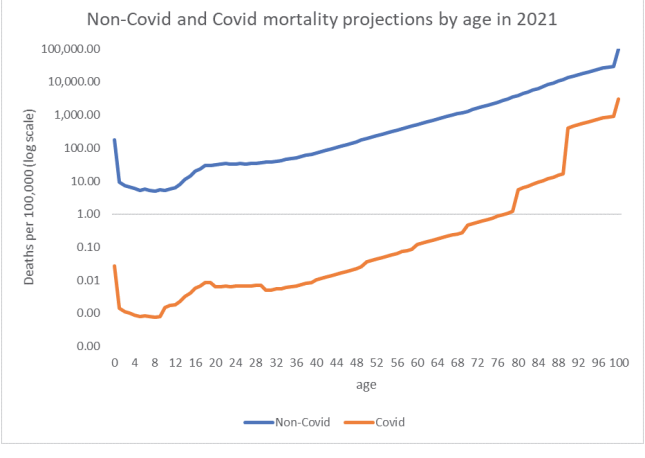

Figure 1. Non-COVID-19 and COVID-19 death projections by age for the year 2021.

As Figure 1 shows, the number of deaths from COVID-19 proportionally follows the trend in mortality for all causes of deaths, except for older ages where the proportion of deaths appears higher. This suggests a relationship between age and mortality from COVID-19, with a mortality shock currently present.

3.2. Financial Scenario

We estimate the Vasicek model parameters α, β, and σ using EURO SWAP maturing at one year (1Y) and ten years (Y10) from 31 January 2005 to 31 December 2020.[4] Figure 2 shows both the Y1 and Y10 EURO SWAP time series.

Figure 2 shows a generalised reduction in interest rates. The decreasing trend affects the values of the simulated interest rate structures using both the annuity instalments variation and the discounted cash flows best estimate. The Vasicek parameters are shown in Table 1.

As Table 1 shows, the parameter α is very close to zero, suggesting a strong persistence in the time series, as also observed in Figure 2, with no strong fluctuations with respect to the decreasing trend. The parameter β is estimated at around 1.20%, being affected by a period in which rates even exceeded 3% (up to 2009) and the most recent periods of negative rates (from 2016). The parameter σ is 0.48 suggesting quite high volatility. Therefore, according to the estimated model, a divergent trend from the mean is expected,

consistent with the most recent time interval in which rates are downward and continue to decrease with non-negligible volatility.

Figure 2. Y1 and Y10 EURO SWAP time series from 31 January 2005 to 31 December 2020.

Table 1. Vasicek parameters estimation using the Y1 and Y10 EURO SWAP time series.

Parameter	Estimation
α	0.00069
β	1.20514
σ	0.48054

3.3. Cash Flow Analysis

We perform the cash flow analysis considering the conditions shown in Table 2. Important to note is that the A62I unisex table with 50% male and 50% females is the most used by insurance companies for annuity contracts.

Table 2. Cash flow analysis variables.

Variable	Notation	Values
Contract years	k	2022, 2024, 2026, 2032
Policyholder ages	x	20, 40, 60
Mortality table	l_x	A62I unisex with 50% male and 50% female
Initial annual instalment	R_0	EUR 1000
Technical rate	i	0%
Guaranteed minimum rate	m_g	0%
Retained rate	m_t	1%
Loading rate for instalment payment	α	1.50%
Loading rate for administrative costs	β	5%
Annual management costs at time t		EUR 0.50
Annual inflation of management costs		2%
Cost of capital increasing rate	∂	1.00
Cost of capital rate	C	6%

Using these data, the segregated fund return rate is simulated based on a zero-coupon-bond forward rate at one year for the period 2022 to 2142 for a total 1000 scenarios.

Tables 3 and Tables 5–7 show the effects of COVID-19 acceleration, comparing (for an immediate annuity contract for policyholders of age x = 20, 40, and 60), the pure premium (PT), the best estimate of liability (BE), the solvency capital requirement (SCR), the cost of capital (CoC), the expected value of the profit ($E(U)$), and the $RORAC$. Table 3 relates to an annuity contract signed in 2022.

Table 3. Effects of COVID-19 for an annuity contract signed in 2022.

Year Demographic Table Individual Age	2022 Base 20	2022 Base 40	2022 Base 60	2022 Accelerated 20	2022 Accelerated 40	2022 Accelerated 60	2022 Difference 20	2022 Difference 40	2022 Difference 60
PT	73,064	52,302	31,917	73,064	52,302	31,971	0	0	0
BE	65,844	44,896	25,806	66,767	44,822	25,735	−77	−74	−71
SCR	5867	3433	2475	5792	3416	2451	−75	−17	−24
CoC	11,584	4886	2465	11,516	4852	2178	−68	−34	−287
$E(U)$	−4364	2521	3646	−4219	2628	4004	145	107	358
$E(U)/PT$	−6.0%	4.8%	11.4%	−5.8%	−5.0%	−12.5%	0.2%	0.2%	1.1%
$RORAC = E(U)/SCR$	−74.4%	73.4%	147.3%	−72.8%	76.9%	163.4%	1.5%	3.5%	16.1%

As Table 3 shows, for policyholders aged 20, the contract is at a loss even without COVID-19 acceleration. This is due to the technical basis used to determine the expenses loaded premium, already inadequate to determine future longevity of the age considered. Furthermore, the $RORAC$ is negative, and the mortality increase due to COVID-19 determines an increment of only 1.5%. For the year 2022, the pandemic acceleration causes an increase in profitability at most equal to 16.1% of $RORAC$. Furthermore, for ages 40 and 60, there is a huge profit for the insurance company even without considering the effects of the pandemic on mortality.

We further explore the profitability of annuity contracts in Table 4 showing the annual cash flows for the three ages considered for one hundred years forward, comparing the baseline mortality table, ignoring the pandemic effects, and the accelerated mortality table.

Table 4. Cash flow analysis for one hundred years forward.

t	Base 20	Accelerated 20	Base 40	Accelerated 40	Base 60	Accelerated 60
1	1051	1051	1050	1050	1046	1046
2	1051	1051	1050	1050	1041	1041
3	1052	1052	1051	1051	1036	1036
4	1053	1053	1051	1051	1030	1030
5	1054	1054	1051	1051	1023	1023
6	1054	1054	1051	1051	1016	1016
7	1055	1055	1051	1051	1008	1008
8	1056	1056	1050	1050	1000	1000
9	1057	1057	1050	1050	990	990
10	1057	1058	1049	1049	980	979
11	1058	1059	1049	1049	969	968
12	1059	1060	1048	1048	956	956
13	1060	1061	1047	1047	943	942
14	1061	1062	1046	1046	928	927
15	1062	1063	1045	1045	911	910
16	1063	1064	1043	1043	893	892
17	1063	1066	1041	1041	873	871
18	1064	1067	1039	1039	851	849
19	1065	1068	1036	1036	827	825
20	1066	1069	1033	1033	800	797
30	1070	1080	975	975	387	372
40	1056	1077	806	805	36	34
50	997	1029	395	383	19	17
70	401	416	19	19	0	0
90	20	21	0	0	0	0
100	0	0	0	0	0	0

As Table 4 for all ages, the expected cash flows for the baseline scenario and the accelerated scenario are similar, showing some differences only for very large values of t that do not affect the value of BE. Furthermore, no particular differences emerge when

comparing the *BE* distributions by age and mortality basis. The results are shown in Figures 3–5. Therefore, both in terms of expected values and variability, cash flows and *BE*s are little affected by the mortality shock due to COVID-19.

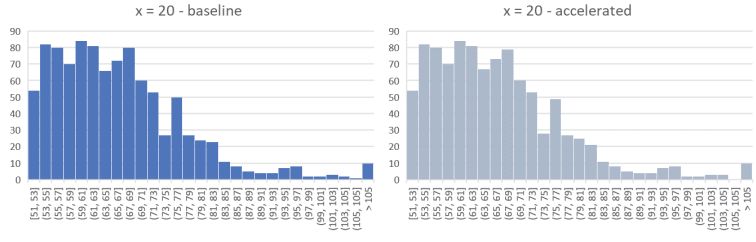

Figure 3. *BE* distribution for the baseline and accelerated mortality tables for age 20 (EUR/thousands).

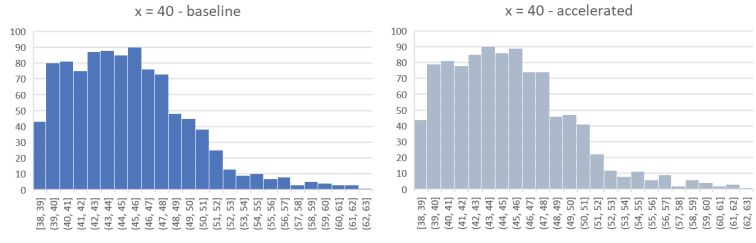

Figure 4. *BE* distribution for baseline and accelerated mortality tables for age 40 (EUR/thousands).

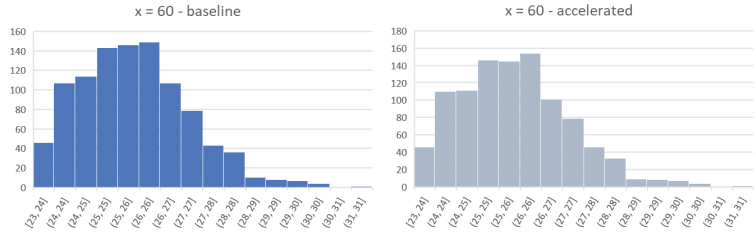

Figure 5. *BE* distribution for baseline and accelerated mortality tables for age 60 (EUR/thousands).

Table 5 shows the results of an annuity contract signed on 1 January 2024.

Table 5. Effects of COVID-19 for an annuity contract signed in 2024.

Year Demographic Table Individual Age	2024 Base 20	2024 Base 40	2024 Base 60	2024 Accelerated 20	2024 Accelerated 40	2024 Accelerated 60	2024 Difference 20	2024 Difference 40	2024 Difference 60
PT	73,063.66	52,302.43	31,916.68	73,063.66	52,302.43	31,916.68	0.00	0.00	0.00
BE	66,473.08	45,310.30	26,085.22	66,391.41	45,233.16	26,011.08	−81.67	−77.15	−74.15
SCR	5967.65	3473.89	2496.08	5892.18	3456.21	2471.78	−75.47	−17.68	−24.30
CoC	11,828.06	4971.35	2233.67	11,757.23	4936.24	2213.17	−70.84	−35.11	−20.49
$E(U)$	−5237.49	2020.77	3597.79	−5084.98	2133.03	3692.43	152.51	112.26	94.64
$E(U)/PT$	−7.2%	3.9%	11.3%	−7.0%	4.1%	11.6%	0.2%	0.2%	0.3%
$RORAC = E(U)/SCR$	−87.8%	58.2%	144.1%	−86.3%	61.7%	−149.4%	1.5%	3.5%	5.2%

As Table 5 shows, not all the contracts are in profit. For policyholders aged 20, the insurance company is at loss, with $RORAC$ −87.8%, and the adjustment of the tables to

the effects of COVID-19 allows partial recovery only at 1.5%. For policyholders aged 40 and 60, the contract always has positive expected profitability both with and without the COVID-19 acceleration adjustment. In summary, for an annuity contract signed in 2024, the COVID-19 acceleration allows increasing profitability by only 5.2% of *RORAC* for a policyholder age 60. Conversely, with very young policyholders, it does not allow full recovery of the loss due to the increase in longevity from 2022 to 2024.

Table 6 shows the effects of COVID-19 for an annuity contract signed on 1 January 2026.

Table 6. Effects of COVID-19 for an annuity contract signed in 2026.

Year Demographic Table Individual Age	2026 Base 20	2026 Base 40	2026 Base 60	2026 Accelerated 20	2026 Accelerated 40	2026 Accelerated 60	2026 Difference 20	2026 Difference 40	2026 Difference 60
PT	73,063.66	52,302.43	31,916.68	73,063.66	52,302.43	31,916.68	0.00	0.00	0.00
BE	67,114.49	45,732.18	26,368.39	67,028.23	45,651.28	26,290.94	−86.25	−80.90	−77.45
SCR	6070.58	3515.85	2517.68	5994.27	3497.69	2493.14	−76.31	−18.17	−24.54
CoC	12077.99	5058.48	2270.46	12003.72	5022.09	2249.39	−74.27	−36.40	−21.07
$E(U)$	−6128.82	1511.77	3277.82	−5968.30	1629.07	3376.35	160.52	117.30	98.52
$E(U)/PT$	−8.4%	2.9%	10.3%	−8.2%	3.1%	10.6%	0.2%	0.2%	0.3%
$RORAC = E(U)/SCR$	−101.0%	43.0%	130.2%	−99.6%	46.6%	135.4%	1.4%	3.6%	5.2%

As Table 6 shows, for a policyholder aged 20, the insurance company is at loss with huge negative $RORAC$ −101.0%, which reduces only to −99.6% considering the COVID-19 effects. Contracts with policyholders aged at least 40 maintain reduced profitability compared to the previous two years but are still satisfactory, even more so considering an increase in $RORAC$ with acceleration due to COVID-19 of at least 3.6%. In summary, considering the data relating to the year 2026, the acceleration of mortality due to COVID-19 entails a negligible increase in profitability compared to the increase in longevity from the year 2022 to the year 2026.

Table 7 shows the results for an annuity contract signed on 1 January 2032.

Table 7. Effects of COVID-19 for an annuity contract signed in 2032.

Year Demographic Table Individual Age	2032 Base 20	2032 Base 40	2032 Base 60	2032 Accelerated 20	2032 Accelerated 40	2032 Accelerated 60	2032 Difference 20	2032 Difference 40	2032 Difference 60
PT	73,063.66	52,302.43	31,916.68	73,063.66	52,302.43	31,916.68	0.00	0.00	0.00
BE	69,134.24	47,057.37	27,254.28	69,033.10	46,964.43	27,166.33	−101.14	−92.94	−87.95
SCR	6395.46	3648.20	2585.94	6316.43	3628.56	2560.78	−79.03	−19.64	−25.16
CoC	12867.52	5332.32	2385.92	12782.22	5291.93	2363.12	−85.29	−40.39	−22.80
$E(U)$	−8938.10	−87.26	2276.48	−8751.67	46.07	2387.24	186.43	133.32	110.76
$E(U)/PT$	−12.2%	−0.2%	7.1%	−12.0%	0.1%	7.5%	0.3%	0.3%	0.3%
$RORAC = E(U)/SCR$	−139.8%	−2.4%	88.0%	−138.6%	1.3%	93.2%	1.2%	3.7%	5.2%

As Table 7 shows, for policyholders aged 20, the insurance company is heavily at loss with a reduction in $RORAC$ compared to the previous decade (2022) equal to 65%. For all the ages considered in the year 2032, the acceleration of mortality due to Covd-19 entails a negligible increase in profitability compared to the increase in longevity from the year 2022 to the year 2032. Considering a balanced portfolio in terms of the age of policyholders, the empirical evidence suggests that in 2032, insurance companies need to update the currently used A62I mortality table.

3.4. Focus on Profitability

Figures 6–8 show the *RORAC* indicator trend by year for the three ages considered. To note is that for all ages analysed, the impact of COVID-19 is very modest and decreases over the years, except for policyholders aged 60, for which in 2022 the impact of COVID-19 determines a consistent reduction in *RORAC*. In addition, as noted in Tables 3 and 5–7, for all three ages considered, the *RORAC* trend decreases with significant variations over the years. This trend confirms the significant weight of the longevity risk in the management of annuities.

Furthermore, looking more deeply at the longevity risk and how much it can affect profitability, the distributions of expected profit and *RORAC* for the year 2022 shown in Figures 9–11 indicate high variability of profit and consequently *RORAC* in all scenarios considered and for all ages:

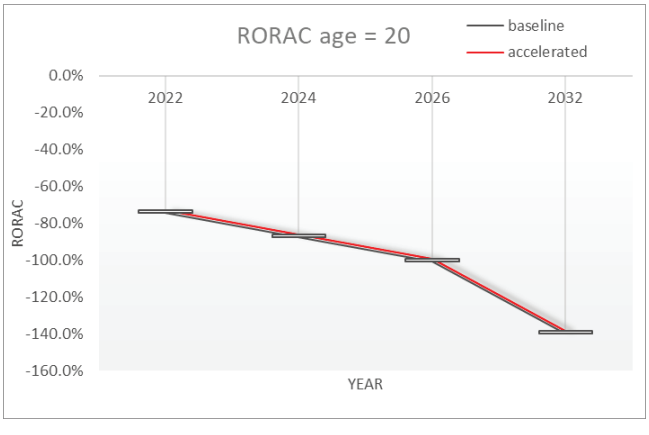

Figure 6. *RORAC* by year for a policyholder aged 20.

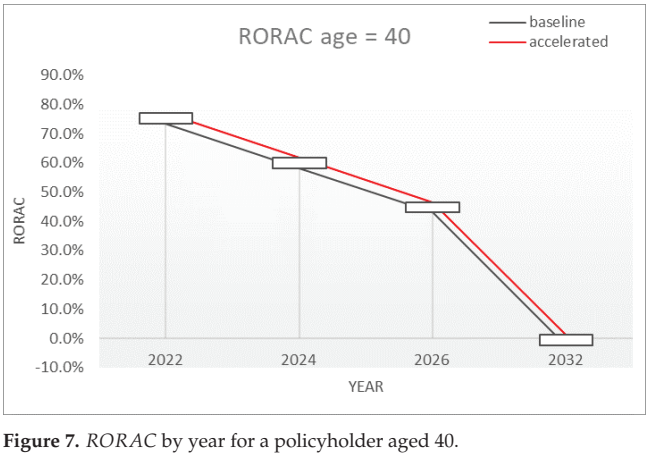

Figure 7. *RORAC* by year for a policyholder aged 40.

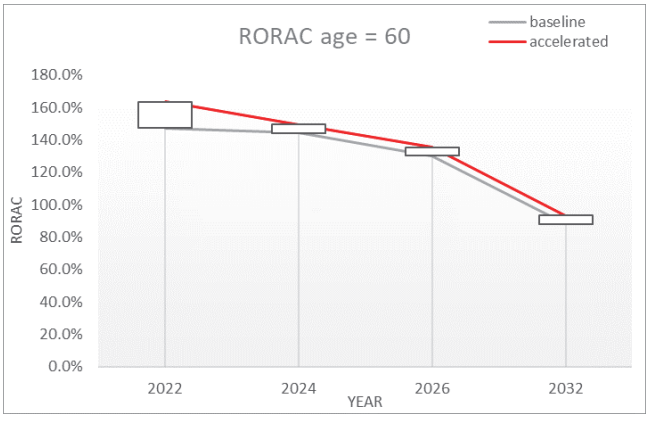

Figure 8. *RORAC* by year for a policyholder aged 60.

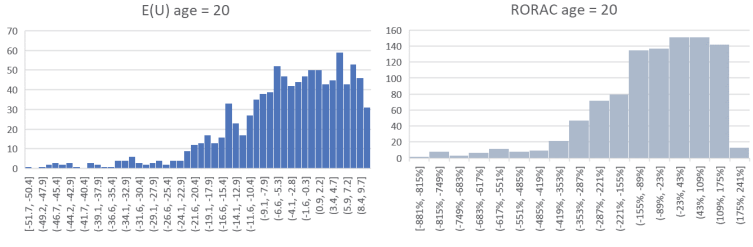

Figure 9. Expected profit and *RORAC* distributions for a policyholder aged 20.

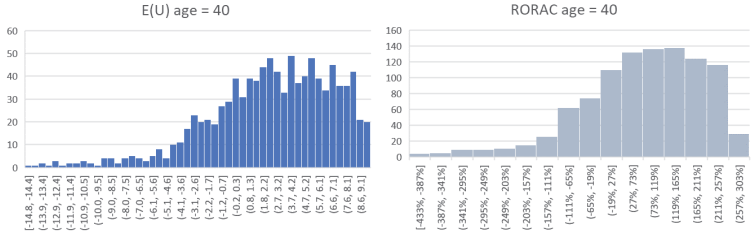

Figure 10. Expected profit and *RORAC* distributions for a policyholder aged 40.

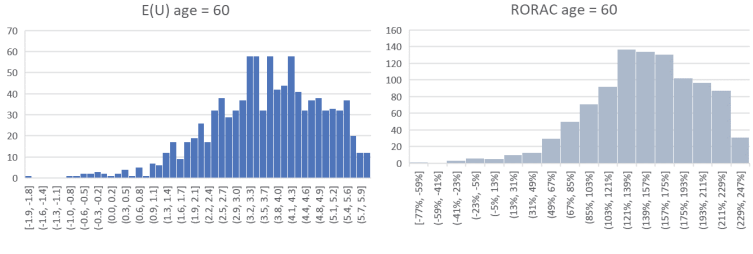

Figure 11. Expected profit and *RORAC* distributions for a policyholder aged 60.

Estimating the expected profit and relative distribution, we obtain the probability of a negative profit, which could prove very useful to understand that even in the presence of a positive profit value, the risk of obtaining a negative result could be high. For example, taking into account the 2022 contracts, the probability of a negative profit is equal to 0.596 for policyholders at age 20, 0.253 at age 40, and 0.012 at age 60. Therefore, while for policyholders aged 60 the probability of obtaining a negative result is negligible, for policyholders aged 40, despite a very positive value of profit and *RORAC*, this probability is to be taken into account and confirms the importance of a good pricing and longevity risk monitoring system.

3.5. Discussion

The analysis of profitability is of great practical and policy value to study how the pandemic affects the insurance market. In particular, the study provides useful indications we can re-formulate as valuable recommendations. In order to increase the resilience of the life insurance business to the COVID-19 pandemic, proactive risk management is required. We suggest taking into account the profitability in the long run by implementing prompt premium adjustments. Due to the long-run dynamics of the mortality characterised by a decreasing effect of the COVID-19 acceleration, accurate safety loadings are necessary to guarantee stability for the insurance industry. In order to evaluate the effects of the acceleration of mortality in the life insurance business, we initially define a framework to operate. In this sense, we analyse the demographic scenario, which shows a greater acceleration of mortality due to COVID-19 for older ages, and the financial scenario, which shows that interest rates tend to decrease in the long term with a certain volatility. The two scenarios make it possible to define the contractual conditions of the immediate annuities for which the cash flow and profitability from 2022 to 2032 are analysed. With regard to cash flow, it is observed that the acceleration in mortality does not generate large differences, with the exception of the older ages and considering a rather long period of time. Regarding profitability, it is noted that age and time are the determining factors to be taken into consideration. In particular, if we consider a short time horizon, adapting the mortality tables to the acceleration from COVID-19 allows obtaining greater profitability for the older ages, while it does not allow to remedy the inadequacy of the tables themselves for the older ages, recording a loss. Similarly, the broader the time horizon, the lower the margin obtained from the use of tables that take acceleration into account while the improvement in longevity tapers the margin more and more, increasing the losses for the younger age and also recording losses for the middle ages. In accordance with our results, Harris et al. (2021) observe an adjustment in life insurance market profitability in presence of some particular health condition or old age, although to a limited extent.

4. Concluding Remarks

The pandemic phenomenon has a non-material impact on the profitability of annuity contracts as it has an instant impact since in a pandemic event there is an increase in mortality only in the first years of the contract and therefore for medium and long-term contracts such as annuities, post-shock mortality quickly tends to mortality without considering the COVID-19 effect.

Therefore, for these contracts, with medium and long durations, this effect with an accidental and unsystematic nature leads to non-material increases in profitability with respect to the same contracts without COVID-19 effects with the same contractual conditions.

On the other hand, as regards the opposite phenomenon, that is the longevity risk, it is a systematic risk that has a material impact over the entire duration of the contract and for such contracts, with medium or long durations, this risk is significant. In fact, if we consider a contract with a very young insured, for example with age $x = 20$, we always have negative returns that increase in material measure passing from the marketing year 2022 to the year 2032 or to the year 2042. For example if we consider the RORAC for $x = 20$

passing from the year 2022 to 2024 we have a contract always with negative profitability and a loss of RORAC without the COVID-19 effect equal to 13.4% while with the COVID-19 effect this loss of RORAC is equal to 13.5%. If we consider the year 2026 the differences become even more significant, in fact without the COVID-19 effect there is a loss of RORAC equal to 26.6% while with the COVID-19 effect this loss is equal to 26.8%.

Therefore, we can conclude that in just two calendar years, the longevity risk and therefore the increase in the life expectancy of the insured lead to an increase in losses for the insurer of approximately 13% while considering four years this increase in loss exceeds 26%.

These conclusions are also fully consistent with the same ones in the paper by Carannante et al. (2021c) in which the authors analyse a pure mortality risk insurance product such as term insurance which cover the opposite risk compared to those of annuities.

Even for these contracts, the acceleration of mortality from COVID-19 would lead to price increases with the same profitability always lower than 0.5%.

Besides in the paper we show that COVID-19 would bring material increases in profitability for insurance companies only in the case of old insureds, in fact for instance if we consider in the commercial year 2022 an insured 60 years old we have, after COVID-19 mortality shock, a RORAC increase equal to 16%, but in our opinion, this case is not real because if we analyse a real new business Italian insurance portfolio the majority of the insured are younger than 50 years old. We conclude that from a theoretical point of view the COVID-19 phenomenon has brought benefits to insurers for non-young policyholders but from a real point of view given the real age of the policyholders of annuity insurance portfolios, the profit margins are not material.

Therefore, the study confirms that it is much more important how the estimated trend of post-COVID-19 mortality realigns to what was predicted in the ante-COVID-19 situation, rather than the shock level recorded in a very short period (1–2 years), i.e., during the pandemic.

The effects of COVID-19 are expected to continue hitting some property-casualty lines harder than others. Nevertheless, pension schemes and annuity portfolios are also exposed to the aftermath of the pandemic. According to Deloitte (2021), the growth and profitability in annuities and many non-term life insurance products will likely be impacted throughout 2021 and beyond with persistently low interest rates. The profitability of life offices also seems to be threatened by the temporary shock of mortality.

In light of these considerations, our paper explores how the COVID-19 pandemic mortality shock might affect the profitability of insurance companies considering immediate annuity contracts, as well as the financial and actuarial aspects. Unlike the commonly assumed post-pandemic effects, COVID-19 mortality acceleration did not and will not bring insurance companies a huge increase in annuity contract profitability, considering a risk portfolio with different ages.

On the other hand, the increasing longevity issue will remain the main problem over the years and will lead insurance companies to adjust their mortality tables with a frequency that never exceeds five years, particularly if the portfolio is composed of a rather low mean policyholder age (see Supplementary Materials).

Supplementary Materials: The following are available online at https://www.mdpi.com/article/10.3390/risks10020040/s1.

Author Contributions: Conceptualization, V.D. and S.F.; methodology, S.F. and P.F.; software, G.M. and M.C.; validation, V.D. and M.C.; formal analysis, S.F., G.M.; data curation, M.C. and G.M.; writing—original draft preparation, S.F. and V.D.; writing—review and editing, M.C. All authors have read and agreed to the published version of the manuscript.

Funding: This research received no external funding

Data Availability Statement: Publicly available datasets were analysed in this study. Human Mortality Database data can be found here: https://www.mortality.org/, accessed on 28 September 2021. Euroswap data can be found here: https://www.eurex.com/ex-en/markets/int/eur-swap/eur-swap-fut/, accessed on 25 September 2021.

Conflicts of Interest: The authors declare no conflict of interest.

Notes

[1] https://www.mortality.org/, accessed on 28 September 2021.
[2] https://www.epicentro.iss.it/coronavirus/sars-cov-2-decessi-italia, accessed on 5 October 2021.
[3] https://www.istat.it/it/archivio/240401, accessed on 5 October 2021.
[4] https://www.eurex.com/ex-en/, accessed on 25 September 2021.

References

Andersson, Patrik, and Mathias Lindholm. 2021. A Note on Pandemic Mortality Rates. Available online: https://ssrn.com/abstract=38058811 (accessed on 11 October 2021).

Bacinello, Anna Rita. 2001. Fair pricing of life insurance participating policies with a minimum interest rate guaranteed. *ASTIN Bulletin* 31: 275–97. [CrossRef]

Bacinello, Anna Rita. 2003a. Fair valuation of a guaranteed life insurance participating contract embedding a surrender option. *The Journal of Risk and Insurance* 70: 461–87. [CrossRef]

Bacinello, Anna Rita. 2003b. Pricing guaranteed life insurance participating policies with annual premiums and surrender option. *North American Actuarial Journal* 7: 1–17. [CrossRef]

Bryan, Ana Ferguson, and Thomas C. Tsai. 2021. Health Insurance Profitability during the COVID-19 Pandemic. *Annals of Surgery* 273: 88–90. [CrossRef] [PubMed]

Cairns, Andrew J. G., David Blake, Amy R. Kessler, and Marsha Kessler. 2020. *The Impact of COVID-19 on Future Higher-Age Mortality*. London: Pensions Institute. Available online: https://papers.ssrn.com/sol3/papers.cfm?abstract$_$id=3606988 (accessed on 11 October 2021).

Carannante, Maria, Valeria D'Amato, and Guido Iaccarino. 2021a. Stochastic Charlson Comorbidity Index: A projection of the mortality acceleration due to the COVID-19. *Statistics in Medicine. under review*.

Carannante, Maria, Valeria D'Amato, and Steven Haberman. 2021b. COVID-19 accelerated mortality shocks and the impact on life insurance: The Italian situation. *Annals of Actuarial Science. under review*.

Carannante, Maria, Valeria D'Amato, Paola Fersini, and Salvatore Forte. 2021c. Gli effetti della pandemia COVID-19 sulla popolazione italiana e sul pricing dei prodotti assicurativi di puro rischio. In *Diritto Economia e Società dopo la pandemia*. Edited by D'Ambrosio I. and Palumbo P. Naplesm. Napoli: Edizione Scientifica, pp. 19–29.

Deloitte. 2021. Insurance Industry Outlook. Deloitte Insights. Available online: https://www2.deloitte.com/us/en/insights/industry/financial-services/financial-services-industry-outlooks/insurance-industry-outlook.html (accessed on 11 October 2021).

ECB. 2021. The role of financial stability considerations in monetary policy and the interaction with macroprudential policy in the euro area. *Occasional Paper Series 272*. Available online: https://www.ecb.europa.eu/pub/pdf/scpops/ecb.op272~dd8168a8cc.en.pdf (accessed on 14 December 2021).

EIOPA. 2014. Commission Delegated Regulation (EU) 2015/35 of 10 October 2014 Supplementing Directive 2009/138/EC of the European Parliament and of the Council on the Taking-up and Pursuit of the Business of Insurance and Reinsurance (Solvency II). Available online: https://eur-lex.europa.eu/legal-content/EN/TXT/PDF/?uri=CELEX:32015R0035$&$from=EN (accessed on 11 October 2021).

EIOPA. 2020a. EIOPA's Response to the Coronavirus Crisis. Available online: https://www.eiopa.europa.eu/content/eiopas-responsecoronavirus-crisis$_$en (accessed on 20 December 2021).

EIOPA. 2020b. European Insurers Face Increased Risk Exposures Due to COVID-19, but Market Perceptions and Imbalances Remained at Medium Level. Available online: https://www.eiopa.europa.eu/content/european-insurers-face-increased-risk-exposuresdue-covid-19-market-perceptions-and$_$en (accessed on 20 December 2021).

Farooq, Umar, Nasir Adeel, Bilal, and Muhammad Umer Quddoos. 2021. The impact of COVID-19 pandemic on abnormal returns of insurance firms: A cross-country evidence. *Applied Economics* 53: 3658–78. [CrossRef]

Gründl, Helmut, Danjela Guxha, Anastasia Kartasheva, and Hato Schmeiser. 2020. Insurability of pandemic risks. *Journal of Risk and Insurance* 88: 863–902. [CrossRef]

Harris, Timothy F., Aaron Yelowitz, and Charles Courtemanche. 2021. Did COVID-19 change life insurance offerings? *Journal of Risk and Insurance* 88: 831–61 [CrossRef] [PubMed]

Karlsson, Fredrik. 2020. Time for a Rethink? The Insurance Industry Faces up to COVID-19. Available online: https://latinlawyer.com/article/1225838/time-for-a-rethink-the-insurance-industry-faces-up-to-covid-19 (accessed on 20 December 2021).

Marsh. 2021. COVID-19: Considerations for the Insurance Industry. Available online: https://www.marsh.com/uk/risks/pandemic/insights/covid-19-considerations-for-insurance-industry.html (accessed on 11 October 2021).

Milesky, Moshe A. 2021. Is COVID-19 a Parallel Shock to the Term Structure of Mortality? Is COVID-19 a Parallel Shock to the Term Structure of Mortality? With Applications to Annuity Valuation. Available online: moshemilevsky.com (accessed on 11 October 2021).

Moody's Analytics. 2020. EIOPA Risk Assessment Shows Increase in Credit and Market Risks. Available online: https://www.moodysanalytics.com/regulatory-news/May-18-20-EIOPA-Risk-Assessment-Shows-Increase-in-Credit-and-Market-Risks (accessed on 20 December 2021)

Nguyen, Duc Khuong, and Dinn-Tri Vo. 2020. Enterprise Risk Management and Solvency: The Case of the Listed EU Insurers. *Journal of Business Research* 113: 360–69. [CrossRef]
Olivieri, Annamaria, and Ermanno Pitacco. 2015. *Introduction to Insurance Mathematics. Technical and Financial Features of Risk Transfers*, 2nd ed. EAA Series. Cham: Springer Nature.
Pułanska, Karolina. 2021. Financial Stability of European Insurance Companies during the COVID-19 Pandemic. *Journal of Risk and Financial Management* 14: 266. [CrossRef]
Renshaw, Arthur, and Steven Haberman. 2003. Lee–Carter mortality forecasting: A parallel generalized linear modelling approach for England and Wales mortality projections. *Applied Statistics* 52: 119–37. [CrossRef]
Scism, Leslie. 2020. Less driving, fewer accidents: Car insurers give millions in coronavirus refunds. *The Wall Street Journal*. Available online: https://www.wsj.com/articles/car-insurer-american-family-gives-200-million-in-coronavirus-refundsas-accidents-decline-11586175602 (accessed on 20 December 2021).
Spiegelhalter, David. 2020. Use of "normal" risk to improve understanding of dangers of COVID-19. *BMJ* 370: 3259. [CrossRef]
Vasicek, Oldrich. 1977. An equilibrium characterization of the term structure. *Journal of Financial Economics* 5: 177–88. [CrossRef]
Wang, Yating, Donghao Zhang, Xiaoquan Wang, and Qiuyao Fu. 2020. How Does COVID-19 Affect China's Insurance Market? *Emerging Markets Finance and Trade* 56: 2350–62. [CrossRef]

risks

MDPI

Article

Proposal to Extend Access to Loans for Serious Illnesses Using Open Data

Frédéric Planchet *,†, Édouard Debonneuil *,‡ and Marie Péju §

ISFA—SAF Laboratory, Institut de Science Financière et d'Assurances (ISFA), Laboratoire SAF EA2429, University Lyon, Université Claude Bernard Lyon 1, F-69366 Lyon, France; peju.marie@gmail.com
* Correspondence: fred@planchet.net (F.P.); edebonneuil@yahoo.fr (É.D.)
† Frédéric Planchet is Professor at ISFA and Partner Actuary at PRIM'ACT.
‡ Edouard Debonneuil is manager of ActuRx.
§ Marie Péju is an independent *data scientist*.

Abstract: In France, access to a loan requires one to obtain loan insurance and the presence of a pathology in the applicant may be a reason for refusal. Improving knowledge of health risks and pooling risks are two methods of broadening access to loans. We attempt to analyse these possibilities using open data and risk pooling scenarios. We find that the removal of medical selection can be ensured if the current framework is adjusted. We also demonstrate how to use open data to estimate loan insurance premiums for a variety of diseases. We take two examples: breast cancer and type 1 diabetes. Broadening access to borrowing would be beneficial for patients and for the development of the economy associated with these projects.

Keywords: borrower insurance; mortality; serious illnesses

Citation: Planchet, Frédéric, Édouard Debonneuil, and Marie Péju. 2022. Proposal to Extend Access to Loans for Serious Illnesses Using Open Data. *Risks* 10: 51. https://doi.org/10.3390/risks10030051

Academic Editors: Anna Rita Bacinello and Nadine Gatzert

Received: 12 November 2021
Accepted: 21 February 2022
Published: 28 February 2022

Publisher's Note: MDPI stays neutral with regard to jurisdictional claims in published maps and institutional affiliations.

1. Introduction

Every year, borrowers are refused loans for the purchase of a property or the creation of a business because of their health status. The human impact is all the greater, as these patients did not choose to be ill. The impossibility of supplementing their financial resources with a loan to help them achieve a life goal can be perceived as discrimination. These refusals also have an economic impact beyond the loan itself, as these life projects would have contributed to the development of the economy.

Some of these refusals are due to insurers' insufficient knowledge of health risks. This refusal is the insurer's response to a risk of financial loss deemed too great due to the risks of death or temporary or permanent disability.

It may seem that insurers would have no issue in appreciating the risk. Insurers' actuaries generally know how to rate contracts on the basis of policyholder statistics. They also know how to deal with illnesses in various ways; in the underwriting process of protection insurance for products with death and disability benefits, premiums are increased notably when medical examinations reveal the presence of an illness. In some countries, such as in the United Kingdom, lower premiums are even applied for annuities in the presence of illness (Ridsdale 2012).

Still, for diseases that are currently refused, insurers do not have the corresponding statistics. It is not easy to find external information for reasons of health privacy. We have only partial access to data that enable us to construct statistics from such sources as health or life insurance data or national health data. Expert assessments of the risks associated with diseases are not unanimous; there are many diseases and associated risk factors, and scientific advances and changes in behaviour modify the risk levels. Faced with this lack of knowledge, insurers take a cautious approach (and they are obliged to do so to avoid bankruptcy and failure to honour their guarantees) and in practice have no choice but to

replace excessively high rates with a refusal to accept them in order to avoid a significant image risk (and they are obliged not to exceed a usury rate).

Furthermore, pooling high risks with low risks comes up against population behaviour. Within the existing framework, an insurer who creates a loan contract without medical selection, therefore being maximally inclusive with regard to pathologies, risks seeing an influx of patients who have been refused a loan elsewhere without this influx being compensated for by a sufficient influx of low-risk individuals; the experiment would come to nothing.

Thus, the existing framework does not favour the detailed knowledge of risks associated with pathologies or the pooling of high health risks with lower risks. Here we try to use open data and our knowledge of insurance to find ways out of the current situation. Throughout the paper we take breast cancer and diabetes as application examples. After an overview of mortality risks and the insurability of removing medical selection, we describe a generic approach to estimating loan insurance pure premiums for patients and apply it to breast cancer and type 1 diabetes. Throughout, we distinguish between mortality and temporary or permanent disability risks and provide elements for inclusive approaches. We hope that these elements can contribute to widening access to borrowing.

2. Overall Picture Based on French Mortality Benchmarks

For about fifty pathologies, the pathology sheets on the Ameli website (Ameli 2018a) provide information on the level of mortality in the general population. They give (at the top of their second page) mortality rates by age group. In Figure 1, we plot these mortality risks by age groups on a log scale for two pathologies, diabetes (Ameli 2018d) and breast cancer—both the risky active breast cancers (Ameli 2018b) and the less risky under (SEER 2020) breast cancers (Ameli 2018c). We also plot the mortality risks of various French populations not defined by pathology in order to compare them with the mortality risks of patients.

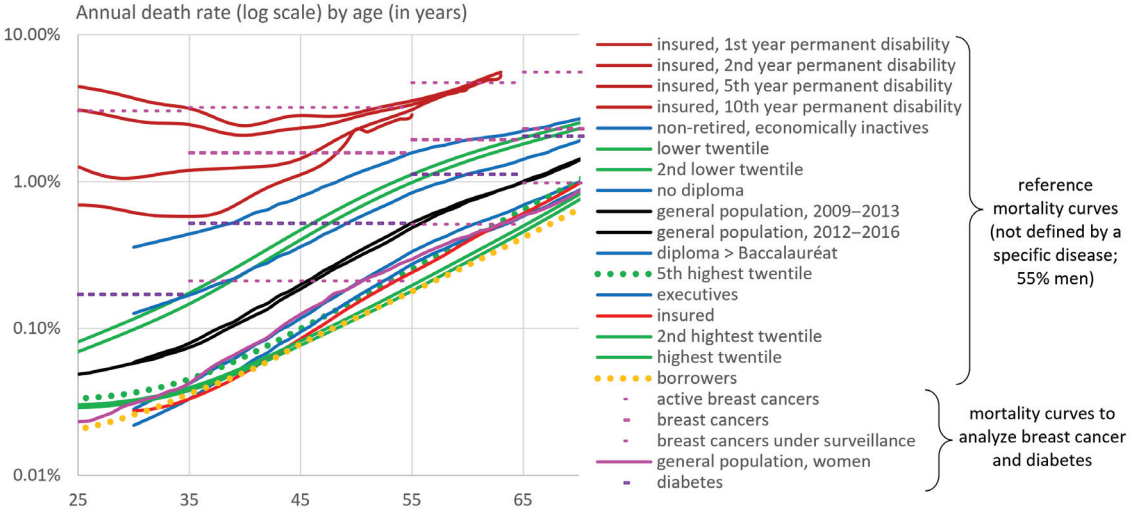

Figure 1. Annual mortality rate in France between the ages of 25 and 65 for different populations (55% men and 45% women)[1].

We can first observe the consistency of the risks of populations not defined by a pathology. The general French population had a similar risk (represented in black) in 2016 (noted general population in 2009–2013 (Blanpain 2016)) and 2018 (noted general population 2021–2016 (Blanpain 2018)) with a decreasing trend. When segmented in green by income twenties (Blanpain 2018) and in blue by diplomas (Blanpain 2016), the level of

mortality falls as one's socio-professional level increases. In red, the average risk of insured individuals, from a table known as "IA 2013" (Tomas and Planchet 2014), is around the line of executives and higher intellectual professionals (which is the lowest blue curve). In yellow-dotted lines, an average of actuarial tables in loan insurance[2], corresponding to the subscription to high incomes and an absence of severe pathology, demonstrates a risk lower than that in red of policyholders in general, which are, on average, less selected or even lower than the first twentieth in terms of income. The risk of death in case of disability, from tables known as "BCAC 2013" (Bagui 2013), is particularly high. Although it decreases in the early years (following an accident or illness, probably due to the death of those most at risk and a stabilization of health conditions for the others) before rising with age, it remains higher than for non-retired inactive individuals (disabled or not). We are used to the use of the latter curves and know that the order of magnitude is correct.

Secondly, the coherence observed between these reference curves allows us to reconstruct mentally and approximately what would be the mortality risks given by the Amelie pathology records if they were available in finer age brackets (the horizontal segments in Figure 1 would be inclined, similarly to the close reference curves, with approximately the same centres). We see that the risks of active breast cancer are of the order of those of disabled insured individuals in the years following the cause of disability and that the risks of the general population with breast cancer or diabetes are much higher than those of the borrower population, even in the case of breast cancer under surveillance. It is therefore necessary to study in greater detail the risks associated with different forms of disease and the transposition of risk to the socio-professional status of borrowers. This is conducted in Section 3.

Before moving to Section 3, however, it is interesting to note that Figure 1 helps us to appreciate what the risk of borrowers would be in the absence of medical selection. As the majority of loan applicants are executives, especially when weighted by amount, the risk should be close to the lowest blue curve. In the absence of medical selection, the risk should be similar to the red curve (tends to be higher due to this, tends to be lower due to the financial resources needed to borrow). Associating these professional categories with a twentieth, this would then correspond to the 5th twentieth of the French population, represented by the green-dotted line, i.e., an increase in risk of the order of 40% compared to current borrowers (yellow-dotted line)—or perhaps less, as patients with serious health conditions are likely to be less inclined to seek a loan and because fixed costs embedded into the insurance premiums absorb the risk (by definition they do not increase with the risk of borrowers). Given fixed insurance costs that do not increase with the risk of borrowers, commercial premiums that would keep current margins would be increased by less than 40% for all borrowers compared to current ones. However, given the almost 100-fold difference between these risks and those of people with active breast cancer, for example, this theoretical view's framework is insufficient and severe conditions are over-represented in one or a handful of insurers rather than being distributed evenly between insurers.

3. A Generic Method to Estimate Loan Insurance Premiums for Patients

We observe that if the framework is to be adjusted, it is important to refine our knowledge of the risks according to factors related to the pathology to minimize patient exclusion. In this section, we describe a method of finding aggregate open data in a way that estimates loan insurance premiums for a variety of pathologies. We do not claim that this is optimal; on the contrary, it sets the scene for potential improvements by other authors. We focus on France, but the approach is not limited to France.

3.1. Mortality Risk of Patients in the General Population According to Various Risk Factors

Finding mortality risks for specific diseases can typically be done with a Google or PubMed search on the disease and on keywords such as "survival", "age", "mortality rate", "death rate", "mortality", "death", "breast cancer", and "type 1 diabetes" (or their equivalents in French). As illustrated in Section 4 with breast cancer and diabetes, articles

are found that model mortality from national datasets, clinical trials, or epidemiologic studies, along with various risk factors.

We performed this for a number of diseases. Trade-offs have to be made between choosing recent articles or articles with more data and more risk factors. Otherwise article results must be combined to get the most out of different articles. Sometimes no adequate study is found in France or the desired country and studies from other countries are transposed while adjusting the results to macro statistics in France.

This step is relatively specific to each pathology.

3.2. Transposition to Borrowers

The mortality risks obtained so far correspond to patients in the general population, not to patients who have the typical wealth and lifestyle of borrowers. However, as observed in Figure 1, the mortality of current policyholders and insured borrowers is, on average, 2 to 2.5 times lower than that of the general population. Thus, do loan applicants with a medical condition have the normal risk of patients with that condition or about half the risk?

3.2.1. Theoretical Considerations and Definition of a Relative Risk Multiplier

It is logical that mortality in the event of illness is lower among loan applicants than the general population: they are, on average, more educated about health and therefore get screened earlier, have better living conditions and fewer co-morbidities and therefore recover more easily from health problems. Thus, the more the survival of a disease depends on these elements, the higher the survival of the insured persons compared to the general population.

A mathematical perspective provides an a priori idea of quantification for certain diseases. Insured populations are typically half as likely to die from all causes. This translates into a reference ratio for causes of death: the death rate for a given cause (death rate relative to the size of the population, not the diagnosed population) is 2 + x times less than that of the general population, where x is centred in some way around zero (sometimes positive, sometimes negative, depending on the pathology).

In particular, if a condition is very common, x is likely to be small in absolute terms (because if x were large, the other causes of death would have to have a large x on average in the other direction for all-cause mortality to be what it is). Mortality from this condition is itself decomposed as the product of incidence and mortality, if diagnosed. Here, depending on the disease considered, knowledge of the qualitative link between incidence and socio-professional category gives an idea of post-diagnosis mortality. Thus, in the case of breast cancer, the death rate (relative to the population size) of insured women can be expected to be about half that of women in the general population. Considering that screening is much more frequent and early in the higher socio-professional status, the incidence in the diagnostic sense and not in relation to a stage of the pathology should tend to be greater in insured women: we can expect the mortality rate in the case of breast cancer to be less than half that in the general population.

Cancers are special in that their early detection radically changes the associated survival—hence the screening approaches for breast cancer, melanoma, or colon cancer. For other diseases, we expect a lower incidence in the insured population than in the general population due to better health on average. However, the insured population tends to see the doctor earlier, so there is a tendency not to be very far from the incidence in the general population. Thus, the factor two of all-cause mortality would be found more in terms of mortality in the case of pathology than in terms of incidence.

Thus, the consensus is that the relative risk between mortality in the presence or absence of a specific pathology—the "relative mortality risk" due to that pathology—should be on average a little larger for insured individuals than for the general population, and smaller in the case of pathologies, such as cancers, for which insured individuals are screened particularly early. This is why we define the "relative risk multiplier" as the ratio

between these two relative risks, which should, therefore, on average, be a little higher than 1 but lower than 2, and probably lower than 1 for breast cancer.

3.2.2. Mathematical Definition of the Multiplier and How to Obtain it

Let us consider four populations: A′, B′, C′, and D′. The prime is, here, to indicate that they are chosen to compute a risk multiplier ρ' that does not exactly correspond to any one insurance loan. Let us use the same letters to represent their annual mortality risk: ${q_x}^{A'}$, ${q_x}^{B'}$, ${q_x}^{C'}$, and ${q_x}^{D'}$. Table 1 shows how to choose the definition of these populations to obtain a relative mortality multiplier by combining their mortality risks.

Table 1. Risk multipliers.

	Population with a Pathology	**Healthy Population (*)**	**Relative Mortality Risk Due to Disease**
Higher socio-professional status	${q_x}^{A'}$	${q_x}^{B'}$	${q_x}^{A'}/{q_x}^{B'}$
General population	${q_x}^{C'}$	${q_x}^{D'}$	${q_x}^{C'}/{q_x}^{D'}$

(*) Here, the word "healthy" is an abuse of language to indicate that the population has not been selected for a particular pathology.

The relative risk multiplier ρ is then defined by:

$$\rho' = \frac{{q_x}^{A'}/{q_x}^{B'}}{{q_x}^{C'}/{q_x}^{D'}}$$

It is very difficult to find ${q_x}^{A'}/{q_x}^{B'}$ on the Internet as it requires articles that focus on a pathology in high socioeconomic populations, whereas articles that focus on a pathology tend to also focus on social inequalities and more particularly on low socioeconomic populations. However, the multiplier can be rewritten as follows:

$$\rho' = \frac{{q_x}^{A'}/{q_x}^{C'}}{{q_x}^{B'}/{q_x}^{D'}}$$

This might seem a pure change of notation, but it leads us to search for other types of articles in the scientific literature that are easier to find, as social inequalities are an important issue for social and health policies. It is what permits one to use open data to estimate the risks of borrowers with a disease without having to guess what ρ' might be. ${q_x}^{A'}/{q_x}^{C'}$ is found in articles that study the impact of socioeconomic status on survival outcome in the case of a disease. ${q_x}^{B'}/{q_x}^{D'}$ is found in articles that study the impact of socioeconomic status on mortality in the general population; it is important to find the same definition of socioeconomic status for the two ratios to be comparable (diplomas, occupations, salaries, etc.).

The relative risk multiplier is therefore computed with the definitions of high socioeconomic status and the pathology found in such articles. Let us remove primes when defining the relative risk multiplier that would be based on borrowers with a specific definition of the pathology related to the insurance contract and underwriting process:

$$\rho = \frac{{q_x}^{A}/{q_x}^{C}}{{q_x}^{B}/{q_x}^{D}}$$

Of note, D and D′ represent the same general population. The mortality rate of loan applicants with a medical condition is then derived from the definition of ρ:

$${q_x}^{A} = {q_x}^{B} \times \frac{{q_x}^{C}}{{q_x}^{D}} \times \rho$$

In this formula,

- ${q_x}^B$ (annual mortality rate of borrowers) and ${q_x}^D$ (annual mortality rate in the general population) are functions of age and possibly gender. ${q_x}^B$ is an average of placeholder borrower tables calculated by the laboratory; an insurer can apply its own experience table;
- ${q_x}^C$ (annual mortality rate of persons with the pathology) depends on age and possibly gender but also on disease-related variables, such as how long ago the diagnosis was made and elements of disease severity;
- ${q_x}^A$ (annual mortality rate of borrowers with the pathology) has all these variables;
- ρ is theoretically a function of age, wealth, history of disease, and any other characteristic associated with the loan applicant.

We make the assumption $\rho \approx \rho'$; we assume that the multiplier established with populations A′, B′, C′, and D′ is sufficient to rate contracts if it is a mortality adjustment. To validate this hypothesis, for a given pathology it can be useful to establish ρ' for various countries to ensure that it is robust with similar values despite different environments. Additionally, if ρ' were greater than 150% or less than 75%, for example, this assumption would need to be adjusted, for example by considering different categories of the pathology and different categories of high socio-professional status (at the cost of difficult internet searches).

In the case of breast cancer, we obtain a multiplier ρ of 83% for French data. For diabetes, we obtain a multiplier of 115% for France, 108% for Korea, 111% for the United States, and 123% for Scotland. It should be noted that these multipliers are in line with the most likely expectations expressed at the beginning of the section: multipliers slightly below 1 when early diagnosis in the higher socio-professional status makes a difference to the risks and slightly above 1 for frequent pathologies.

At this stage, it is therefore possible for insurers to establish mortality tables for an inclusive or partially inclusive approach for various conditions, bearing in mind that mortality risk is the most important guarantee in loan contracts.

3.2.3. Temporary Disability

As for mortality, for each disease the first step is to look for sources of data or studies that can be used to model the transition to temporary disability, or at least to work stoppage, and the continuation of temporary disability. This search is not easy, as the available data mentioning a specific disease in connection with work stoppage are often very macroscopic indicators. Luckily, in terms of modelling, mortality is the most important guarantee of loan insurance, thus approximations are more acceptable than when modelling mortality risk.

A solution is to rely on the American open data database made available by the National Center for Health Statistics (NHIS 2016). As this is an American database, the risks of temporary disability are lower and the prevalence of certain pathologies, such as diabetes, is higher. It is then a question of comparing the macroscopic indicators to appreciate the differences, modelling the risk in the United States, and adjusting it to the French macroscopic indicators within the framework of the understanding obtained when comparing the indicators.

This American database was compiled from a questionnaire sent each year between 2010 and 2018 to different, randomly selected individuals. It consists of 284,809 individuals, 55% of whom are women. A total of 3.3% of the women were diagnosed with breast cancer and the mean and median ages of these women are 68 and 70 years, respectively. The mean age at diagnosis is 56 years. It is possible to test different combinations of variables and thus select the most relevant ones.

With this database, we can model the annual probability i_x to get into work stoppage of more than d days, and the average duration of work stoppage that follows d_x. The risk is then the product of both ($i_x d_x$). Similar to mortality, we can define populations A, B, C, and D and their associated risks ${i_x}^A$, ${i_x}^B$, …, ${d_x}^D$, and we get the formula that defines a risk multiplier ρ:

$$ {i_x}^A {d_x}^A = {i_x}^B {d_x}^B \times \frac{{i_x}^C {d_x}^C}{{i_x}^D {d_x}^D} \times \rho $$

Here, A and B still represent French borrowers, but C and D represent American workers, with a specific pathology in the case of A and C. ${i_x}^C{d_x}^C$ and ${i_x}^D{d_x}^D$ are modelled based on the American database, ${i_x}^B{d_x}^B$ comes from knowledge of French insurers and we make the assumption that the risk multiplier is the same as for mortality: $\rho \approx \rho'$ (a higher mortality is associated with a more severe disease and greater risk of disability).

For applications for breast cancer and diabetes we decided to model incidence (${i_x}^C$ and ${i_x}^D$) and duration (${d_x}^C$ and ${d_x}^D$) separately to facilitate the modelling in a Markovian approach.

1. For incidence, we considered a logistic regression giving the annual probability of a work stoppage greater than three days. We chose a logistic regression because this annual incidence is a probability is between 0 and 1, but other models could have been chosen. The three-day threshold was chosen by expert judgement to differentiate temporary disability from pure work stoppage.
2. For duration, we considered a gamma regression, giving the duration of a work stoppage greater than 3 days. We chose a gamma regression because it leads to durations that are positive, but other models could have been chosen.

The use of regressions improves the understanding of the relationship between temporary disability and risk factors. It is important to look for the most relevant explanatory variables for the condition under study.

${i_x}^B$ is an average of placeholder borrower tables calculated by the laboratory using the same approach as for mortality. An insurer can use its own experience table. For ${d_x}^B$ we used the BCAC 2013 tables (Bagui 2013).

The approach we described here is limited in terms of risk factors compared to the risk factors that are typically found in articles related to mortality risks. As cases that lead to higher mortality risk likely also lead to higher disability risks, we should include mortality-related risk factors with some proportionality rules and interpolations on the risk factors already modelled for disability risk.

3.2.4. Permanent Disability

As with temporary disability, it is particularly difficult to find permanent disability statistics related to diseases but we found an approach for modelling temporary disability with open data.

As shown in Table 2, a French study (Cuerq et al. 2008) provides the probabilities P_3 and P_{10} of becoming disabled 3 years and 10 years after diagnosis for various pathologies. It is possible to interpolate and extrapolate these data to model permanent disability risk as a function of time.

Table 2. Percentage of patients in permanent disability 3 and 10 years after the start of long-term sickness in France.

	Rate (%)	
Long-Term Sickness	**3 Years Later**	**10 Years Later**
Multiple sclerosis	14.0	23.4
Incapacitating stroke	19.8	21.9
Severe active rheumatoid arthritis	10.1	7.1
Chronic arteriopathies with ischemic manifestations	10.6	17.0
Coronary artery disease	9.9	15.1
Heart failure, severe heart disease	9.6	14.3
Severe chronic kidney disease and nephrotic syndrome	7.6	13.2
Severe forms of neurological conditions, severe epilepsy	8.8	13.0
Long-term psychiatric conditions	9.9	13.0
Severe chronic respiratory failure	9.0	12.6
Severe ankylosing spondylitis	8.0	12.5
Malignant tumors	8.4	10.8
Severe high blood pressure	5.1	9.8
Chronic active liver disease and cirrhosis	5.9	8.6
Type 1 and 2 diabetes	3.3	7.6
Crohn's disease and active ulcerative colitis	2.2	4.7
Severe primary immunodeficiency, AIDS	1.9	3.6

Let us denote the annual probability of entering permanent disability as p_x. Here, also, let us consider four populations, A, B, C, and D, and let us reuse the mortality risk multiplier ρ (that transposes relative risk to policy-holders) so that the following can be written:

$$p_x{}^A = p_x{}^B \times \frac{p_x{}^C}{p_x{}^D} \times \rho$$

where A and B represent policy-holders, C and D the population of workers, and A and C are identified as having a specific pathology.

Using constant values of $p_x{}^C$ between 0 and 3 years following diagnosis, noting that $q'_x{}^C$ is the annual death rate of people from population C when in permanent disability, and considering the average values of $p_x{}^C$, $q_x{}^C$ and $q'_x{}^C$ over the first three years post-diagnostic, P_3 is the probability of entering permanent disability in the first, second, or third year without dying:

$$P_3 = p_x{}^C\left(1 - q'_x{}^C\right)^2 + \left(1 - q_x{}^C - p_x{}^C\right)p_x{}^C\left(1 - q'_x{}^C\right) + \left(1 - q_x{}^C - p_x{}^C\right)^2 p_x{}^C$$

Considering that $p_x{}^C$, $q_x{}^C$, and $q'_x{}^C$ are small and that the product of more than two of these numbers is negligible compared to 1, the probability of ending up with permanent disability after 3 years is:

$$P_3 \approx p_x{}^C\left(3 - 3q'_x{}^C - 3q_x{}^C - 3p_x{}^C\right).$$

As a result, $p_x{}^C \approx P_3/3$ in the first three years following diagnosis and this estimation is slightly prudent. A simpler approach is to neglect mortality, as we see that it is slightly prudent with respect to $p_x{}^C$. Neglecting mortality, the probability of remaining out of permanent disability is:

$$1 - P_3 \approx \left(1 - p_x{}^C\right)^3$$

As a result, $p_x{}^C \approx 1 - (1 - P_3)^3$ is a refined approximation that is still slightly prudent overall from diagnosis to 3 years later.

Similarly, if we neglect mortality up to 10 years following diagnosis, the probability of remaining out of permanent disability starting from the percentage $1 - P_3$ of people 3 years after diagnosis is:

$$\frac{1 - P_{10}}{1 - P_3} \approx \left(1 - p_x{}^C\right)^7$$

As a result, $p_x{}^C \approx 1 - \left(\frac{1-P_{10}}{1-P_3}\right)^{1/7}$ is an estimation that is slightly prudent from year 3 to 10 after diagnosis. We use it for any year following the first three years post-diagnosis, and this might be prudent because, as diseases stabilise, the risk of entering long-term disability is lower.

For a given pathology, we have just defined $p_x{}^C$ as two numbers that represent weighted means over age, gender, and disease risk factors. This is why we define $p_x{}^D$ similarly. Concretely, we multiply the probability of entering disability during at least one month (Kusnick-Joinville et al. 2006) by the probability to remain in disability and enter permanent disability based on the BCAC 2013 tables as performed by (Bagui 2013), averaged over working ages. $p_x{}^B$ is an average of placeholder borrower tables calculated by the laboratory using the same approach as mortality.

We detailed how to compute the annual probability of entering permanent disability, $p_x{}^A$. We also need to define the annual probability of dying when in permanent disability, $q'_x{}^A$. In real life, it is greater than the death rate when not in permanent disability, but to evaluate loan insurance premiums it does not have great importance and $q_x{}^A$ already represents the weighted average of the two death rates, thus $q_x{}^A$ can be used as well.

3.2.5. Premium Calculation

A Markov model is a simple approximation for assembling mortality and temporary or permanent disability risks[3]. A four-state Markov model is shown in Figure 2.

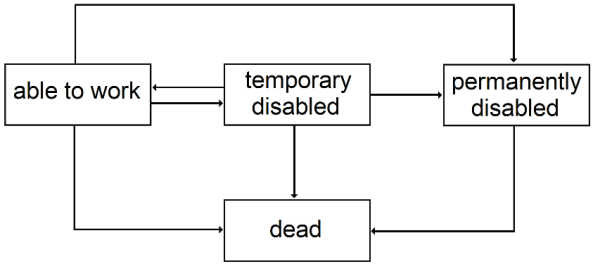

Figure 2. Diagram of a Markov model with four states.

Each arrow corresponds to a probability; the probability of death from one of the three other states, probability of going into temporary disability, of going into permanent disability before the end of the three years in temporary disability (after three years the transition is automatic), and the probability of returning to the work state. These probabilities would typically be functions of age, pathology characteristics, and length of time in the state or length of time in the diagnosis in a semi-Markovian framework.

In practice, it is difficult to find data for each arrow. A three-state Markov model shall thus be used, as described in Figure 3, with steps of one year.

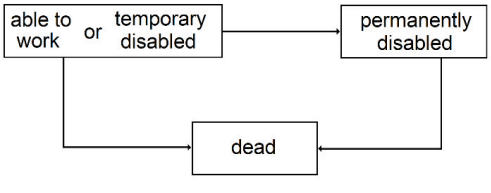

Figure 3. Diagram of a Markov model with three states.

At t = 0, the proportion of borrowers is 1 in the "Work or Disability" state and 0 in the other two states. It is therefore represented by a vector (1; 0; 0). At each subsequent time step, the proportion of borrowers in each state is the product of, on the one hand, the transition matrix made up of the annual transition probabilities and, on the other hand, the vector of the proportion of borrowers in the states of the previous time step.

Note that the matrix is as follows (in Table 3) and that its numerical value is different for each date (t = 0, 1, etc. over the duration of the contract) depending on the age and the initial characteristics of the pathology.

Table 3. Transition matrix.

$1-q_x^A-p_x^A$	p_x^A	q_x^A
0	$1-q_x{}^A$	$q_x{}^A$
0	0	1

The pure premium is the sum of the amounts the insurer must pay to the borrowers in the year for each state multiplied by the proportion of borrowers in the state. The simplest example is that of a loan covered by a borrower's insurance policy for death only, as it

does not depend on parameters related to disability. Each year $t \geq 0$ the proportion S_t of patients is alive:

$$S_0 = 1 S_t = \prod_{x=x_0}^{x=x_0+(t-1)} 1 - {q_x}^A$$

who have borrowed an amount C at age x_0 for a term T with an interest rate r. In the case of death, the insurer must take over the payment of the remaining balance, or capital remaining due (CRD):

$$CRD_t = [\frac{C}{T}\Big(1+r\Big)^T\Big](T-t)$$

assuming in this loan that the same amount, in square brackets, is to be repaid every year. Then, the pure premium P^A is:

$$P^A = \sum_{t=0}^{T} S_t \; {q_{x_0+(t-1)}}^A \; CRD_t$$

Note that in a two-state model (alive, dead) S_t is obtained by reading the proportion in the first state; in the three-state model (work-or-disability, disability, and death) S_t is the sum of the proportions of the first two states.

The inclusion of charges (e.g., distribution, claims handling, and reinsurance costs) would result in a commercial premium that is higher than the pure premium.

This pure premium P^A for a borrower with a medical condition can be compared to the pure premium P^B for a borrower under usual conditions by replacing A with B in the transition matrix. The additional premium $P^A - P^B$ due to the pathology can be defined as a percentage p of the usual premium or a permillage m:

$$p = \frac{P^A - P^B}{P^B} 100$$

$$m = \Big(P^A - P^B\Big) 1000$$

In practice, not all expenses are proportional to the risk: there are fixed costs. The fixed costs do not increase with risks; therefore, surcharges in real life should be lower than the one we computed here.

Examples are given below for breast cancer and diabetes.

4. Application to Two Diseases: Breast Cancer and Diabetes

We apply the modelling to breast cancer and type 1 diabetes.

4.1. Breast Cancer

4.1.1. Mortality by Risk Factor

Dabakuyo et al. (2008) modelled mortality in women with active invasive breast cancer. This study was based on data from 3831 French women with breast cancer. The data were collected between 1982 and 1997, with a median follow-up time of 9 years, on women aged 19 to 99 at diagnosis (mean and median age of 61 years). They model risk ratios (HR) based on 2615 women and the following risk factors:

- Age at diagnosis;
- Oestrogen receptor function;
- TNM stage;
- SBR grade.

The impact of these risk factors was calculated with a Cox model using the following reference population:

- Age between 45 and 59;
- Stage T of 1;

- Stage N of 0;
- Stage M of 0;
- Oestrogen receptor dysfunction;
- SBR grade of 1.

We do not provide the results of the model here; the goal is to illustrate the type of information one finds to model loan insurance risks.

Such a model of mortality risk must be transposed from the general population to the insured population using a multiplier defined as $\rho' = \frac{{q_x}^{A'}/{q_x}^{C'}}{{q_x}^{B'}/{q_x}^{D'}}$.

To obtain ${q_x}^{A'}/{q_x}^{C'}$, a ratio of mortality risks of women with breast cancer but different socio-professional groups, we relied on the study by (Gentil-Brevet et al. 2008). This study is based on a sample of 1150 French women with invasive breast cancer diagnosed between 1995 and 1997 who were followed up with to 2006. It is important to carefully note the distribution of socio-professional status in the study in order then to compute ${q_x}^{B'}/{q_x}^{D'}$ accordingly:

- 42.5% were in the higher socio-professional status (SPS+) group defined as "executives, middle professional group, and clerical employees". Their survival 5 and 7 years post-diagnosis was $\left(1-{q_x}^{A'}\right)^5 = 88.2\%$ and $\left(1-{q_x}^{A'}\right)^7 = 83.0\%$, thus on average ${q_x}^{A'} = 1 - 88.2\%^{\frac{1}{5}}$ and ${q_x}^{A'} = 1 - 83.0\%^{\frac{1}{7}}$;
- 16.6% did not have a specified SPS;
- 40.9% were in the lower socio-professional status (SPS−) group defined as "famers, artisans, manual workers, unemployed"; Their survival 5 and 7 years post diagnosis was 77.4% and 69.4%.

The general population being approximately represented by as many SPS+ as SPS−, we computed ${q_x}^{C'}$ as the average of the mortality rate of the two populations: ${q_x}^{C'} = \left[1 - 88.2\%^{\frac{1}{5}} + 1 - 77.4\%^{\frac{1}{5}}\right]/2$ over 5 years and ${q_x}^{C'} = \left[1 - 83.0\%^{\frac{1}{5}} + 1 - 69.4\%^{\frac{1}{5}}\right]/2$.

This leads to $\frac{{q_x}^{A'}}{{q_x}^{C'}} = 66.4\%$ from diagnosis to 5 years later and $\frac{{q_x}^{A'}}{{q_x}^{C'}} = 68.1\ \%$ from diagnosis to 7 years later. Thus, we have two possible values.

To obtain ${q_x}^{B'}/{q_x}^{D'}$, a ratio of mortality risks depending on socio-professional status, we used mortality tables by sex and standard of living quintile (Blanpain 2018). As in the article by (Gentil-Brevet et al. 2008), we separated the socio-professional status into two groups (SPS+ and SPS−). We used the same weighting as the article for the population affected by breast cancer: 25% of women are under 50 years of age, approximately 50% are between 50 and 70 years of age and 25% are between 71 and 85 years of age. We obtained the mortality rates of 686 and 860 per 100,000 persons, respectively, for the SPS+ and SPS− populations: $\frac{{q_x}^{B'}}{{q_x}^{D'}} = \frac{686}{860} = 80\%$.

Alternatively, ${q_x}^{B'}/{q_x}^{D'}$ can be obtained with mortality tables by sex and the socio-professional status provided by (Blanpain 2016). It needs to be combined with the distribution of socio-professional status among females, such as those provided by (Maruani and Meron 2012) to make weighted average mortality rates that have similar socio-professional statutes, as in (Gentil-Brevet et al. 2008). We do not detail the calculation, as it is long and does not bring much to this article—we obtained $\frac{{q_x}^{B'}}{{q_x}^{D'}} = 85\%$.

The multiplier is then one of four different values depending on the choice of the numerator and denominator: $\rho' = \frac{66.4\ \%}{80\ \%} = 83\%$ or $\frac{68.1\ \%}{80\ \%} = 85.1\%$ or $\frac{66.4\ \%}{85\ \%} = 78.1\%$ or $\frac{68.1\ \%}{85\ \%} = 81.1\%$. We chose the first value, as it is close to the average of the four values and slightly higher—thus closer to more prudent premiums (additionally, while building these values we felt it had the best match of assumptions between the numerator and denominator).

4.1.2. Short-Term Disability

Using the American database, incidence and duration were modelled among women as follows:

- A logistic regression (glm function in R, using "family=binomial(logit)") yields the following average incidence rate:

$$i_x = \frac{1}{1 + \mathrm{e}^{-(\alpha+\beta x+\gamma\ 1_{breast\ cancer})}}$$

where $1_{breast\ cancer}$ is 1 or 0 depending on whether the person was diagnosed with breast cancer or not. We then have ${i_x}^D = \frac{1}{1+\mathrm{e}^{-(\alpha+\beta x)}}$ and ${i_x}^C = \frac{1}{1+\mathrm{e}^{-(\alpha+\gamma+\beta x)}}$. Our regression found that $\beta = -0.019$ (more frequent work stoppage at younger ages) and $\gamma = 0.53$ (effect of cancer). α was adjusted to match the average frequency of work stoppage in France (Kusnick-Joinville et al. 2006);

- A gamma regression (glm function in R, using "family = Gamman(link = 'log')") yields the following average duration:

$$d_x = \mathrm{e}^{-(\alpha+\beta x+\gamma\ 1_{breast\ cancer})}$$

We then have ${d_x}^D = \mathrm{e}^{-(\alpha+\beta x)}$ and ${d_x}^C = \mathrm{e}^{-(\alpha+\gamma+\beta x)}$. Here, $\beta = 0.018$ (longer work stoppage with age) and $\gamma = 0.73$ (effect of cancer). α was adjusted to match the average frequency of work stoppage in France (Kusnick-Joinville et al. 2006).

4.1.3. Long-Term Disability

In Table 2, we do not have data for breast cancer, only for cancers ("tumours"). We still considered the latter, which is prudent, as breast cancer has a similar prognostic value to most cancers.

- ${p_x}^C = 1 - (1 - 0.084)^{1/3} = 2.88\%$ for t between 0 and 3 years.
- ${p_x}^C = 1 - \left(\frac{1-0.108}{1-0.084}\right)^{1/7} = 0.38\%$ for t beyond 3 years.

4.1.4. Results

Table 4 illustrates additional premiums, in the last column, depending on various breast cancer cases described in the other columns. These are the m values we obtain for women who are 42 years old at the time of application for a 10-year loan and were diagnosed 3 years ago with a non-metastatic breast cancer.

The additional commercial premium may be smaller than the additional pure premium due to fixed costs (and commercial decisions).

It is possible to pool some cases, as shown in Table 5, to provide loan access to a maximum number of patients. The weighting used to calculate the average excess premiums is the distribution of such cancers found in SEER[4], a free application that provides very precise statistics on cancers in the United States.

Figures 4 and 5 show the additional disability pure premium (this time expressed as a percentage p) as a function of the age of the borrower at the time of application. Here, all severities of breast cancers have been pooled.

Of note, it would not have made much sense to express additional mortality premiums as a percentage p. This is because it would have been particularly high for young women (who have a particularly low mortality risk in the absence of breast cancer)—according to the model we developed, we observe that Tables 3 and 4 are roughly valid for all ages. Additionally, it would not have made much sense to express additional disability premiums as a permillage m. This is because long-term disability is limited at higher ages.

Table 4. Detailed additional pure mortality premiums.

T Stage	N Stage	M Stage	SBR Grade	Oestrogen Receptor Function	m
1	0	0	1	Positive	2.2
2	0	0	1	Positive	6.4
3	0	0	1	Positive	8.9
1	1	0	1	Positive	5.9
2	1	0	1	Positive	14.6
3	1	0	1	Positive	19.7
1	0	0	2	Positive	5.8
2	0	0	2	Positive	14.4
3	0	0	2	Positive	19.4
1	1	0	2	Positive	13.2
2	1	0	2	Positive	31.0
3	1	0	2	Positive	41.3
1	0	0	3	Positive	8.3
2	0	0	3	Positive	20.0
3	0	0	3	Positive	26.8
1	1	0	3	Positive	18.4
2	1	0	3	Positive	42.4
3	1	0	3	Positive	56.2
1	0	0	1	Negative	3.2
2	0	0	1	Negative	8.5
3	0	0	1	Negative	11.7
1	1	0	1	Negative	7.8
2	1	0	1	Negative	18.9
3	1	0	1	Negative	25.4
1	0	0	2	Negative	7.7
2	0	0	2	Negative	18.7
3	0	0	2	Negative	25.1
1	1	0	2	Negative	17.2
2	1	0	2	Negative	39.7
3	1	0	2	Negative	52.7
1	0	0	3	Negative	10.9
2	0	0	3	Negative	25.8
3	0	0	3	Negative	34.4
1	1	0	3	Negative	23.8
2	1	0	3	Negative	54.1
3	1	0	3	Negative	71.3

Table 5. Pooled additional pure mortality premiums.

T Stage	N Stage	M Stage	SBR Grade	Oestrogen Receptor Function	*p*
-	-	0	-	-	13.5
1	-	0	-	-	5.8
2	-	0	-	-	21.1
3	-	0	-	-	31.7
4	-	0	-	-	36.7
-	1	0	-	-	7.2
-	0	0	-	-	24.9
-	-	0	1	-	3.5
-	-	0	2	-	11.5
-	-	0	3	-	21.1
-	-	0	-	Negative	21.4
-	-	0	-	Positive	11.3

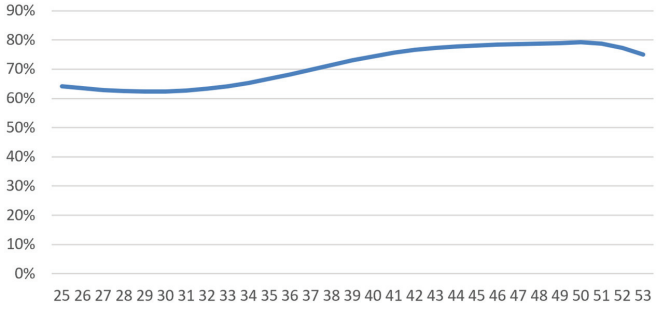

Figure 4. Additional pure premium p for short-term disability as a function of age.

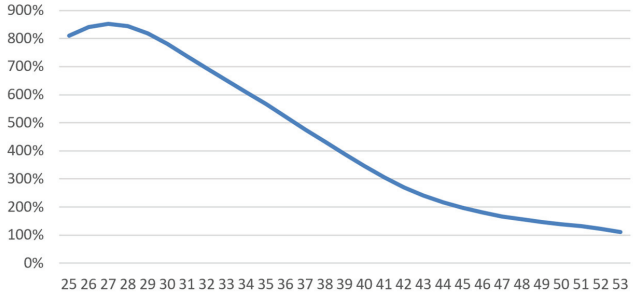

Figure 5. Additional pure premium p for long-term disability as a function of age.

4.2. Diabetes

There is much open data about diabetes in France but little about type 1 diabetes. Thus, to take a more complex example and appreciate the limits of what open data brings, we present the modelling of type 1 diabetes.

4.2.1. Mortality by Type of Diabetes

We failed to identify French articles that finely modelled type 1 diabetes mortality, thus we searched for articles from neighbouring countries. We selected a Danish study that investigated the evolution of relative and absolute mortality rates in 4821 type 1 diabetic patients followed between 2002 and 2011 (Jørgensen et al. 2013). Of these, 54% were male, the median age was 44 years, and the median follow-up time was 18 years.

Standard-mortality ratios (SMR) are calculated relative to the general population by sex, current age, age at diagnosis, and the presence or not of kidney disease, as diabetic nephropathy is a complication that can progress to renal failure. They are presented in Figure 6.

Unsurprisingly, mortality is higher for those diagnosed at a young age and for those with kidney disease. Given the high risk associated with kidney disease, in what follows we decided to limit the mortality risk to other cases of type 1 diabetes.

To model the mortality rates of diabetics in France, we apply the Danish SMR to the mortality rates of the general French population. The model must then be transposed from the general population to the insured population using a multiplier defined as $\rho' = \frac{{q_x}^{A'}/{q_x}^{C'}}{{q_x}^{B'}/{q_x}^{D'}}$.

We did not find articles to produce this multiplier specifically for type 1 diabetes in France, so we decided to simply estimate it for diabetes (essentially type 2).

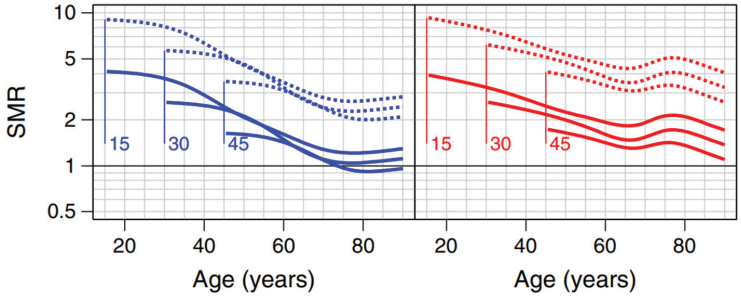

Figure 6. SMR by age at diagnosis and current age[5].

To obtain ${q_x}^{A'}/{q_x}^{C'}$, a ratio of mortality risks with diabetics from different socio-professional groups, we relied on a French article (Piffaretti et al. 2016). They studied the mortality of 7218 individuals with type 2 diabetes who answered a questionnaire in 2001 and 2007 and were followed until 2013. Figure 7 shows the relative risks according to their socio-professional category.

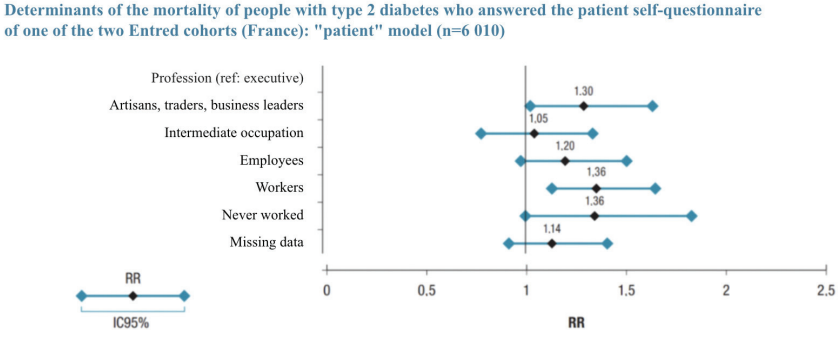

Figure 7. Relative risks according to socio-professional category with executives as reference (source: Piffaretti et al. 2016).

Figure 8 shows the distribution of socio-professional status. Based on the two figures, we estimate $\frac{{q_x}^{A'}}{{q_x}^{C'}} = \frac{1}{{q_x}^{C'}/{q_x}^{A'}}$ where A′ are executives with diabetes and C′ is decomposed into various categories:

$$\frac{{q_x}^{A'}}{{q_x}^{C'}} = \frac{1}{1 * 9.6\% + 1.36 * 9.0\% + 1.05 * 11.7\% + 1.20 * 18.4\% + 1.36 * 26.7\% + 1.36 * 6.3\% + 1.14 * 18.3\%} = 82\%$$

For ${q_x}^{B'}/{q_x}^{D'}$, we use mortality tables by sex and socio-professional status (Blanpain 2016). In order to be able to compare the average relative risks, we used the age and sex weighting of the article used for diabetes (Piffaretti et al. 2016).

We obtain $\frac{{q_x}^{B'}}{{q_x}^{D'}} = 71.6\%$.

This leads to the multiplier $\rho' = \frac{{q_x}^{A'}/{q_x}C'}{{q_x}^{B'}/{q_x}D'}$ =82%/71.6% = 115%.

We searched for multipliers from other countries and found articles from which it is straightforward to obtain a multiplier for Scotland (Walter et al. 2011), the United States (Dray-Spira et al. 2010), and South Korea (Kim et al. 2016). We observe that the French multiplier is of the same order of magnitude as these multipliers, which are presented in Table 6.

Baseline characteristics of the Entred 2001 and Entred 2007 cohorts and mortality rate of people with type 2 diabetes who responded to the patient self-questionnaire (N=7 218), France

		Frequency (%)	Mortality rate for 1000 patients
Occupation and socio-professional category	Artisans, traders, business leaders	9.0	41.0
	Executive	9.6	29.2
	Intermediate occupation	11.7	24.4
	Employees	18.4	22.8
	Workers	26.7	31.7
	Never worked	6.3	30.4
	Missing data	18.3	36.5

Figure 8. Distribution of socio-professional status.

Table 6. Multiplier for diabetes in various countries.

South Korea	108%
United States	111%
Scotland	123%
France	115%

4.2.2. Short-Term Disability by Age and Age of Diagnosis

To model disability in type 1 diabetes, we relied on American database statistics from 2016 and 2017 due to the diabetes type variable only being present for these two years. During this period, 60,000 Americans completed questionnaires, capturing the impact of type 1 diabetes on the incidence and maintenance of disability. We modelled the incidence and duration as follows:

- A logistic regression yields the following average incidence rate:

$$i_x = \frac{1}{1 + \mathrm{e}^{-(\alpha+\beta x+\gamma\ 1_{diabetes\ type\ 1}+\delta\ \tau)}}$$

where $1_{diabetes\ type\ 1}$ is 1 or 0 depending on whether the person was diagnosed with breast cancer or not, and τ is the time since diagnosis (set to 0 for those without type 1 diabetes). We then have ${i_x}^D = \frac{1}{1+\mathrm{e}^{-(\alpha+\beta x)}}$ and ${i_x}^C = \frac{1}{1+\mathrm{e}^{-(\alpha+\gamma+\beta x+\delta\ \tau)}}$. Regression found $\beta = 0.003$ (almost no impact of age, overall), $\gamma = 0.14$ (effect of type 1 diabetes), and $\delta = -0.04$. α was adjusted to match the average frequency of work stoppage in France (Kusnick-Joinville et al. 2006).

- A gamma regression yields the following average duration:

$$d_x = \mathrm{e}^{-(\alpha+\beta x+\gamma\ 1_{diabetes\ type\ 1}+\delta\ \tau)}$$

We then have ${d_x}^D = \mathrm{e}^{-(\alpha+\beta x)}$ and ${d_x}^C = \mathrm{e}^{-(\alpha+\gamma+\beta x+\delta\ \tau)}$. Here, $\beta = 0.024$ (longer work stoppage with age) and $\gamma = 0.32$ (effect of type 1 diabetes). α was adjusted to match the average frequency of work stoppage in France, observed in (Kusnick-Joinville et al. 2006).

4.2.3. Long-Term Disability

In Table 2, we do not have data for type 1 diabetes, only for type 1 or 2 diabetes. We still considered the latter. We think it is prudent, as our short-term disability analysis in the US database demonstrates lower risks for type 1 diabetes than type 2 (data not shown).

- $p_x{}^C = 1 - (1 - 0.033)^{1/3} = 1.11\%$ for t between 0 and 3 years.
- $p_x{}^C = 1 - \left(\frac{1-0.076}{1-0.033}\right)^{1/7} = 0.65\%$ for t beyond 3 years.

4.2.4. Results

Figure 9 shows additional mortality premiums expressed in percentage depending on applicant age and how long ago the applicant was diagnosed with type 1 diabetes.

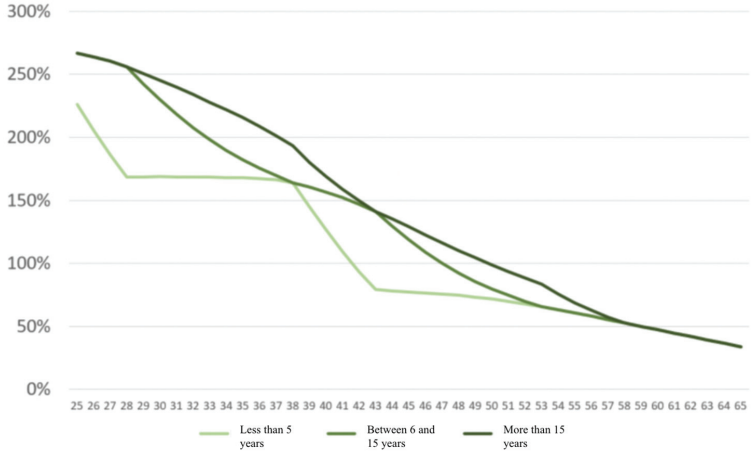

Figure 9. Additional pure premium p for mortality risk as a function of applicant age and whether diagnosis is recent or not (three cases).

Figure 10 shows the additional pure premium for disability (both short-term and long-term) as a function of applicant age and time since the diagnosis of type 1 diabetes.

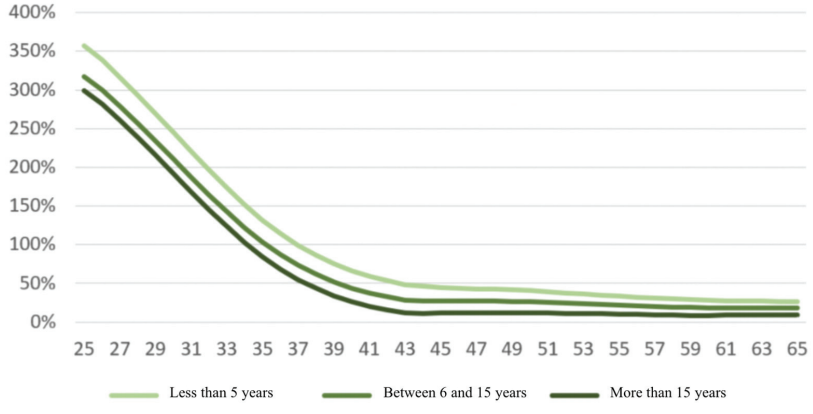

Figure 10. Additional pure premium p for disability risk as a function of applicant age, if diagnostic is recent or not (three cases).

As we can observe, the processes of obtaining premiums for type 1 diabetes and breast cancer were relatively similar. This suggests that the same process can be conducted for all severe diseases, in the worst case grouping them, such as grouping type 1 and 2 diabetes or taking prudent approximations, such as taking long-term disability risks associated with cancers instead of breast cancer. The process we conducted is the one described in

Section 3. It is an example of the process and other means to estimate risks based on open data that can lead to the best estimations, such as adjusting disability risks based on the risk of mortality.

5. Conclusions

This study has demonstrated that, based on open data, it is possible to significantly refine the description of the risks of mortality and disability for serious pathologies that currently lead to numerous insurance refusals. A more precise assessment of these risks makes it possible to include more people in the insurance with excess risks, which allows the premium to be kept to a reasonable level.

The methodology presented makes it possible to extend the work to many other diseases, even if each disease requires significant bibliographic and information cross-checking efforts. The examples of diseases taken suggest it is sometimes possible to estimate risks related to great details for some pathologies, such as the exact grade of and oestrogen receptor function of a breast cancer, and that it is sometimes not necessarily feasible except by taking prudent approximations, such as using all-cancer long-term disability risk instead of breast cancer. This means that it is possible to cover a large range of diseases without taking strongly prudent approximations if one accepts that the granularity of disease definition is sometimes coarse, depending on the found open data.

A difficult question was how to transpose risks from the general population to high socio-economic profiles. We defined this transposition via the definition of a multiplier that interestingly permits us to transpose studies that link social inequalities and mortality risks into loan insurance premiums—a different field. We were able to suggest that the multiplier would tend to be slightly smaller than one when mass screenings exist for the studied disease, and slightly greater than one otherwise (and if the disease is a frequent one). This was perfectly verified in the examples we considered.

Beyond the technical aspects of being able to use a diverse set of open data to generate loan insurance premiums comes the question of how to pool diseases to facilitate access to loans. The results we observed for breast cancer and type 1 diabetes suggest that non-metastatic breast cancers could be covered as a whole, as well as type 1 diabetes in the absence of nephropathy.

For even greater inclusion of patients, a framework would be needed to mutualize severe risks with low risks, e.g., by covering all cases of breast cancer and diabetes or even by eliminating medical selection. The latter option would dilute the excess risk across all insured individuals, with a potential but limited increase in basic premiums as we find in part 1, but runs the risk of high risks being concentrated in the first insurer or insurers to try this.

Author Contributions: This article is a group work to which all authors contributed equally. All authors have read and agreed to the published version of the manuscript.

Funding: This work was supported by the FUI ASPRET, co-financed by BPSI and Sogecap.

Institutional Review Board Statement: Not applicable.

Informed Consent Statement: Not applicable.

Data Availability Statement: All data used are listed in the references.

Conflicts of Interest: The authors declare no conflict of interest.

Notes

[1] For insured risks this gender breakdown is based on expert opinion, as the data at our disposal does not distinguish between the sexes.

[2] Average, maximum and minimum of best estimate actuarial tables among a group of French insurer for the mortality and temporary disability incidence of borrowers. Female risks were obtained by dividing by 1.5 (expert judgement) and male risks where deducted by considering that the tables contained 55% males (expert judgement).

[3] Since the conditional transition probabilities depend on the time spent in the state, semi-Markovian models are better suited, but given the context of this study, this simplification is acceptable.

[4] Surveillance Research Program, National Cancer Institute SEER* Stat software (seer.cancer.gov/seerstat) version 8.3.9.

[5] In blue and red for men and women respectively. The solid lines represent those without kidney disease. The numbers associated with the curves (15, 30 and 45) are the ages at diagnosis.

References

Ameli. 2018a. «Fiches sur les Pathologies» Available on the Website Ameli.fr. Available online: https://assurance-maladie.ameli.fr/etudes-et-donnees/entree-par-theme/pathologies/cartographie-assurance-maladie/donnees/fiches-pathologies/fiches-pathologies (accessed on 5 November 2021).

Ameli. 2018b. *Femmes prises en charge pour cancer du sein actif*. Fiche Pathologie. Available online: https://assurance-maladie.ameli.fr/etudes-et-donnees/cartographie-fiche-cancer-sein-femme-actif (accessed on 5 November 2021).

Ameli. 2018c. *Femmes prises en charge pour cancer du sein sous surveillance*. Fiche Pathologie. Available online: https://assurance-maladie.ameli.fr/etudes-et-donnees/cartographie-fiche-cancer-sein-femme-sous-surveillance (accessed on 5 November 2021).

Ameli. 2018d. *Diabète*. Fiche Pathologie. Available online: https://assurance-maladie.ameli.fr/etudes-et-donnees/cartographie-fiche-diabete (accessed on 5 November 2021).

Bagui, Hasna. 2013. *Refonte des lois de maintien en incapacité temporaire de travail*. Mémoire de Master. ISFA. Available online: http://www.ressources-actuarielles.net/C12574E200674F5B/0/CA2755D9E71E059AC1257C78006164B9 (accessed on 20 February 2022).

Blanpain, Nathalie. 2016. *Les inégalités sociales face à la mort. Tables de mortalité par catégorie sociale et par diplôme*. INSEE, Résultats. Available online: https://www.insee.fr/fr/statistiques/1893092 (accessed on 20 February 2022).

Blanpain, Nathalie. 2018. *Tables de mortalité par niveau de vie*. INSEE, Résultats. Available online: https://www.insee.fr/fr/statistiques/3311422 (accessed on 20 February 2022).

Cuerq, Anne, Michel Païta, and Philippe Ricordeau. 2008. *Points de repère Ameli n°16: Les causes médicales de l'invalidité en 2006*. Available online: https://assurance-maladie.ameli.fr/etudes-et-donnees/2008-causes-medicales-invalidite-2006 (accessed on 20 February 2022).

Dabakuyo, Tienhan Sandrine, Franck Bonnetain, Patrick Roignot, Marie-Laure Poillot, Gilles Chaplain, Thierry Altwegg, Guy Hedelin, and Patrick Arveux. 2008. Population-based study of breast cancer survival in Cote d'Or (France): Prognostic factors and relative survival. *Annals of Oncology* 19: 276–83. Available online: https://www.annalsofoncology.org/article/S0923-7534(19)41345-8/fulltext (accessed on 20 February 2022).

Dray-Spira, Rosemary, Tiffany Gary-Webb, and Frederick Brancati. 2010. Educational disparities in mortality among adults with diabetes in the US. *Diabetes Care* 33: 1200–5. Available online: https://www.ncbi.nlm.nih.gov/pmc/articles/PMC2875423/ (accessed on 20 February 2022).

Gentil-Brevet, Julie, Marc Colonna, Arlette Danzon, Pascale Grosclaude, Gilles Chaplain, Michel Velten, Franck Bonnetain, and Patrick Arveux. 2008. The influence of socio-economic and surveillance characteristics on breast cancer survival: A French population-based study. *British Journal of Cancer* 98: 217–24. Available online: https://www.ncbi.nlm.nih.gov/pmc/articles/PMC2359707/ (accessed on 20 February 2022).

Jørgensen, Marit Eika, Thomas Peter Almdal, and Bendix Carstensen. 2013. *Time Trends in Mortality Rates in Type 1 Diabetes from 2002 to 2011*. Available online: https://pubmed.ncbi.nlm.nih.gov/23949580/ (accessed on 20 February 2022).

Kim, Nam Hoon, Tae Joon Kim, Nan Hee Kim, Kyung Mook Choi, Sei Hyun Baik, Dong Seop Choi, Yousung Park, and Sin Gon Kim. 2016. Relative and combined effects of socioeconomic status and diabetes on mortality: A nationwide cohort study. *Medicin* 95. Available online: https://www.ncbi.nlm.nih.gov/pmc/articles/PMC5265873/ (accessed on 20 February 2022).

Kusnick-Joinville, Odile, Céline Lamy, Yvon Merlière, and Dominique Polton. 2006. *Points de repère Ameli n°5: Déterminants de l'évolution des indemnités journalières maladie*. Available online: https://assurance-maladie.ameli.fr/sites/default/files/2006-11_determinants-evolution-indemnites-journalieres-maladie_points-de-repere-5_assurance-maladie.pdf (accessed on 20 February 2022).

Maruani, Margaret, and Monique Meron. 2012. *Un siècle de travail des femmes en France*. Paris: La Découverte.

NHIS (National Health Survey). 2016. Centers for Disease Control and Prevention. Available online: https://www.cdc.gov/nchs/nhis/1997-2018.htm (accessed on 20 February 2022).

Piffaretti, Clara, Anne Fagot-Campagna, Grégoire Rey, Juliana Antero-Jacquemin, Aurélien Latouche, and Laurence Mandereau-Bruno. 2016. Déterminants de la mortalité des personnes diabétiques de type 2. Cohortes Entred, France, 2002–2013. *Bulletin Epidémiologique Hebdomadaire-BEH* 681–90. Available online: https://www.santepubliquefrance.fr/maladies-et-traumatismes/diabete/documents/article/determinants-de-la-mortalite-des-personnes-diabetiques-de-type-2.-cohortes-entred-france-2002-2013 (accessed on 20 February 2022).

Ridsdale, B. 2012. Annuity underwriting in the United Kingdom. Note for the International Actuarial Associ-ation Mortality Working Group. Available online: https://www.actuaries.org/CTTEES_TFM/Documents/Zagreb_item19_underwriting_annuities_UK.pdf (accessed on 20 February 2022).

SEER. 2020. Surveillance, Epidemiology, and End Results (SEER) Program SEER*Stat Database: Incidence—SEER Research Data, 9 Registries, Nov 2020 Sub (1975–2018)—Linked to County Attributes—Time Dependent (1990–2018) Income/Rurality, 1969–2019 Counties, National Cancer Institute, DCCPS, Surveillance Research Program, Released April 2021, Based on the November 2020 Submission. Available online: https://seer.cancer.gov/seerstat/ (accessed on 5 November 2021).

Tomas, Julien, and Frédéric Planchet. 2014. Prospective mortality table and portfolio experience. In *Computational Actuarial Science with R*. Edited by A. Charpentier. The R Series; Chapman and Hall: chp. 9. Available online: http://www.ressources-actuarielles.net/gtmortalite (accessed on 20 February 2022).

Walter, Jeremy, Shona Livingstone, Helen Colhoun, Robert Lindsay, John McKnight, Andrew Morris, John Petrie, Sam Philip, Naveed Sattar, Sarah Wild, and et al. 2011. Effect of socioeconomic status on mortality among people with type 2 diabetes: A study from the Scottish Diabetes Research Network Epidemiology Group. *Diabetes Care* 34: 1127–32. Available online: https://www.ncbi.nlm.nih.gov/pmc/articles/PMC3114515/ (accessed on 20 February 2022).

MDPI
St. Alban-Anlage 66
4052 Basel
Switzerland
Tel. +41 61 683 77 34
Fax +41 61 302 89 18
www.mdpi.com

Risks Editorial Office
E-mail: risks@mdpi.com
www.mdpi.com/journal/risks

MDPI
St. Alban-Anlage 66
4052 Basel
Switzerland

Tel: +41 61 683 77 34
Fax: +41 61 302 89 18

www.mdpi.com

ISBN 978-3-0365-3828-0